

**THE UNIVERSITY OF TURKISH AERONAUTICAL ASSOCIATION
INSTITUTE OF SCIENCE AND TECHNOLOGY**

**ANALYSIS AND SIMULATION OF COMPOSITE MATERIALS PROPERTIES
AND BEHAVIOUR USED FOR MANUFACTURING WIND POWER BLADES
STUDY**

MASTER THESIS

ALI I.Y.AL-FARIS

ID: 1406080016

**INSTITUTION OF SCIENCE AND TECHNOLOGY
MECHANICAL AND AERONAUTICAL ENGINEERING DEPARTMENT
MASTER THESIS PROGRAM**

DECEMBER 2017

**THE UNIVERSITY OF TURKISH AERONAUTICAL ASSOCIATION
INSTITUTE OF SCIENCE AND TECHNOLOGY**

**ANALYSIS AND SIMULATION OF COMPOSITE MATERIALS
PROPERTIES AND BEHAVIOUR USED FOR MANUFACTURING WIND
POWER BLADES STUDY**

MASTER THESIS

ALI I.Y.AL-FARIS

Ref.No: 10172228

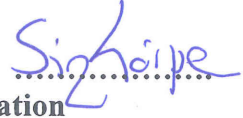
**IN PARTIAL FULFILLMENT OF THE REQUIREMENT FOR THE
DEGREE OF MASTER OF SCIENCE IN MECHANICAL AND
AERONAUTICAL ENGINEERING**

Supervisor: Asst. Prof. Dr. Durmuş SİNAN KÖRPE

ALI. I. AL FARIS, having student number **1406080016** and enrolled in the Master program at the Institute of Science and Technology at the University of Turkish Aeronautical Association, after meeting all the required conditions contained in the related regulations, has successfully accomplished, in front of jury, the presentation of the thesis prepared with the title of: **“Analysis and Simulation of Composite Materials Properties and Behaviour Used for Manufacturing Wind Power Blades Study”**.

Supervisor:

Asst. Prof. Dr. Durmuş SINAN KÖRPE
University of Turkish Aeronautical Association



Jury Members:

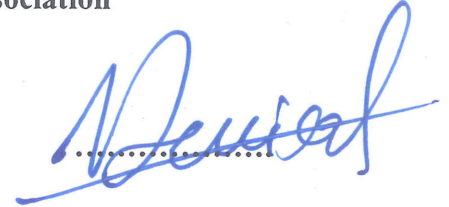
Asst. Prof. Dr. Durmuş SINAN KÖRPE
University of Turkish Aeronautical Association



Assoc. Prof. Dr. Tahsin ÇAĞRI ŞİŞMAN
University of Turkish Aeronautical Association



Assoc. Prof. Dr. Murat Demiral
Çankaya University



Thesis Defense Date: 04.12.2017

STATEMENT OF NON-PLAGIARISM PAGE

I at this moment declare that all information in this document has been obtained and presented in accordance with academic rules and ethical conduct. I also declare that, as required by these rules and conduct, I had fully cited and referenced all material and results that are not original to this work.

A handwritten signature in blue ink, consisting of a large, stylized loop followed by a horizontal line and a small vertical stroke at the end.

ALI. I. AL--FARIS

04.12.2017

ACKNOWLEDGMENTS

This is a nice opportunity to show deep thankfulness to all those who helped and supported me in completing this piece of work. First of all, I would like to show sincere thankful to my supervisor Asst. Prof. Dr. Durmuş SİNAN KÖRPE, who willingly shared his knowledge, experience, and ideas with me, where without his excellent courses, guidance, and remarkable patience I don't think I would ever have finished this work. I would like to thank all the academic staff in the Mechanical and Aeronautical Engineering Department for allocating their valuable time and effort during these years of study. Also, I would like to thank Dr. Wael R. ABDULMAJEED for his valuable support. My appreciation is also for a student in the Aeronautical Engineering Department in THK Univ. Ozan T. ISMAILOGLU for his cooperation with me in a part of my work. I want to express my sincere gratitude to my parents, wife, brother, children, and all my family for their complete reliance, unconditional love, and moral support throughout my academic years.

ALLI.AL FARIS

DECEMBER 2017

TABLE OF CONTENTS

STATEMENT OF NON-PLAGIARISM PAGE	iii
ACKNOWLEDGMENTS	iv
TABLE OF CONTENTS	v
LIST OF TABLES.....	viii
LIST OF FIGURES.....	x
ABSTRACT	xiii
ÖZET	xv
CHAPTER ONE.....	1
GENERAL INTRODUCTION	1
1.1. Introduction	1
1.2. The aim of the study.	2
1.3. Literature Review	3
1.4. Thesis Objective	6
1.5. Thesis Organization	6
CHAPTER TWO.....	8
COMPOSITE MATERIALS BACKGROUND IN WIND ENERGY SECTOR.....	8
2.1. Introduction	8
2.2. Blade Concepts.....	9
2.3. Loads Acting on Wind Blades.....	12
2.4. Wind Blade Requirements	13
2.5. Composite Materials	14
2.6. The Advantages of Composite Materials	15
2.7. Composite Material Properties	17
2.7.1. Common Fiber Types	17
2.7.2. Common Matrix Types.....	22

CHAPTER THREE.....	26
THEORETICAL PART.....	26
3.1. Introduction	27
3.1.1. Why Helios Composite?	28
3.2. Stacking Sequence	29
3.3 Global Coordinates and Local Coordinates	29
3.4. CLT (classical laminate theory)	30
3.5. CLT Equations:	31
3.6. An Important Assumptions and Work Simplifications.....	33
3.7. Failure Criteria.....	34
3.7.1. Hashin Criterion	34
3.7.2. Christensen Criterion.....	35
3.7.3. Maximum Stress Criterion.....	35
3.8. Failure Criteria Similarities.....	36
CHAPTER FOUR	37
METHODOLOGY	37
4.1. Introduction	37
4.2. Description of the Work.....	37
4.3. Work organization	39
4.4. Pure Axial Load Analysis	41
4.4.1. Failure Mood Analysis According Different Failure Criterion.....	41
4.4.2. Failure Behavior of Composites with Different Failure Criteria.....	47
4.5. Progressive Failure Analysis (failure envelope)	49
4.5.1. Failure Envelope Analysis With Specific Criteria - Different Composites (Axial with Transverse Loaded).	49
4.5.2. Analysis with Certain Composite -Different Criteria (Axial with Transverse Loaded).	53
4.5.3. Analysis with Certain Criterion -Different Composites (axial with shear loaded).	56

4.5.4. Analysis with Certain Composite -Different Criteria (axial with shear loaded).....	60
4.6. Pure Shear Load Analysis.....	64
4.7. Aerodynamic Force Analysis Using QBlade Software Version 0.963.....	68
4.8. Composite Material Behavior Due to Aerodynamic Force Analysis.....	72
4.8.1. Assumptions.....	72
4.8.2. Calculations.....	73
CHAPTER FIVE.....	75
CONCLUSION AND SUGGESTIONS.....	75
5.1. Conclusion.....	75
5.2. Suggestions.....	76
REFERENCES.....	77

LIST OF TABLES

Table 1	: Properties of Carbon, Glass and Aluminum fibers.....	20
Table 2	: Failure mood definitions in the study tables below.....	41
Table 3	: Failure mood sequence of the three composites at maximum. Stress criterion.....	42
Table 4	: Failure mood sequence of the three composites at Christensen criterion.....	43
Table 5	: Failure mood sequence of the three composites at hashin criterion.....	45
Table 6	: Failure envelope turning values of (S_{11}, S_{22}) of the composites using Max.Stress Criterion.....	50
Table 7	: Failure envelope turning values of (S_{11}, S_{22}) of the composites using Christensen Criterion.....	52
Table 8	: Failure envelope turning values of (S_{11}, S_{22}) of the composites using Hashin Criterion.....	53
Table 9	: Failure envelope turning values of (S_{11}, S_{12}) of the composites using Max. Stress Criterion.....	57
Table 10	: Failure envelope turning values of (S_{11}, S_{12}) of the composites using Christensen criterion.....	58
Table 11	: Failure envelope turning values of (S_{11}, S_{12}) of the composites using Hashin criterion.....	60
Table 12	: Failure envelope turning values of (S_{11}, S_{12}) of the IM7-977-3 with different failure criteria.....	61
Table 13	: Failure envelope turning values of (S_{11}, S_{12}) of the AS4-8552 with different failure criteria.....	62

Table 14	: Failure envelope turning values of (S_{11} , S_{12}) of the AS4-3501-6 with different failure criteria.	64
Table 15	: shear load failure mood sequence of the three composites at maximum Stress criteria.....	64
Table 16	: shear load failure mood sequence of the three composites at Hashin criterion.	66
Table 17	: shear load failure mood sequence of the three composites at Christensen criterion.	67
Table 18	: SANDIA_SERI-8 model database.	69
Table 19	: max. deflection table for all sections of the three composites.	74

LIST OF FIGURES

Figure 1	: Schematic cross-section of a blade.	10
Figure 2	: Cross section of blade with overall integrated beam and shell	11
Figure 3	: Section of the blade with load-carrying box and attached shells Perspective view, (b) cross-sectional view.....	11
Figure 4	: Durability of wind blades compared with other blades.....	12
Figure 5	: The flap wise and edgewise load directions	13
Figure 6	: Fiber, resin stress-strain sketch	15
Figure 7	: Stress-strain curve for most fibers used with the resin	17
Figure 8	: Composite materials: The picture of the fiberglass composite material	18
Figure 9	: Carbon fiber.....	19
Figure 10	: The picture of the carbon composite material	20
Figure 11	: The structure of Kevlar is mesh-like, allowing it to absorb impact energy effectively.	21
Figure 12	: Composite materials: The picture of the Kevlar composite material.....	21
Figure 13	: Chemical crosslinking results in the permanent curing of a thermoset composite.....	23
Figure 14	: Thermoset polymers are amorphous (left) while thermoplastics are typically semi-crystalline (center), but do not have chemical cross-linking (right).....	24
Figure 15	: Normal compressive stress (left) causes a material to become shorter and wider, a tensile stress (right) lengthens and thins out the material	26
Figure 16	: Shear stresses result in a change in shape	27

Figure 17	: Composite Layers.	29
Figure 18	: The plies (laminas) are stacked together to form a laminate (left), Coordination of the axes for each ply and the angle is shown at right.	30
Figure 19	: Kirchhoff's hypothesis requires normal to the mid-plane remains normal to the mid-plane during bending.	30
Figure 20	: Z is measured from the geometric mid-plane, with the positive direction being downwards.....	32
Figure 21	: Micromechanics levels.	37
Figure 22	: Composite laminate plies with stacking sequence.	38
Figure 23	: The three orthogonal planes.	38
Figure 24	: Coordinates system and loads directions definitions.	39
Figure 25	: Failure mood sequence of the three composites at maximum Stress criterion.	43
Figure 26	: Failure mood sequence of the three composites at Christensen criterion.....	45
Figure 27	: Failure mood sequence of the three composites at Hashin criteria.....	46
Figure 28	: Breaking axial load for IM7-977-3 Composite Material.	47
Figure 29	: Breaking axial load for AS4-8552 Composite Material.....	48
Figure 30	: Breaking axial load for AS4-3501-6 Composite Material.	49
Figure 31	: Failure Envelope Diagram for Composites Using Max.Stress Criteria.	50
Figure 32	: Failure Envelope Diagram for Composites Using Christensen Criterion.....	51
Figure 33	: Failure Envelope Diagram for Composites Using Hashin Criterion.....	52
Figure 34	: Failure envelope for IM7-977-3by applying different failure criterion.....	54
Figure 35	: Failure envelope forAS4-8552 by applying different failure criteria.....	54

Figure 36 : Failure envelope for AS4-3501-6 by applying different failure criteria.....	55
Figure 37 : Failure envelope using max. stress criteria on the three composites.	56
Figure 38 : Shape of failure envelope using Christensen criteria on the three composites.	57
Figure 39 : Shape of failure envelope using Hashin criteria on the three composites.	59
Figure 40 : Failure envelope of axial with shear load for IM7-977-3 using different failure criteria.	60
Figure 41 : Failure envelope of axial with shear load for AS4-8552 using different failure criteria.	61
Figure 42 : Failure envelope of axial with a shear load for AS4-3501-6 using different failure criteria.	63
Figure 43 : laminate stacking sequence.	65
Figure 44 : Shear load failure mood sequence of the three composites at maximum. Stress criterion.	66
Figure 45 : shear load failure mood sequence of the three composites at Hashin criterion.....	67
Figure 46 : Shear load failure mood sequence of the three composites at Christensen criterion.	68
Figure 47 : SANDIA_SERI-8.	69
Figure 48 : SANDI_SERI-8 simulation at $v=15\text{m/s}$	70
Figure 49 : Normal force at different time steps on the blade.....	71
Figure 50 : (a) the blade segment number, (b)main I-beam sections for spar, (c) I-beam spar cross section dimensions, (d) I-beam spar average dimensions, (e) I-beam spar average cross section, (f) main cord values for spar sections (blade top view).	73

ABSTRACT

ANALYSIS AND SIMULATION OF COMPOSITE MATERIALS PROPERTIES AND BEHAVIOUR USED FOR MANUFACTURING WIND POWER BLADES STUDY

AL FARIS. ALI

Master. Department of Aeronautics and Mechanical Engineering

Thesis Supervisor: Asst. Prof. Dr. Durmuş SİNAN KÖRPE

December 2017, 81 Pages

The materials which are used in the wind turbine are wide and varied. The differences which existed between the large and small machines are substantial and in terms of design, it includes expected changes and it may need to enter new materials and technologies during the manufacturing process. During the next 10 years, the work opportunities on the wind turbines and its materials and components will be expanded. This study is a try to assist some of the composite materials that are commonly used in the wind energy manufacturing sector by using software that recently becoming used for more precise prediction of the composite behavior. Auto Desk Helius Composite software has been used in this study, where three composite materials have been chosen to investigate their properties, behavior, failure sequence which is IM7-977-3, AS4-8552, and AS4-3501-6. Those composites have been tested according to three failure criteria which are Maximum Stress, Christensen, Hashin failure criteria. A comparison between the usages of each composite has been made. The effect of using a different failure criterion on a specific composite has been studied. A comparison between the failure criteria has been made. Failure sequence for each composite under an axial load and shear load separately has been investigated. Failure envelope for each composite has been presented in such a way to help the designers take the right decision by knowing the failure stresses constraints of

each composite. QBlade open source software has been used in this study to fulfill the aerodynamic part analysis. SANDIA_SERI-8 wind blade model has been chosen as a case study to make a simulation for a wind turbine model under a steady state wind speed of 15m/s. Acting force on the blade has been calculated from the aerodynamic analysis part with QBlade and has been introduced in the composite analysis part with Helius Composite to find out the deflection of each composite material. An approximation of the blade model dimensions has been made to make it possible to use with the Auto Desk Helius Composite software.

Keywords: Auto Desk Helius Composite software, QBlade open source software, deflection calculation, failure envelope analysis, failure mood sequence, composite materials, aerodynamic force analysis, wind blade composite materials.

ÖZET

RÜZGÂR TÜRBİNİ BIÇAĞI ÜRETİMİNDE KULLANILAN KOMPOZİT MATERYALLERİN ÖZELLİK VE DAVRANIŞLARININ SİMÜLASYONU VE ANALİZİ ÜZERİNE BİR ÇALIŞMA

AL FARIS. ALI

Yüksek Lisans Tezi, Makine Mühendisliği Anabilim Dalı

Tez Danışmanı: Yrd. Doç. Dr. Durmuş SİNAN KÖRPE

Aralık 2017, 81 sayfa

Rüzgâr türbinlerinde çok çeşitli malzemeler kullanılır. Küçük ve büyük makineler arasında büyük farklılıklar vardır ve tasarımlarda yeni malzeme teknolojileri ve imalat yöntemlerine ihtiyaç duyulacağı öngörülen değişiklikler vardır. Rüzgâr türbinleri bileşenleri ve malzemeleri en azından önümüzdeki 10 yıl boyunca önemli ve genişleyen iş fırsatlarıdır. Bu çalışma, son zamanlarda kompozit malzemelerin daha kesin olarak öngörülmesi için kullanılan yazılımları kullanarak rüzgâr enerjisi üretiminde yaygın olan bazı kompozit malzemelere yardımcı olmaya çalışmaktadır. Bu çalışmada, Auto Desk Helius Composite yazılımı kullanıldı; burada, IM7-977-3, AS4-8552, AS4-3501-6 olan özelliklerini, davranışlarını, arıza sıralarını incelemek üzere üç kompozit malzeme seçildi. Bu kompozitler Maksimum Stres, Christensen, Hashin başarısızlık kriterleri olmak üzere üç başarısızlık kriterine göre test edilmiştir. Her kompozitin kullanımı arasında bir karşılaştırma yapılmıştır. Belli bir kompozit üzerinde farklı bir arıza kriterinin kullanılmasının etkisi çalışılmıştır. Başarısızlık ölçütleri arasında bir karşılaştırma yapılmıştır. Her kompozit için bir aksiyal yük altında kesme sırası ve kesilme yükü ayrı olarak araştırılmıştır. Her bir kompozit için başarısızlık zarfı, tasarımcıların her bir kompozitin başarısızlık zorlamaları kısıtlamalarını bilerek doğru kararı almasına yardımcı olacak şekilde sunulmuştur. Bu çalışmada aerodinamik parça analizini gerçekleştirmek

için QBlade açık kaynaklı yazılım kullanılmıştır. SANDIA_SERI-8 rüzgâr bıçağı modeli, 15m / s'lik sabit bir rüzgar hızı altında bir rüzgar türbini modelinin bir simülasyonunu yapmak için bir vaka çalışması olarak seçilmiştir. Bıçak üzerindeki etki kuvveti, QBlade'li aerodinamik analiz bölümünden hesaplandı ve her bir kompozit malzemenin sapmasını bulmak için Helius Composite ile bileşik analiz bölümünde tanıtıldı. Auto Desk Helius Composite yazılımı kullanımını mümkün kılmak için bıçak model boyutlarının bir yaklaştırması yapılmıştır.

Anahtar Kelimeler: Auto Desk Helius Kompozit yazılımı, QBlade açık kaynaklı yazılım, sapma hesaplama, arıza zarf analizi, arıza durum dizisi, kompozit malzemeler, aerodinamik kuvvet analizi, rüzgâr bıçağı kompozit malzemeler.



CHAPTER ONE

GENERAL INTRODUCTION

1.1. Introduction

The three basic components where the wind turbine depends are three basic components including the blade materials, blade angle and blade shape. Thus, turbine blade's material represents a significant role in the wind turbines. The materials of the blade must retain long fatigue life, high difficulty, and low density. The components of turbines have been changed when the technology improved and evolved. The lighter weight systems became desirable in the last periods. The materials which characterize by low cost and light weight are significant in the blades. The wind turbine uses a wide range of materials. The differences which existed between the large and small machines are substantial and in terms of design, it includes expected changes and it may need to enter new materials and technologies during the manufacturing process. The number of materials which used in the manufacturing process is two materials only. The first material (the matrix or binder) fixes a cluster of fibers or the fragments of a much stronger material with each other and the other material (the reinforcement) which surroundings this fragment or fibers. The researchers aim to develop the first material by making it most resistance to effect [1]. The components of fibrous materials are beneficial in terms of the mechanical and physical characteristics if compared with the other construction materials of wind turbine blades. The high strength and low weights are the most benefits of this material [2] [3]. Thus, the wind turbine blade which is constructed with combined materials has less weights if compared with the conventional construction.

Currently, the glass fiber-reinforced-plastic (GRP) is the basic material which through most of the rotor blades are constructed. In addition, other materials have been experienced comprising steel, numerous composites and carbon filament-reinforced-plastic (CFRP). The rotor which is used in the large machines must be manufactured from fatigue resistant materials with high strength. Since the wind turbine as developing rapidly, there are materials which can be used in the designing of the wind turbine in the near future including CFRP, steel, GRP, and perhaps other materials will likely come into use. Generally, the blades are manufactured from the GRP whereas the CFRP is used to reduce the cost and weight to some ranges. The most significant drivers which influence the selection of materials are reliability and low cost. The manufacturing of blades includes the use of Carbon fiber reinforcements. They are used to increase the strength of stiffness and tensile at the direction of fiber as compared to material which includes the glass. However, the compressive strength gains are much lower. Therefore, the glass mixture and carbon are economically used with carbon mostly to increase the stiffness of global blades [4].

1.2. The aim of the study.

The exploration of structural and aerodynamic designs effectively and optimal materials examinations led to developing the wind turbine design blades. The experiments and design assessments of the materials and industrial concerns of huge wind turbine blades and rotors resulted in the design provisions and initial designs for candidate blades in the range between 30-70 m in length [5] [6] and rotors between the range from 80-120 m in diameter [7] [8]. The challenges which will face the future design for even greater machines will remain to push the design envelope excesses that is mainly restricted by the growth of weight penalty. As mentioned by Veers et al. [9], the blade design development, performance and manufacturing are always representing the initial goal of the research. It is discovered that the reduction of 10-20% in the weight of blade lead to significant decrease in the other main elements cost including the tower and the drive train. However, the blades of wind turbines account only 10-15% of the capital cost for the entire system. Therefore, according to this reason, in this study, three composite materials have been chosen to make an investigation on them by using three failure criteria. The effect of each

failure criterion on the composites has been investigated. The failure's behavior of each composite with different failure criterion has been investigated. Creating a symmetrical stacking sequence of eight plies to find out their mechanical properties has been done. Axial load and shear load have been applied respectively to find out the permissible loads for each material separately. Failure envelope analysis and failure mood analysis have been done for both axial and shear loads correspondingly. Comparisons for all these analyses have been discussed to establish an efficient way to choose the suitable composite material for a wind turbine blade manufacturing or any other application according to a simple way by using professional software (Helios Composite) and benefits of the pre-design method before relying on practical analysis reposts which are very expensive in general.

1.3. Literature Review

Both in the developing and developed countries, decrease the dependence on the fossil fuel represent a significant goal. To achieve this goal, the renewable energy including the wind energy must be used extensively. This can be noticed through the growth of installing many on-shore and off-shore wind farms which are constructed with extra-large wind turbines due to the high costs of maintenance and compensation of oversized Off-Shore or the wind turbines that distantly installed. The most important part which through the reliability of the wind turbines are measured is the rotor where they must be increased to guarantee the effective operation for more than 20 years. The durability of turbines can be achieved by many issues including the low weight, the high stiffness of blade materials, resistance against the environmental impacts and fatigue. Therefore, to develop the utilization of wind turbines, improved components must be developed.

S. Morgan-Smith at Grandpa's Knob Company in Vermont have built the first wind turbine in to generate the electric power. The turbine constructed in 1941 with basic specifications (53.3 m rotor, two blades. power rating 1.25 MW) and it is prepared with great amounts of steel blades. This turbine operated irregularly only a few hundreds of hours and one of its blades are failed. Thus, the significance of correct selection of materials and the inherent boundaries of materials as a wind blade material has been

proven only at the history beginning of wind energy progress. The second successful example of the wind turbine of energy generation is known as Gedser wind turbine and it has been constructed by Johannes Jul. for the electricity company SEAS at Gedser coast in 1956-57. The turbine is manufactured using composite blades which have been constructed with aluminum shells reinforced steel spears with wooden ribs. The first success story of wind energy turbine was with three blades 24 m rotor, 200 kW. It is operated for 11 years without any maintenance process. Most of the wind turbine which has been produced after 1970 are combined with composite blades [10] [11]. Therefore, the connection between the wind energy generation technology success and the expansion to use combined materials for turbine parts became clear from the first steps of wind energy industrialized. The second turbine that has been constructed from composite blades is succeeded while the first one which has been constructed from still blades is failed.

Mandell, J. F., Samborsky, D. D., & Agastra, P. [2], argued that it is possible to determine the conditions and materials where the high cycles can cause the low strain damage failure. The most distinguished thing that the reasonably new Wind Strand TM based laminates, moreover to abstemiously higher modulus appears outstanding fatigue resistance in both compression loading and tension, compared with E-glass.

Żółkiewski, S. [4], provided that there are fibrous combined materials associated in bolt joints, form joints, and glue joints have been examined. They displayed that the diagram analysis of force-displacement charts showed that the relative strength is increased when increasing the number of classes. The fatigue experiments showed that the decrease in the strength characteristics of composite materials appears after five thousand cycles of loading.

Salman Ali [12], is experienced the characteristics effect and tensile of a composite which configured from matrix reinforced by 50% palm natural fibers and 50% carbon fibers. The palm fiber and carbon fiber fractions of weights are 10, 20, 30, 40, 50, and 60% by weight (wt). The examinations of impact and tensile have been implemented to identify the tensile and impact properties where the greatest strength of impact is $175KJ/m^2$ and fiber weight fraction of 60 %, while $19KJ/m^2$ for virgin polystyrene material and a maximum tensile strength of 358MPa at a weight fraction of fibers 60 %, and 59Mpa for virgin polystyrene material.

Attaf, B [13], has searched for new cost-effective material coupled with high-performance stiffness and/or strength-to-weight ratio; In order to meet wind blades requirement, he used a Unidirectional E-glass fiber (UD 900 g/m²), orientated principally in the blade longitudinal direction (at 0°) with some layers (UD 450 g/m²). Orientated at +/-45°, E-glass mat (UNIFIL 450 g/m²), which is a quasi-isotropic material in the 1-2 plan. The fiber volume fraction (V_f) of the selected composites is estimated to be 60%. In his work, development has been investigated for improvement of design and manufacturing of future wind turbine blades using fiber-reinforced composites. Also, environmental impacts and requirements regarding health, hygiene, and safety have been considered while remaining consistent with a logic cost-efficiency ratio.

Shokrieh et al. [14], has adjusted the standards of Hashin failure through considering the non-linear properties of the materials, in addition, to implement the rule of sudden material degradation

Van der Meer et al. [15], have simulated the progressive failure analysis of fiber failure using phantom-node calculation technique. The calculation results have been validated with the experimental results of the tension checks.

Puck et al. [16], has Developed one of the most realistic Puck's failure standard of advanced failure analysis depending on the Mohr-Coulomb hypothesis using the analytical technique. They deliberated a deterministic method depending on the classical lamination theory (CLT) and advanced degradation model.

Sun et al. [17], expected failure envelopes and stress/strain performance for unidirectional and complicated combined laminates using linear laminate theory. As well as, they approved ply-by-ply discount technique with parallel spring decrease model for material characteristics degradation.

Vasjaliya et al. [18], define SERI-8 wind turbine blade to improve its aerodynamic and structural performance depending on the multidisciplinary design optimization (MDO) process. Their operations have been separated into five stages where the first stage are aerodynamically optimal twist angles of airfoils for the blade cross-sections beside the blade spanwise trend, and the delivery of pressure besides the blade at greatest lift and wind circumstances. The performance of Airfoil has been expected with XFOIL/QBlade, whereas the analysis of CFD has been implemented by CFX software. The second stage

produces optimal material, structural analysis to progress a fluid-structural interaction (FSI) system for SERI-8 composite blade to exploit aerodynamic effectiveness and structural strength whereas decreasing the blade mass and cost.

Kim, Y., Al-Abadi, A et al. [19], they investigate to maximize the performance of wind turbine under different wind condition. They took two approaches to investigate the problem. The 1st approach was an experimental setup for generation and measurement of turbulence with specially designed laboratory scale wind turbine which has been made in a wind tunnel. The 2nd approach was a computational simulation which is performed for NREL Phase VI wind turbine by using QBlade, which enables to simulate the aerodynamic and wake performance of wind turbines under a range of turbulent flows. The results showed that high turbulence improves the power coefficient.

1.4. Thesis Objective

This study is a try to investigate composite materials in a way to give more understanding about composite properties, failure behavior, failure sequence providing detailed information to be used when you try to choose one composite among others, which fits a specific condition in the wind blade manufacturing sector.

1.5. Thesis Organization

This study comes with five chapters as follows:

Chapter one starts with a general introduction about the importance of wind turbine blades in wind turbine units and what is the requirement to design wind blades. The importance of choosing the right composite to build a blade has been stated. What is the composite consists of and their advantages and disadvantages have been discussed. In this chapter the importance of this study has been stated and a quick literature review for what the researchers have done before concerning of this study.

Chapter two starts with a briefing about renewable energy and wind turbine importance among other renewable energy types. The philosophy of the wind blades and its structure has been discussed. Types of the loads that are acting on wind blades and wind blades requirements to carry the loads have been stated. Types of composite that

have been used and their advantages, disadvantages types and properties of them have been discussed.

Chapter three contains the theoretical part of this study. Where all the equations that have been used and the theories have been stated. The coordination systems and stacking sequence have been assumed. The assumption that has been adopted to make this study has been stated.

Chapter four explains how the loads have been applied to the composite materials and the description of the work procedure until the results started to appear. Categorizing the results as groups for more clear discussions and more clarity.

Chapter five contains the conclusion of this study and what could be the future and the suggestion to complete this work to consider the sides that have not been covered here.

CHAPTER TWO

COMPOSITE MATERIALS BACKGROUND IN WIND ENERGY SECTOR

2.1. Introduction

The average of renewable energy growth is increased at rates of 10-60% a year at the end of 2014 which passed on many technologies that include the renewable energy. Many renewable technologies including the wind technologies are grown increasingly since 2009 as compared to their growth in the past years. The amount of wind energy which obtained in 2009 is more than the amount of energy which is obtained by using all the other technologies. Nevertheless, the PV has been increased with fast growth which exceeds the growth of all the other technologies with 60% annual average growth ratio and it is shown the significance of the renewable energies. In 2010, the renewable power established around a third of the anew created power generation capabilities. The International Panel on Climate Change stated that there are limited general technical limitations to incorporate the technologies of renewable energies to comprise most of the entire universal energy demands. The supporters of the renewable energy did not expect the increasing growth and interest in its consumption. The renewable energy is considered a main source of energy to about 30% of the countries around the world. The air flow is used to turn the wind turbines and operates it and then obtain the energy that generated from this movement. Latest utility-scale wind turbines are prolonged from 600 kW to 5 MW of rated power. The most common commercial use of wind turbine is rated about 1.5–3 MW. The amount of energy which generated by the wind turbine depends on the wind speed and thus, whenever the speed of wind increase, the amount of generated energy will be increased. The best results can be gotten in the regions where the winds

are fast such as offshore and high-altitude farms. Typical capability elements are 20-40%, with values at the higher end of the range in typically promising sites [20].

2.2. Blade Concepts

Rotor blades are similar to the wings of aircraft where they comprise two appearances, the suction side and the pressure side where both of them form an enhanced aerodynamic shape as shown in Figure 1. At the leading and trailing edges, the appearances are met where the leading edge is curvy, and the trailing edge is sharp. The chord line is a name which is called on the straight line between the leading and trailing edges at identified cross-section and its length represents the chord. WTG blades do not similar the aircraft wings where they are a built-in twist which pledges that the operative attack angle of the blade and the air is set away approximately persistent beside the blade. Many turbine designs must include a rotating angle to preserve the required angle of attack when the speed of wind change. This mechanism can also be used as a braking system. The brake can be implemented using the electrical or mechanical means or just by rotating the tip of the blade which is called tip brakes. When describing the applied loads on blades, the edgewise is used to refer the deformation of loading and bending in the chord line path while flap-wise displays the route regular to this which is the most flexible direction. Loads of winds represent the main loads on the turbine blades that configure both flap-wise and edgewise bending, and gravity which generates edgewise bending when the blade is horizontal and other axial compression or tension when the blade is vertical. And torsional bends because of the asymmetry of the blade cross section similarly essential to be taken into consideration when loadings related to accelerations.

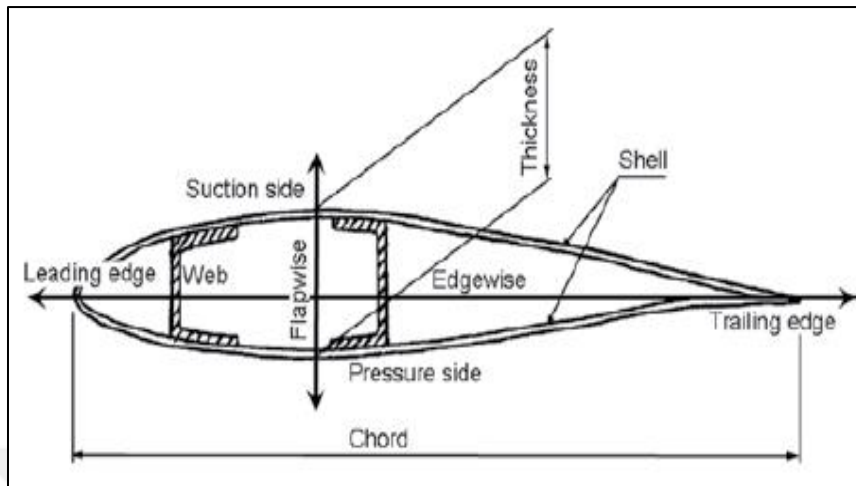


Figure 1: Schematic Cross-Section of a Blade [21].

- 1- The turning and airflow disorder by the tower cause the change of loads with time. As the case with any related beam-like structure, bending a blade arouses to form longitudinal tensile stresses in part of the blade section and compressive pressures in the residues. For flap wise bending include, in general, the stress and suction sides correspondingly. As well as, in specific parts of the blades, Shear (tangential) stresses are generated. While the efficient struggle to flap wise bending is the key concern in the design of the blade, and the external shell cannot implement this issue without the assistance of some internal stiffening, as presented schematically in Figure 1. The required stiffness and bending strength can be provided using two key measures as in Figure 2, thicken the upper and lower parts of the blade shell to transfer the longitudinal pressures which generated by the bending loads. They can be joined by one or more essential webs, which assist to constrain buckling of the shell and carry the pressures of shear associated to flap wise bending.
- 2- The alternative procedure utilizes a box beam or spar to which the upper and lower shells are adhesively involved Figure 3. The similar function is performed by the flanges and webs of the box beam as the parts of thickened shell and webs of the 1st procedure. Uncorroborated slices of the external shells that provide the aerodynamic shape are constructed in the form of sandwich structures.

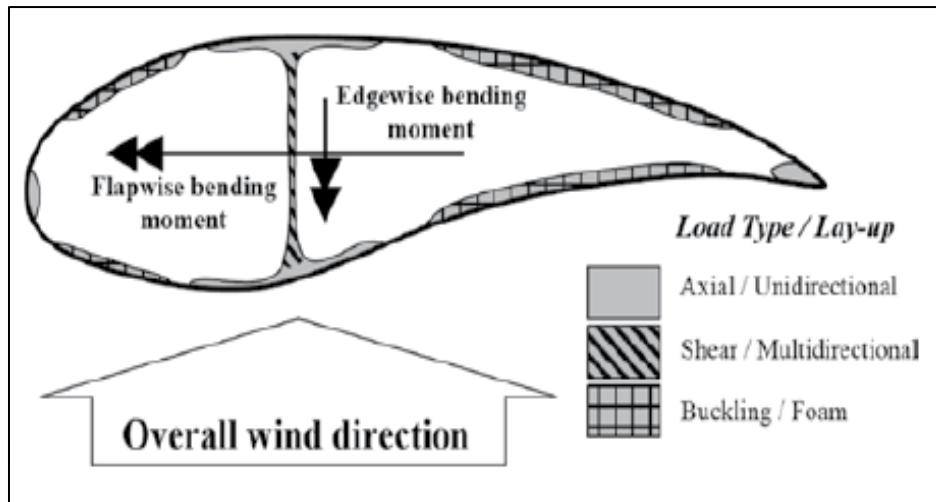


Figure 2: Cross Section of The Blade with Overall Integrated Beam and Shell [22].

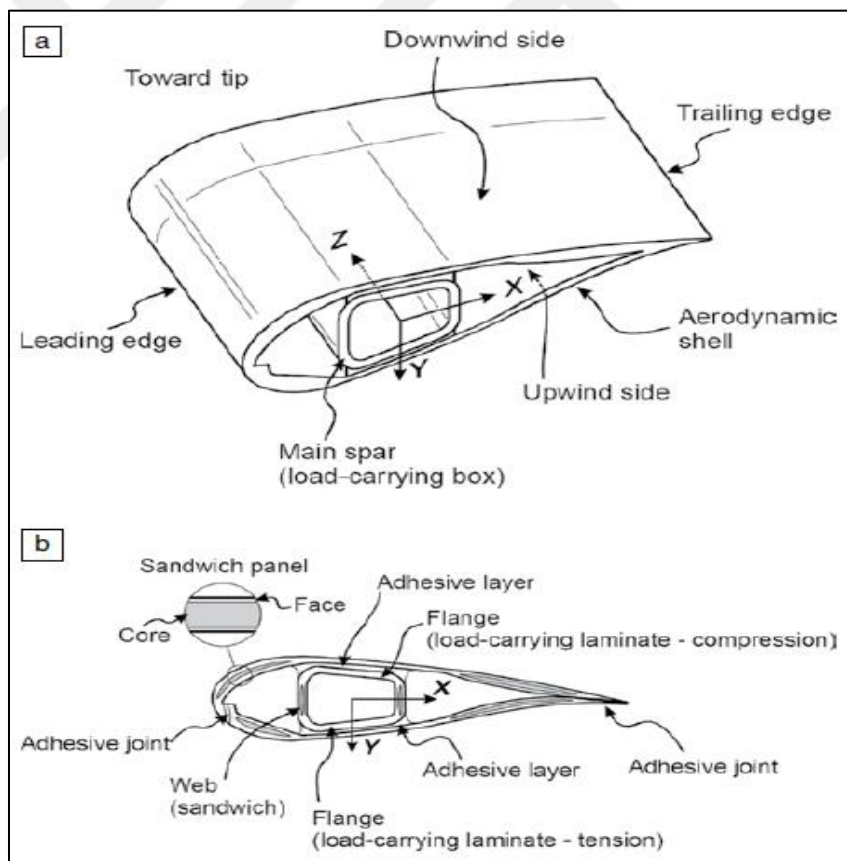


Figure 3: Section of The Blade with Load-Carrying Box and Attached Shells Perspective View, (B) Cross-Sectional View [23].

2.3. Loads Acting on Wind Blades

Wind turbine blades are exposed to the outer loading that contains the flap-wise and edgewise bending loads, inertia forces, gravitational loads, loads of pitch acceleration, also torsional loading. The flap wise load has been produced mainly by the wind pressure. Whereas the edgewise load has been produced both by gravitational forces and torque load. At the blade root, the most significant edgewise bending moment lies. Main cyclic loads are made by gravity (edgewise bending) and by changing winds (flap wise bending) the predictable fatigue life of a wind turbine is between of 20-25 years (more than 10^8 cycles) as shown in Figure 4.

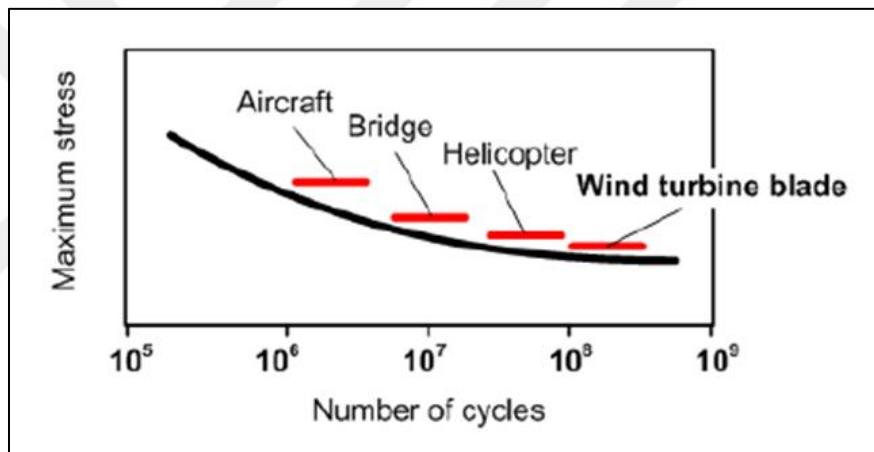


Figure 4: Durability of Wind Blades Compared with Other Blades [24].

The flap-wise and edgewise bending loads are a reason for high tensile, compressive and longitudinal pressures in the material as shown in Figure 5. The downwind side of the blades is exposed to compression pressures. Whereas the upwind side is subject to tensile. The flap wise and edgewise bending moments because the fatigue damage growing. Those instants are liable for 97% of the hurt in blades [25].

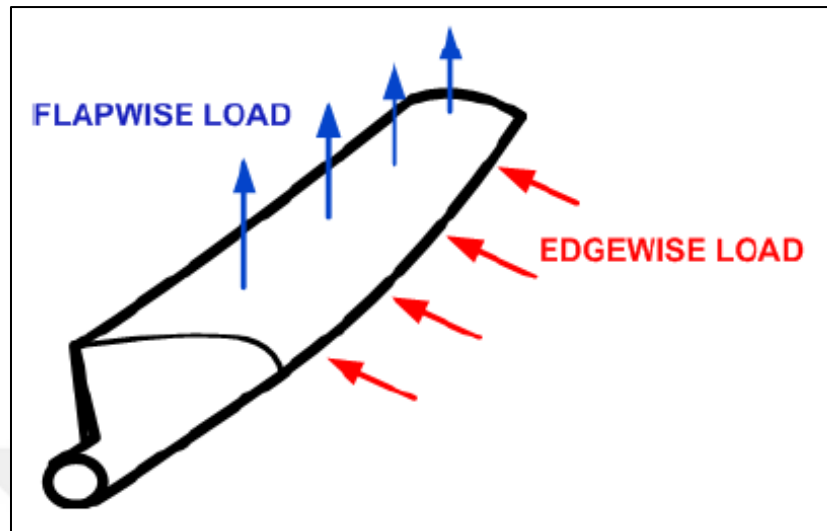


Figure 5: The Flap Wise And Edgewise Load Directions [24].

2.4. Wind Blade Requirements

The blades of wind turbines must be strong enough to endure the loads of applied without breaking. Therefore, the fatigue strength must be enough to hold the variable loads with time and the strength at the end enough to hold the high loads. As well as, the blades must be strong adequately to prevent the collision with the tower during the dangerous circumstances. On the local level, the stiffness is important to avoid the buckling of the parts when they expose into high pressure. It is necessary to lighten the construction of the blades as possible to decrease the cost of the generated energy. This can be accomplished by the optimal benefit from the structural grounding and dimensions inconsistent with the chosen materials. For confirming that the production of the blades is consistent with the expectations of design and computations, the production procedures used in the manufacturing must be organized and adequately trustable. Thus, the blades are normally producing from stiff, light and strong materials constructed on fiber-reinforced polymers, wood, and combinations of them. The reinforcements are manufactured naturally comprising incessant glass fibers and carbon fibers. These materials are mixed together in a laminated (i.e., layered) structure with thermosetting resins, in general polyester, vinyl ester, or epoxy; the resulting complex materials are normally specified as glass-reinforced plastic (GRP) and carbon fiber- reinforced plastic

(CFRP). Blades which manufactured by wood or hybrid wood/carbon fibers are flooded with epoxy resin. The assessment by Brøndsted et al. [10] And the volume edited by Lilholt et al. [26], Deliberate numerous material subjects in this area. Fiber-reinforced combinations of the type which is used in wind turbine blades are laminates that have collected of various layers of reinforcing fabric flooded with an adhesive resin and held with each other. These laminates can be very strong and rigid when they are loaded on their plane, but due to that the layers or plies, can more readily be pulled apart, they are weaker when they are loaded out-of-plane. The in-plane characteristics are typically determined by the fibers, whereas the out-of-plane characteristics rely strongly on the resin's matrix strength and adhesive competency.

2.5. Composite Materials

According to the definition, mixtures are materials that involve two or more chemically different ingredients with different characteristics [27]. Composite materials are not new-found materials, but they have been obtained by merging materials with different properties in different ways (granular, fibrous, stratified, etc.). It can be said as a mixture of two or more materials at the macroscopic level. The objective is provided that the properties of materials without before construction with putting these materials together. For these features like resistance, wear resistance, aging resistance, thermal properties, fracture toughness, conductivity, weight and corrosion resistance, etc. can be sorted. Technically, after the 1940s, these materials are in progress to be used in the aviation industry.

On the other side, like in the aviation sector, within the selection of materials for wind turbine rotor blade structure, a significant criterion which expresses the ratio of intensity to mechanical properties can be considered as a significant advantage related to specific values of mechanical properties for composite material compared to conventional materials. Glass-reinforced plastics are the type of most chosen composite materials for wind turbine rotor blades. These composite materials are preferred because they are easy and economical if compared with fiber - reinforced plastics in providing lightning in turbine blades. Carbon fiber-reinforced plastics have limited usage in the rotor blades.

Although these composite materials deliver strength and lightning higher than to glass reinforced plastics, their high cost is a disadvantage [20].

2.6. The Advantages of Composite Materials

The most important advantage for fiber composites is its high strength and durability compared with conventional engineering materials as shown in Figure 6. These features afford energy and performance developments which are very significant in the design of engineering structures.

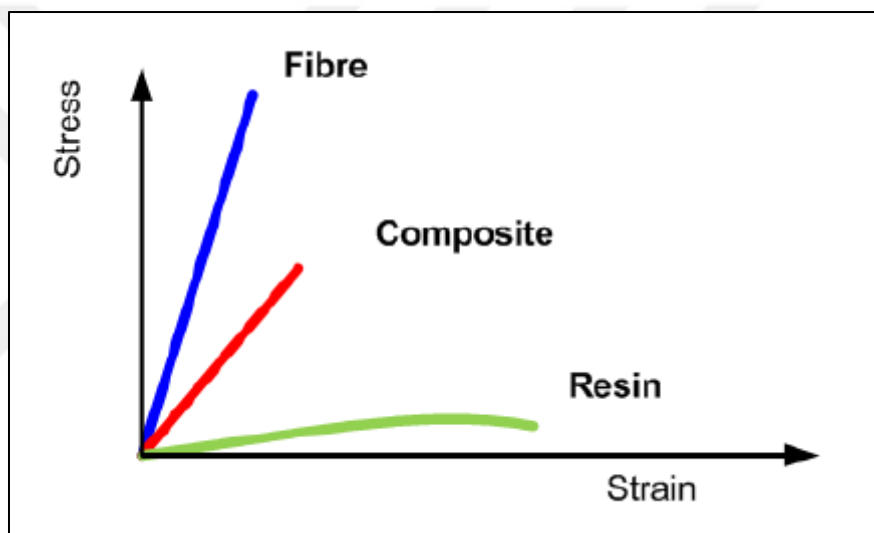


Figure 6: Fiber, Resin Stress-Strain Sketch [24].

For each application, the optimal material properties will be different. Since the material properties of composites are extremely customizable, this case can be considered as an advantage for Composites. Not only can different groupings of materials be used, but the angle of each layer (called a ply or lamina) that has been placed in and their order (the stacking sequence) can be a modification of the configuration the material properties (called a laminate). Since, these combination properties composites can be designed to get the optimal properties in groupings such as stiffness, strength, weight, impact resistance, fatigue life, thermal expansion and corrosion resistance. The interaction allows for enhancements which are just not possible in non-composite materials. For example, the fibers help to arrest fatigue cracks in the matrix, improving the fatigue consequences of composite materials [28].

This wide variety in the design of these materials offers an efficient structure produced by using less material. Also, this diversity enables the use of computers, optimization, skilled systems and artificial intelligence in the manufacture of composite structures and design development. Fatigue Time; fatigue time is one of the main usage motivations in the aerospace industry. Fatigue time is also important for many other structures (transport vehicles, industrial components, bridges, and various structures exposed to wind and water loads).

Polymer and ceramic matrix materials can be carefully chosen to enhance the corrosion resistance of composite materials contrary to moisture and other chemicals. Composites have been produced using this matrix material have needed a less maintenance compared with traditional engineering materials.

Composite material's efficiency reflects very little waste in the production. Production costs are also directly associated with the number of portions in composite materials structure and due to the capability of composite materials to form the final shape in designed time and providing a more efficient mixture of the rivet connection can decrease the number of parts significantly.

Electrical Insulation is desired for many engineering structures. For example; the decrease in the electrical conductivity, glass/polyester ladders and light poles are favorite to make of aluminum and stainless steel. Insulating components are significant for applications for the electronics industry. In the opposite, copper matrix composites are proceeding to use in high-temperature applications because of the high thermal conductivity of copper. Finally, cost calculation of structures that have been made of composite material must contain product's total life cycle cost. Composites are more expensive in general than conventional materials. Though, all other factors must be considered when comparing costs.

- 1- High strength and durability of the composite material.
 - 2- Reducing the cost of production by automation of composite materials.
 - 3- Transportation and setting up costs are usually lower for composite structures.
- Finally, the lifespan of the composite structure is longer than that of traditional materials and need less maintenance throughout their lifespan [20].

2.7. Composite Material Properties

Glass and carbon fibers considered most of fiber reinforced structures. For less weight critical structures, glass fibers give excellent strength and stiffness at a low price. For critical weight structures, carbon fiber increases the strength, stiffness and fatigue resistance but at a higher price. A third fiber which is generally used in impacted structures is Kevlar because of its excellent energy absorption ability. It is clear to guess their behavior from the stress-strain curve in Figure 7.

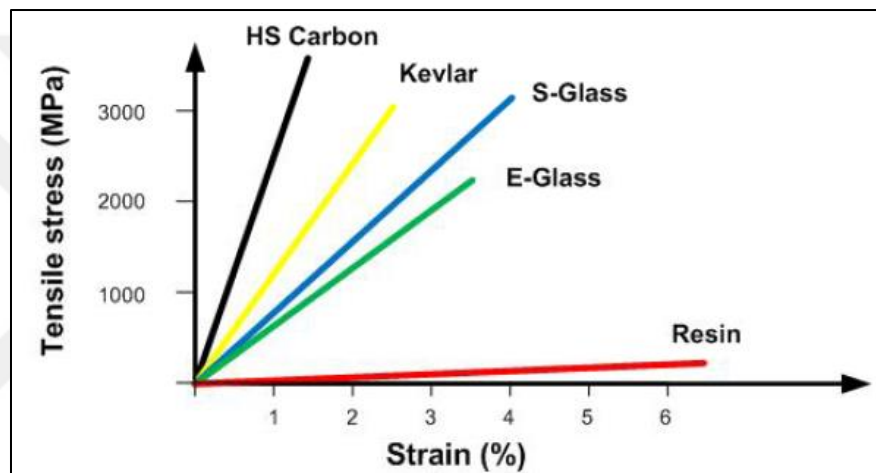


Figure 7: Stress-Strain Curve for Most Fibers Used with The Resin [24].

Thermoset polymers have very good chemical and thermal stability, adequate strength and commercial manufacturability. Therefore, they are the most frequent type of matrix materials have been used in high-performance composites.

Thermoplastic polymers have better effect features, but they are highly expensive and need higher temperatures and pressures to manufacture. Other matrix materials, like ceramics and metals, have been used for more particular applications which need their unique properties [28].

2.7.1. Common Fiber Types

Fibers are caring the load in the composite. Therefore, the serious properties in the fiber that must possess are high stiffness, low density, and high strength. These necessities have led to the developing of many fiber types, some of them are discussed here. Glass is

the oldest manufactured fiber, where was first frequent produced in the early 1900s. Although it was not strong as other advanced fibers such as carbon, it has low cost and delivers suitable properties. Carbon fiber is most typically used in high-performance structures since it delivers excellent material properties at an acceptable cost. Boron fibers give even better mechanical properties compared with carbon fibers specifically at high temperature, though they typically need high cost for large structures. Kevlar fibers, on the other hand, hold excellent impact resistance, that is why it has been adopted in armor. Finally, basalt and ceramic fibers are frequently used in high heat situations also they offer excellent thermal stability compared with any other materials [28].

2.7.1.1. Glass Fiber

Glass fibers have high similarity to the configuration of window glass as seen in Figure 8. However, they have better material properties than most of the materials because of their small size. Two types of glass fibers are used in composites; E-glass and S-Glass.

E-glass specifies electrical glass and is utmost usually used as it provides a balance of function and price. The electrical properties are exceptional. Therefore, this fiber has been formulated for electrical applications. In case of insufficient strength and stiffness for E-glass, S-Glass is used. It has about 10% larger stiffness and strength than E-glass, also has higher thermal resistance, but it is more expensive. It has been used for high-performance structures applications where carbon fiber or metals cannot be utilized [28].

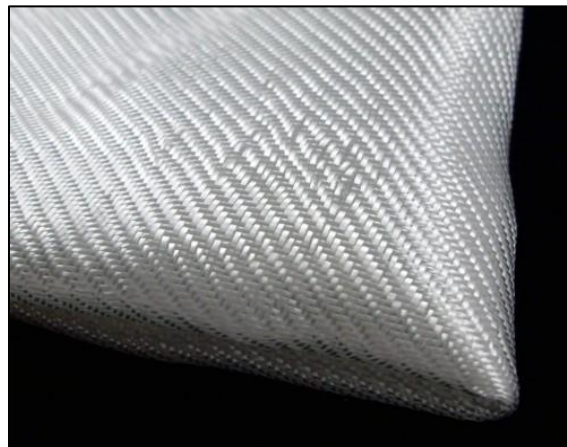


Figure 8: Composite Materials: The Picture of The Fiberglass Composite Material [4].

2.7.1.2. Carbon Fiber

Carbon fibers present much better material properties at a low density if compared with aluminum and glass as shown in Figure 9. The stiffness of it is almost more than four times greater than of aluminum with the strength of at least 10 times greater than aluminum.

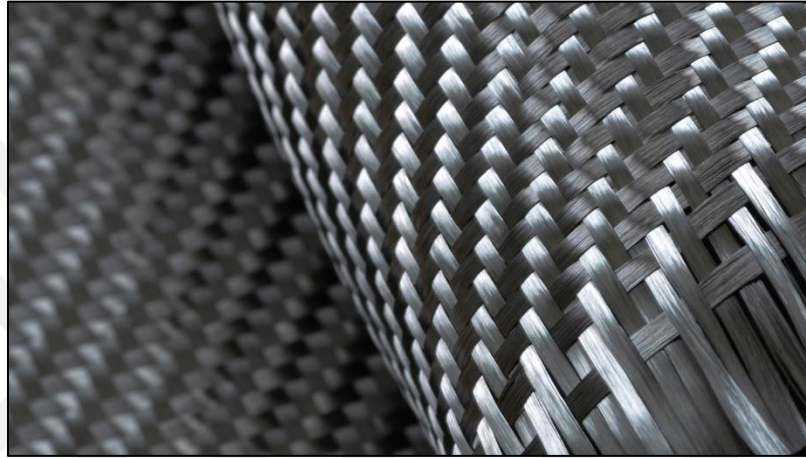


Figure 9: Carbon Fiber [29].

Carbon fibers are very thin, having a diameter of 0.0003 inches or 7-8micron. Millions of tiny fibers can form complex shapes easily. This little size assists to improve the tensile strength of the material. The graphite fiber is very pure, about 99% carbon, and possess very high modulus with $E \geq 50 * 10^6$ psi if compared with $E = 40 * 10^6$ Psi for conventional carbon fibers. Carbon and graphite are dissimilar although both terms are being utilized interchangeably. Because of the cost, most composites that have been used in aircraft today are made of carbon fibers, not graphite fibers. After the production of carbon fibers, they experience a surface treatment in an acid or alkaline bath to improve behavior properties and ensure a quality boundary.

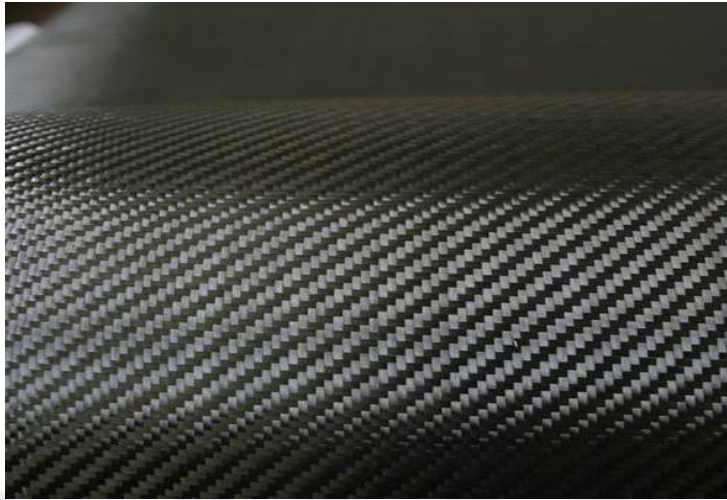


Figure 10: The Picture of The Carbon Composite Material [4].

The excellent strength of carbon fibers, stiffness and light density, make it the most frequently fiber type which has been utilized in high-performance structures. Therefore, carbon fibers have been used mainly in wind turbine companies like Vestas and Gamesa in structural spar caps of large size blades [30]. Typical properties of commercially existing carbon fiber are listed in Table 1 below and compared with the glass fiber properties and aluminum [28].

Table 1: Properties of Carbon, Glass and Aluminum Fibers.

	TORAYT-800 FIBER	HEXCEL IM7 FIBER	GLASS FIBER	ALUMINUM
STIFFNESS	42.6 msi (294GPa)	40.0 msi (276 Gpa)	10.5 msi (72 Gpa)	10 msi (69 Gpa)
TENSILE STRENGTH	796 ksi (5490 MPa)	822 ksi (5670 Mpa)	500 ksi (3447 Mpa)	60 ksi (413 Mpa)
DENSITY	0.065 lb/in ³ (1.81 g/cc)	0.064 lb/in ³ (1.78 g/cc)	0.092 lb/in ³ (2.54 g/cc)	0.098 lb/in ³ (2.7 g/cc)

2.7.1.3.Kevlar Fiber

In addition to a high tensile strength, Kevlar fibers have excellent impact resistance because of their molecular structure Figure. Its look like a microscopic net, the structure

lets the material to deform and captivate impact energy with no fracturing, unlike glass and carbon fibers that are very brittle. Therefore, Kevlar diversities are used for bulletproof vests and other high resistance applications though fiber has an organic nature, Kevlar must be protected from the atmosphere, where ultraviolet light can be the reason of degradation for its strength and stiffness. Also, the Kevlar fiber captivates moisture as shown in Figure 11, and therefore it is not appropriate for application in a wet environment like aircraft control surfaces [28].

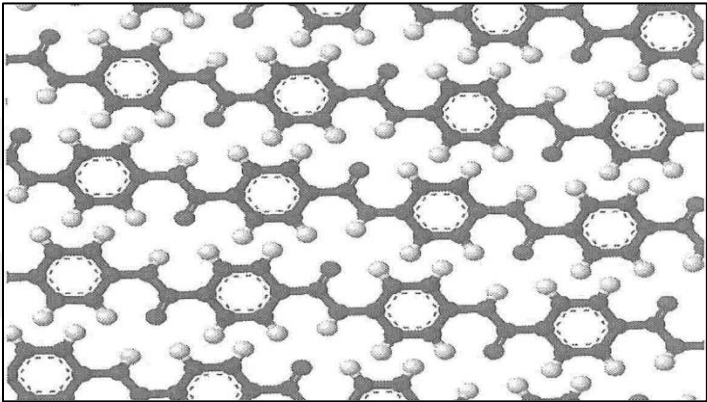


Figure 11: The Structure of Kevlar Is Mesh-Like, Allowing It to Absorb Impact Energy Effectively.

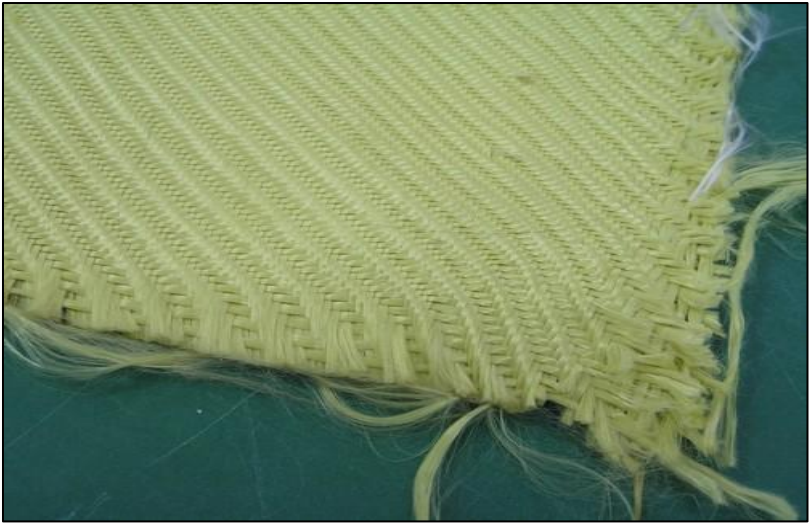


Figure 12: Composite Materials: The Picture of The Kevlar Composite Material [4].

2.7.2. Common Matrix Types

Matrix has more diverse requirements to fulfill its job of binding and protecting the fibers. For the matrix to easily wet out the fibers, the matrix must have sufficiently low surface tension and viscosity. The greater the pressure, the higher the viscosity required to incorporate the fibers and matrix together. Additionally, the interfacial shear strength should be high for a strong joint to be formed with the fiber. If the matrix elongation is less than that of the fibers, the matrix will disintegrate before the fibers breaking, which is undesirable. Finally, the matrix should have reasonable toughness and strength.

The second main job of the matrix is to protect the fibers from adverse conditions. As the fibers are brittle, the matrix must be able to protect them from mechanical abrasion, from a multitude of sources of damage. There are many types of the matrix which are utilized for different composite applications. They can be categorized as polymers, metals, and ceramics. A composite utilizing metal as the matrix material is called metal matrix composites (MMC). Examples of MMC are boron fiber in the aluminum matrix (B/ Al) and silicon carbide fiber in the aluminum matrix (SiC/ Al). These materials yield excellent mechanical properties at elevated temperature. Ceramics can be used as the matrix material to make ceramic matrix composite (CMC). Ceramic materials are utilized in high heat situations, such as turbine burners and brake pads. However, they tend to be brittle and are susceptible to cracking and fracture. This can be solved by using a ceramic matrix reinforced with ceramic fibers to provide the heat resistance and improve the fracture toughness. However, the high processing temperatures and pressures, as well as the high prices to fabricate MMC and CMC, have limited their applications. Today, the most commonly utilized matrix material is polymers [28].

2.7.2.1. Polymer

There are two types of polymers, thermoset, and thermoplastic. The molecular structure and thus physical properties of these two classes of polymers are completely different. There are two different arrangements of the molecules: amorphous, typical of thermosets, and semi-crystalline, typical of thermoplastics.

2.7.2.1.1 Thermoset Polymers

Thermoset polymers, which are represented around 80% of the market of reinforced polymers [31] [22], are the greatest commercial use for composites. They are created through the crosslinking of the molecules as shown in Figure 13, creating a rigid, three-dimensional structure. Because of this chemical reaction, the polymer cannot be reformed after curing. The polymer precursors are typically supplied in liquid (A Stage) or partially cured but malleable (B-Stage) form before curing and are then molded into form. The cure is then typically induced by heat, lending the name to this class of polymers.

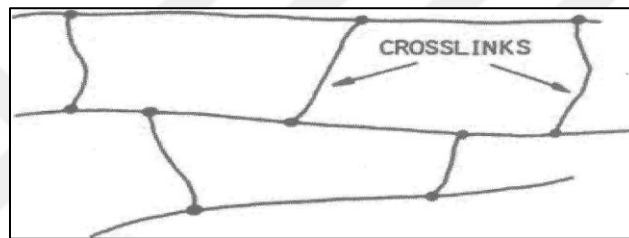


Figure 13. Chemical Crosslinking Results in The Permanent Curing of a Thermoset Composite.

High-performance thermoset materials typically require an elevated temperature to polymerize fully. Higher temperature accelerates the chemical reaction occurring in a thermoset. Although the irreversible chemical reaction prevents the recycling of thermosets, it lends certain advantages to this class of polymers. This rigid cross-linking provides higher thermal and chemical stability. Thermosets suffer minimal softening at elevated temperatures below the glass transition temperature, leading to lower stress relaxation and creep, two-time dependent problems which can lead to unintended changes in part geometry. Additionally, this rigid crosslinking prevents a chemical attack from many aerospace solvents which could degrade the material properties.

All in all, the most famous thermoset polymer for high-performance composites is epoxy due to its excellent mechanical and chemical properties. Other advantages of epoxy are the absence of volatiles through cure and low shrinkage after cure, outstanding opposition to chemicals and solvents as well as outstanding adhesion to glass and carbon fibers. The main weaknesses are reasonably high cost and long cure time. Epoxy-based composites are principally used in aircraft and space applications. The polyester and vinyl-esters resins are generally used in automotive, marine, chemical, and electrical

applications. Note that once cured, the reaction of thermosets cannot be reversed and the cured polymer will have the same shape. If heated, they will burn rather than melt [28].

2.7.2.1.2. Thermoplastic Polymers

Thermoplastic polymers, as the name suggests, soften and become highly malleable with the application of heat and become a solid after cooling. This is possible because the individual molecules are linear in structure and not chemically linked to one another, but instead held together by weak secondary bonds (as shown in Figure 14, right). These bonds can then be broken by the application of heat, allowing the molecules to flow relative to one another. When the heat is removed, and the part cools, the molecules freeze in their new positions as the secondary bonds are restored. This reversible process subsequently means that a thermoplastic polymer can be heat softened, melted, and reformed as many times as desired.

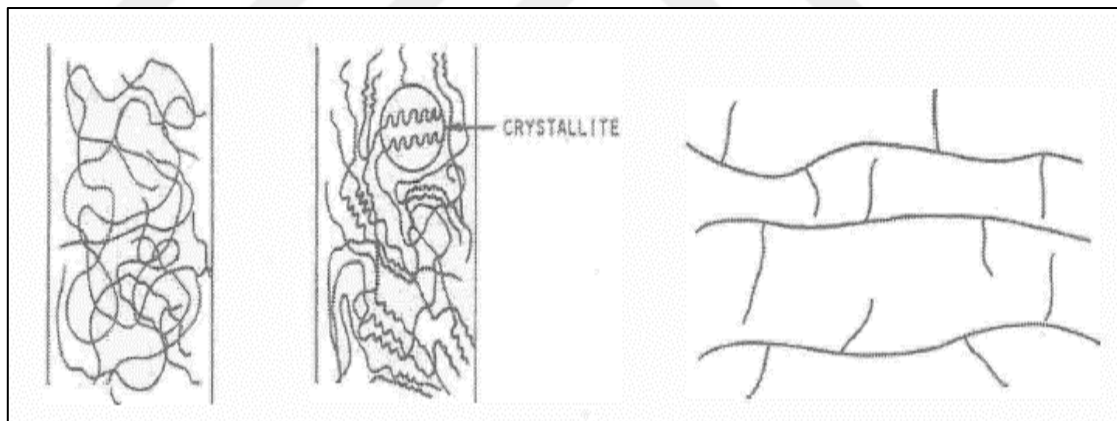


Figure 14: Thermoset Polymers are Amorphous (Left) while Thermoplastics are Typically Semi-Crystalline (Center), But Do Not Have Chemical Cross-Linking (Right).

Thermoplastics have an infinite shelf life. Sheets of thermoplastic or thermoplastic prepreg can be created and stored at room temperature until they are needed. Since the plastic is solid at this temperature, handling is also easier as the material is not tacky like pre-cured thermosets, nor is it a spoilable liquid. Additionally, parts can more easily be repaired by welding of the plastic through heat or solvents as opposed to requiring a carefully prepared bonded repair on thermosets. Finally, parts can be recycled through standard means of melting and recovering the raw materials. Thermoplastics, due to their

weaker molecular structure, also tend to be more ductile compared to thermosets. This yields higher impact strength as energy can be absorbed through plastic deformation of the matrix as opposed to fracture and delamination. Additionally, this ductility tends to create better fracture resistance, helping to prevent the critical damage of delamination. Finally, the strain to failure of thermoplastics is typically higher than that of thermosets for the same reasons.

All in all, thermoplastics will melt when heat is applied. Many consumer goods and bottles are made using thermoplastics due to their relatively simple manufacture and similarity to metal forming techniques. Additional benefits of thermoplastics comprise the greater elongation at fracture, the probability of involuntary processing, and infinite shelf life of raw materials [32].

Typical examples are nylon, polypropylene, polyethylene, PVC and ABS. The thermoplastic matrix materials that can be used in high performance composites include: thermoplastic polyesters (such as PET, PBT), polycarbonate (PC), polyamide-imide (PAI), polyether-ether ketone (PEEK), polysulfide (PSUL), polyphenylene sulfide (PPS), polyetherimide (PEI), with PEEK being the most popular one. The main advantages of the thermoplastic matrix are higher impact strength, better fracture resistant, unlimited storage (shelf-life), and post formability. Additionally, thermoplastics, with their ability to be melted, can be recycled [28].

CHAPTER THREE

THEORETICAL PART

Two types of stresses in here, normal stress and shear stress. Both can break down the bonds of a material and be a reason for material failure. The normal stress, usually symbolized as σ and referred to as tensile or compressive stress, is the applied force that effects perpendicular to the surface. For isotropic materials, this does cause a change in size of the object but does not result distortion or change in shape. As shown in Figure 15 uniaxial compressive stress will affect a bar to become shorter and wider whereas tensile stresses will elongate, but in both cases, it will persist a rectangle in cross-section.

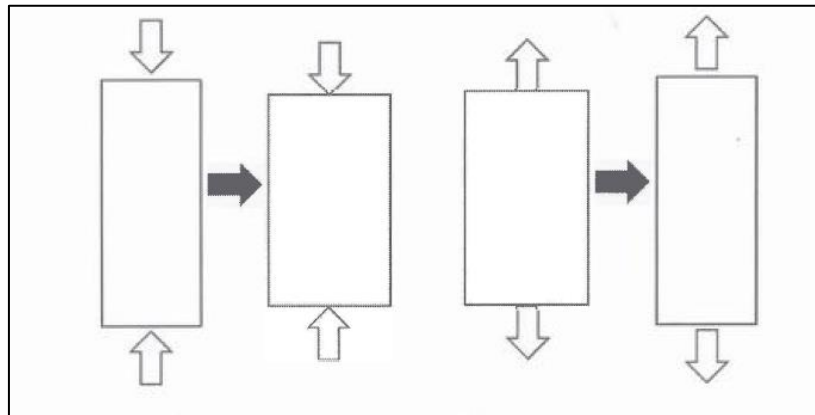


Figure 15: Normal Compressive Stress (Left) Causes A Material to Become Shorter and Wider, A Tensile Stress (Right) Lengthens and Thins Out the Material [28].

Meanwhile, shear stress, most commonly denoted as τ , acts parallel to the surface in question. For isotropic materials, this will result in a change in shape or distortion see

Figure 16. For example, a plate that is subjected to a pure shear stress will change from a square to a parallelogram.

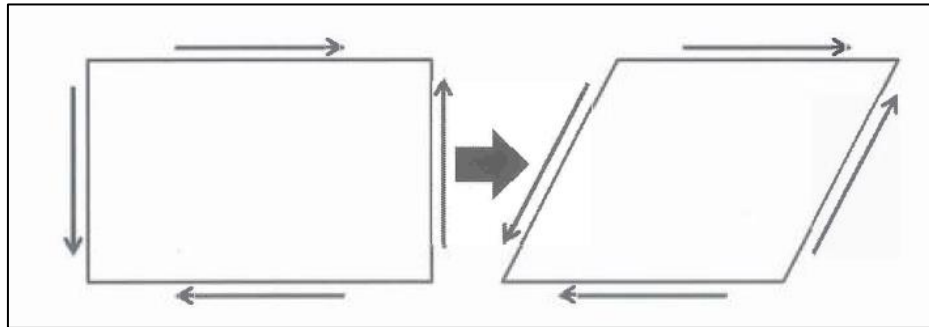


Figure 16: Shear Stresses Result in a Change in Shape [28].

These two kinds of stresses in this study have been applied to the chosen composites through a specific stacking sequence for all to examine the behavior of each according to three different failure theories and a comparison has been conducted:

- 1- For the composite materials to analyze the progressive failure and the mood of failure for each ply.
- 2- The effect of using different failure theories and making a comparison to assist those theories.

3.1. Introduction

In this study, three composite materials have been chosen according to their contributions to wind blade, aerospace industry. IM7-977-3 was taken for the increased application of composite materials in large vehicle structures considerations [33] [34]. The as4-3501-6 composite material has been used in the aircraft and sporting industries with typical products usually involving thin sections with tensile loadings [35] [36]. AS4-8552 is also considered one of the commonly used materials in aircraft, wind energy industry [37]. Auto disk “Helius composite” software has been used. The program is mean to predict laminate failure, once the loads on a section of the laminate are known. Its calculation depends on classical laminate theory **CLT**. For simple geometries and it may be clear what the loading is while for more complicated geometries. The program may be

used as part of a larger calculation to investigate for failure at critical points in the structure.

3.1.1. Why Helios Composite?

The tools in Autodesk Helios PFA and Autodesk Helios Composite allowed us to think outside the box. We were able to leverage the experimental data we had to predict the performance of the composite material we needed¹. Autodesk solutions help NASA CoEx team explore new composite materials virtually while saving time and cost. Composites for Exploration (CoEx), part of the National Aeronautics and Space Administration's (NASA) Advanced Exploration Systems initiative, develops out-of-autoclave composite materials and structures for the next generation of the agency's heavy-lift launch vehicles. The project is intended to enable significant savings in weight and lifecycle cost, while also developing technology NASA engineers can use to produce the largest composite aerospace structures ever made. A common issue that composite engineers face is finding material property data necessary for analysis and simulation. Often, published material data is missing required properties, or resultant lamina data is needed to explore different combinations of composite constituents. CoEx engineers looked for a practical software solution that could give them an accurate, repeatable way to take the information they had and then obtain the data they needed. They decided to take a two-step approach using Autodesk^{Helios} PFA and Autodesk^{Helios} Composite. Through this approach, the CoEx engineers would use a micromechanics-based method to first extract the constituent properties of materials A and B and then apply them to determine the resultant properties of their desired layup. The researchers then can use Autodesk Helios Composite software to apply the extracted constituent properties and calculate the resultant properties of their desired laminate. They also were able to add the new fiber and resins quickly and easily to their existing material database. Also, it can be used Autodesk Helios Composite software to reconstruct laminas A and B to assess the

¹ **Terry Fan**
NASA's Goddard Space Flight Center.

accuracy of the process. The resulting lamina properties predicted by Autodesk Heliu Composite were, on average, within 1.7 percent of the measured values on data sheets A and B. This gave the researchers confidence to use the derived constituent properties to estimate properties for the desired composite layup. The calculated properties were deemed reasonable, and then used for analysis until test data became available [38].

3.2. Stacking Sequence

Is the order that we lay up the plies at a certain angle to create the desired thickness of the laminate. Stacking sequence that is closer to symmetric has higher material properties and lower residual stresses. Stacking sequence with (0,45, -45,90) s has been adopted for composite materials that are used in this work as shown in Figure 17. From a design standpoint, this is optimal as the residual stresses tend to cause delamination. Meanwhile, a higher modulus is obviously desirable from a design standpoint.

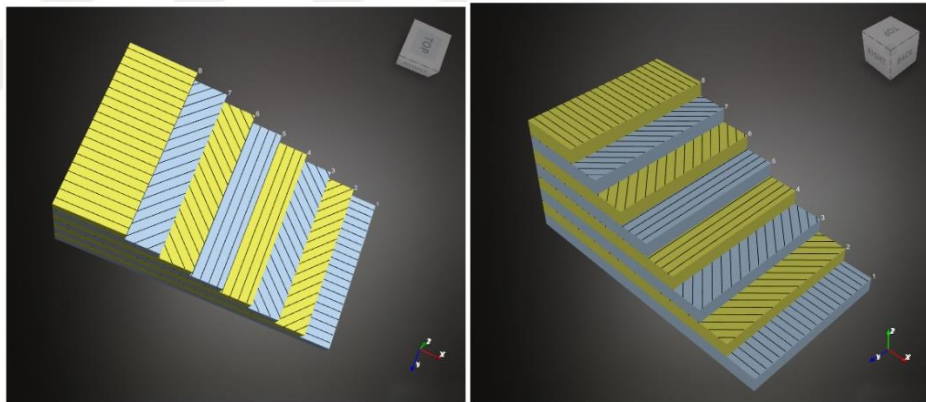


Figure 17: Composite Layers.

3.3 Global Coordinates and Local Coordinates

Continuous fiber composites are utilized, with the fibers running the full length of the part. To appropriately describe the orientation of each ply in a composite laminate, a coordinate system is defined and shown in Figure 18. The global coordinate is the X direction that is located parallel to the direction of loading and Y is perpendicular to the X direction. Meanwhile, each ply has a local coordinate system, denoted by 1 and 2, where the one direction runs parallel to the fibers, and the two directions are perpendicular to the

fiber (1) direction. Each ply is subsequently described by the angle between this X direction and the one direction. For example, when the two align, the ply is considered as 0 ply, when they are perpendicular; it is a 90 ply [28].

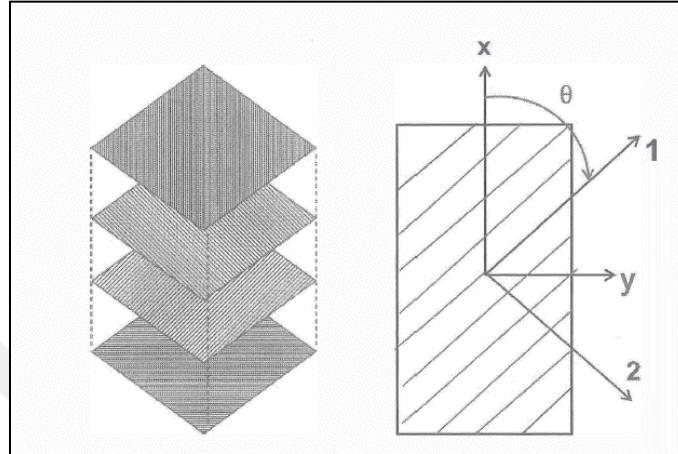


Figure 18: The Plies (Laminas) are Stacked Together to Form a Laminate (Left), Coordination of The Axes for Each Ply and The Angle is Shown at Right [28].

3.4. CLT (classical laminate theory)

Classical Lamination Theory (CLT) is a theory for predicting the relationship between the forces and moments applied to a laminate and the resultant strains and curvatures based on the properties of the individual plies. This theory is based on the plane-stress formulation of Hooke's law for a single ply in arbitrary (x-y) coordinates as well as Kirchhoff's hypothesis for a thin plate. The Kirchhoff hypothesis assumes the straight lines that are normal to the mid-surface remains straight and normal to the mid-surface after deformation, as in Figure 19.

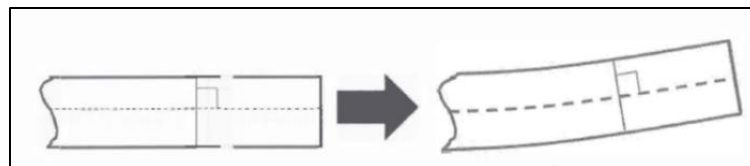


Figure 19: Kirchhoff's Hypothesis Requires Normal to The Mid-Plane Remains Normal to The Mid-Plane During Bending [28].

This suggests that the transverse shear strains are zero, $\gamma_{xz} = \gamma_{yz} = 0$, which is a good approximation only for a thin plate. In thick plates, the transverse strains are

sufficiently large to cause the normal to rotate away from the 90 degrees and a higher order; shear the deformable theory must be used. To be considered as a thin plate, the length a and the width b must be at least 10 times greater than its thickness h , that is $a > 10h$ and $b > 10h$. Furthermore, it is assumed that the plies are perfectly bonded together, the ply materials are linear elastic, and the resulting laminate strains are small. There are no boundary conditions involved in the theory [37].

3.5. CLT Equations:

Based on the above assumptions, results of the CLT equations can be derived as follows for the combined mechanical, thermal and moisture loads [28]:

$$\begin{array}{c}
 \begin{bmatrix} N_x \\ N_y \\ N_{xy} \\ M_x \\ M_y \\ M_{xy} \end{bmatrix} + \begin{bmatrix} N_x^T \\ N_y^T \\ N_{xy}^T \\ M_x^T \\ M_y^T \\ M_{xy}^T \end{bmatrix} + \begin{bmatrix} N_x^m \\ N_y^m \\ N_{xy}^m \\ M_x^m \\ M_y^m \\ M_{xy}^m \end{bmatrix} = \begin{bmatrix} A_{11} & A_{12} & A_{16} & B_{11} & B_{12} & B_{16} \\ A_{12} & A_{22} & A_{26} & B_{12} & B_{22} & B_{26} \\ A_{16} & A_{26} & A_{66} & B_{16} & B_{26} & B_{66} \\ B_{11} & B_{12} & B_{16} & D_{11} & D_{12} & D_{16} \\ B_{12} & B_{22} & B_{26} & D_{12} & D_{22} & D_{26} \\ B_{16} & B_{26} & B_{66} & D_{16} & D_{26} & D_{66} \end{bmatrix} \begin{bmatrix} \epsilon_x^0 \\ \epsilon_y^0 \\ \gamma_{xy}^0 \\ k_x \\ k_y \\ k_{xy} \end{bmatrix} \quad (1) \\
 \begin{array}{c}
 \text{In plane} \\
 \text{forces} \\
 + \\
 \text{moments} \\
 \\
 \text{thermal} \\
 \text{ef} \\
 \text{fect} \\
 \text{forces} \\
 + \\
 \text{thermal} \\
 \text{ef} \\
 \text{fect} \\
 \text{moments} \\
 \\
 \text{moisture} \\
 \text{ef} \\
 \text{fect} \\
 \text{forces} \\
 + \\
 \text{moisture} \\
 \text{endused} \\
 \text{moments} \\
 \\
 \underbrace{\begin{bmatrix} A_{11} & A_{12} & A_{16} \\ A_{12} & A_{22} & A_{26} \\ A_{16} & A_{26} & A_{66} \end{bmatrix}}_{\begin{bmatrix} [A] \\ [B] \end{bmatrix}} \quad \underbrace{\begin{bmatrix} B_{11} & B_{12} & B_{16} \\ B_{12} & B_{22} & B_{26} \\ B_{16} & B_{26} & B_{66} \end{bmatrix}}_{\begin{bmatrix} [B] \\ [D] \end{bmatrix}} \\
 \text{sreain} \\
 + \\
 \text{curvature}
 \end{array}
 \end{array}$$

Where:

[A] is called the extensional stiffness matrix.

[D] is the bending stiffness matrix.

[B] is the coupling stiffness matrix.

[A] extensional stiffness matrix equation has been driven from:

$$[A] = \sum_{k=1}^n [\bar{Q}]_k (Z_k - Z_{k-1}) \quad (2)$$

[B] the bending-extension coupling stiffness matrix equation has been driven from:

$$[B] = \frac{1}{2} \sum_{k=1}^n [\bar{Q}]_k (Z_k^2 - Z_{k-1}^2) \quad (3)$$

[D] the bending stiffness matrix equation has been driven from:

$$[D] = \frac{1}{3} \sum_{k=1}^n [\bar{Q}]_k (Z_k^3 - Z_{k-1}^3) \quad (4)$$

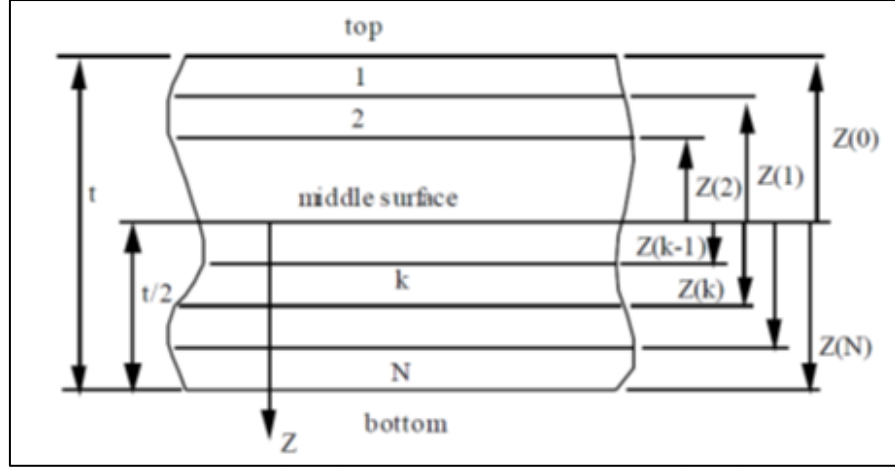


Figure 20: Z is measured from the geometric mid-plane, with the positive direction being downwards.

Z is measured from the mid-plane, as shown in the Figure 20 [28].

Z is negative above the mid-plane and positive below the mid-plane.

Z_k it is the interfaces between plies.

Z_0 referring to the distance from the upper surface to the midplane.

Z_n referring to the lower surface of the nth ply.

n is the total number of plies.

From the equations (2), (3), (4)

$[\bar{Q}]$ is a 3x3 matrix representing the plane stress (or reduced) stiffness matrix for a material ply in a laminate where: $\{\sigma\} = [\bar{Q}]\{\varepsilon\}$

$\{\varepsilon\}$ =global strain

$\{\sigma\}$ =global stress

Where:

$$\text{Transformed Stiffness Matrix}[\bar{Q}] = \begin{bmatrix} \bar{Q}_{11} & \bar{Q}_{12} & \bar{Q}_{16} \\ \bar{Q}_{21} & \bar{Q}_{22} & \bar{Q}_{26} \\ \bar{Q}_{61} & \bar{Q}_{62} & \bar{Q}_{66} \end{bmatrix} \quad (5)$$

To obtain the components of $[\bar{Q}]$ matrix from the next illustrated equations: [39]

$$\bar{Q}_{11} = Q_{11} \cos^4 \theta + 2(Q_{12} + 2Q_{66}) \sin^2 \theta \cos^2 \theta + Q_{22} \sin^4 \theta \quad (6)$$

$$\bar{Q}_{11} = Q_{11} \cos^4 \theta + 2(Q_{12} + 2Q_{66}) \sin^2 \theta \cos^2 \theta + Q_{22} \sin^4 \theta \quad (7)$$

$$\overline{Q_{12}} = \overline{Q_{21}} = (Q_{11} + Q_{22} - 4Q_{66})\sin^2\theta\cos^2\theta + Q_{12}(\sin^4\theta + \cos^4\theta) \quad (8)$$

$$\overline{Q_{22}} = Q_{11}\sin^4\theta + 2(Q_{12} + 2Q_{66})\sin^2\theta\cos^2\theta + Q_{22}\cos^4\theta \quad (9)$$

$$\overline{Q_{16}} = \overline{Q_{61}} = (Q_{11} - Q_{12} - 2Q_{66})\sin\theta\cos^3\theta + (Q_{12} - Q_{22} + 2Q_{66})\sin^3\theta\cos\theta \quad (10)$$

$$\overline{Q_{26}} = \overline{Q_{62}} = (Q_{11} - Q_{12} - 2Q_{66})\sin^3\theta\cos\theta + (Q_{12} - Q_{22} + 2Q_{66})\sin\theta\cos^3\theta \quad (11)$$

$$\overline{Q_{66}} = (Q_{11} + Q_{22} - 2Q_{12} - 2Q_{66})\sin^2\theta\cos^2\theta + Q_{66}(\sin^4\theta + \cos^4\theta) \quad (12)$$

Note that

$$\overline{Q_{16}} = 0 \text{ and } \overline{Q_{26}} = 0 \text{ only if } \theta = 0 \text{ or } \theta = 90$$

3.6. An Important Assumptions and Work Simplifications

- 1- Assume that the composites are symmetric laminates, $[B] = 0$, and extensional forces will result in extensional strains only. However, for an unsymmetrical laminate, $[B]$ is non-zero and extensional forces will result in a curvature. Similarly, bending moments can create extensional in-plane strains in an unsymmetrical laminate as well. This coupling effect is not desirable and should be eliminated by designing asymmetric laminate.
- 2- Matrix $[A]$ is independent of stacking sequence. The sequence in which the plies are laid does not change the value of $[A]$. As a result, the extensional stiffness does not depend on the order a laminate is assembled.
- 3- Both the $[B]$ and $[D]$ matrices are strongly dependent upon stacking sequence as the expressions $(Z_k^2 - Z_{k-1}^2)$ and $(Z_k^3 - Z_{k-1}^3)$ are present.
- 4- No moment applied on the composites.
- 5- No thermal effects on the composites.
- 6- No moisture effects on the composites.

- 7- Balancing a laminate serves to make $A_{16} = A_{26} = 0$. This occurs because $\sin(-\theta) = -\sin\theta$, and $\cos(-\theta) = \cos\theta$, which cause the \overline{Q}_{16} , \overline{Q}_{26} terms for a $+\theta$ ply to be equal and opposite to those of a $-\theta$ ply.

3.7. Failure Criteria

In the following, three exact failure standards of the diagonally isotropic fiber combined case will give.

The three criteria are:

- 1- Hashin Criterion.
- 2- Christensen Criterion.
- 3- Maximum Stress Criterion.

The purpose of giving these three mainstream theories rather than just one is to show the variety of effects and interpretations that are possible.

3.7.1. Hashin Criterion

In this criterion, the failure modes decayed to matrix controlled and fiber controlled groups, reliant to which pressure modules act on the failure planes, these planes being taken parallel and perpendicular to the fiber direction, correspondingly. The entire modes more decayed into tensile controlled and compressive controlled forms, with several of the same terms appearing in each [40]. In Hashin criterion four different modes of failure have been identified for the composite material: compressive fiber failure, tensile fiber failure, tensile matrix failure, and compressive matrix failure.

If $\sigma_{11} \geq 0$, the Tensile **Fiber** Failure Criterion is:

$$F_f^+ = \left(\frac{\sigma_{11}}{S_{11}^+}\right)^2 + \alpha \left(\frac{\sigma_{12}}{S_{12}^+}\right)^2 \geq 1.0 \quad (13)$$

If $\sigma_{11} < 0$, the Compressive **Fiber** Failure Criterion is:

$$F_f^- = \left(\frac{\sigma_{11}}{S_{11}^-}\right)^2 \geq 1.0 \quad (14)$$

If $\sigma_{22} \geq 0$, The Tensile Matrix Failure Criterion is:

$$F_m^+ = \left(\frac{\sigma_{22}}{S_{22}^+}\right)^2 + \left(\frac{\sigma_{12}}{S_{12}^+}\right)^2 \geq 1.0 \quad (15)$$

If $\sigma_{22} < 0$, the Compressive **Matrix** Failure Criterion is:

$$F_m^- = \left(\frac{\sigma_{22}}{2S_{23}} \right)^2 + \left[\left(\frac{S_{22}^-}{2S_{23}} \right)^2 - 1 \right] \frac{\sigma_{22}}{S_{22}^-} + \left(\frac{\sigma_{12}}{S_{12}} \right)^2 \geq 1.0 \quad [2] \quad (16)$$

Note that, the Hashin equations include two user-specified parameters (α and S_{23}).

- α - User-specified coefficient that determines the contribution of the longitudinal shear stress to fiber tensile failure. Allowable range is $(0.0 \leq \alpha \leq 1.0)$, and the default value in the software that has been used is $\alpha = 1$.
- S_{23} - Transverse shear strength of the composite material in the (23) plane [41]. And the default value in the software that has been used is $S_{23} = 76.91 \text{MPa}$.

3.7.2. Christensen Criterion

The transverse shear stress failure property, S_{23} is not involved here, it was in fact eliminated by requiring the independence to hydrostatic pressure. If σ_{22} and σ_{33} are small compared with σ_{11} , then fiber mode just becomes the maximum stress criterion in the fiber direction. While the Hashin criterion shows no interaction at all between them [40], the Christensen criterion uses the following fundamental strengths of the composite material are listed to recognize two different failure modes: matrix failure and fiber failure.

The matrix failure criterion is

$$\left(\frac{1}{S_{22}^+} - \frac{1}{S_{22}^-} \right) (\sigma_{22} + \sigma_{33}) + \frac{1}{S_{22}^+ S_{22}^-} (\sigma_{22} + \sigma_{33})^2 + \frac{1}{S_{23}^2} (\sigma_{23}^2 - \sigma_{22} \sigma_{33}) + \frac{1}{S_{12}^2} (\sigma_{12}^2 + \sigma_{13}^2) \geq 1.0 \quad (17)$$

Where the transverse shear strength S_{23} is supposed to satisfy

$$S_{23} \geq \frac{1}{2} \sqrt{S_{22}^+ S_{22}^-} \quad (18)$$

The fiber failure criterion is

$$\left(\frac{1}{S_{11}^+} - \frac{1}{S_{11}^-} \right) \sigma_{11} + \frac{\sigma_{11}^2}{S_{11}^+ S_{11}^-} \geq 1.0 \quad [41] \quad (19)$$

3.7.3. Maximum Stress Criterion

The simplest theory ignores any interaction between the normal principal stresses and assumes that failure occurs when either of the normal stresses exceeds the ultimate

stress. This failure criterion is perfect for brittle materials and should not use for ductile material like steel, aluminum, and plastics [42].

The Max Stress Criterion identifies three possible failure modes: Longitudinal Failure, Transverse Failure, or Shear Failure.

$$\text{Longitudinal Failure occurs whenever } \sigma_{11} \geq S_{11}^+ \text{ OR } \sigma_{11} \leq S_{11}^- \quad (20)$$

$$\text{Transverse Failure occurs whenever } \sigma_{22} \geq S_{22}^+ \text{ OR } \sigma_{22} \leq S_{22}^- \quad (21)$$

$$\text{Longitudinal Shear Failure occurs whenever } |\sigma_{12}| \geq |\sigma_{12}^{max}| \quad (22)$$

$$\text{Failure Index} = \text{Max. Absolute Value of } \left(\frac{\sigma_{11}}{S_{11}^+}, \frac{\sigma_{11}}{S_{11}^-}, \frac{\sigma_{22}}{S_{22}^+}, \frac{\sigma_{22}}{S_{22}^-}, \frac{\sigma_{12}}{S_{12}^-} \right) \quad (23)$$

Since the failure index is a simple stresses ratio, the failure load can be determined by just dividing the applied load by the failure index.

Where:

S_{11}^+ = Value of σ_{11} at longitudinal tensile failure.

S_{11}^- = Value of σ_{11} at longitudinal compressive failure.

S_{22}^+ = Value of σ_{22} at transverse tensile failure.

S_{22}^- = Value of σ_{22} at transverse compressive failure.

S_{12} = Absolute value of σ_{12} at longitudinal shear failure.

S_{23} = Absolute value of σ_{23} at transverse shear failure.

The three failure criteria just given show the variety of physical effects which can or may occur. These three approaches are interrelated. The second criterion is the simplest of the three. All three criteria are serious, well-considered efforts, and their differences reflect the complexity of the program to determine failure criteria [40].

3.8. Failure Criteria Similarities

The similarities of the three criteria are that they all show an asymmetry in uniaxially tensile and compressive strengths, and they all show a sensitivity to mean normal stress. One of their differences is that of the way fiber direction uniaxial stress σ_{11} interacts with fiber direction shear stress σ_{12} . The Hashin criterion has them interacting when σ_{11} is tensile but not when it is compressive. The Christensen criterion states that the shear stress σ_{12} has a negligible effect on the fiber direction strength, for very strong fiber systems in which there is no rotation of the fiber direction [40].

CHAPTER FOUR

METHODOLOGY

4.1. Introduction

In this chapter the analysis that have been done on the composite materials have been presented. Comparisons of composites behavior under tests have been done by using figures and tables for more clear and comprehensive understanding of the behavior of each composites.

4.2. Description of the Work

Micromechanics uses some expressions to describe the part that has been dealing with, starting from fiber and matrix that form a lamina or ply. A group of plies form a laminate which is used to build a composite structure Figure 21.

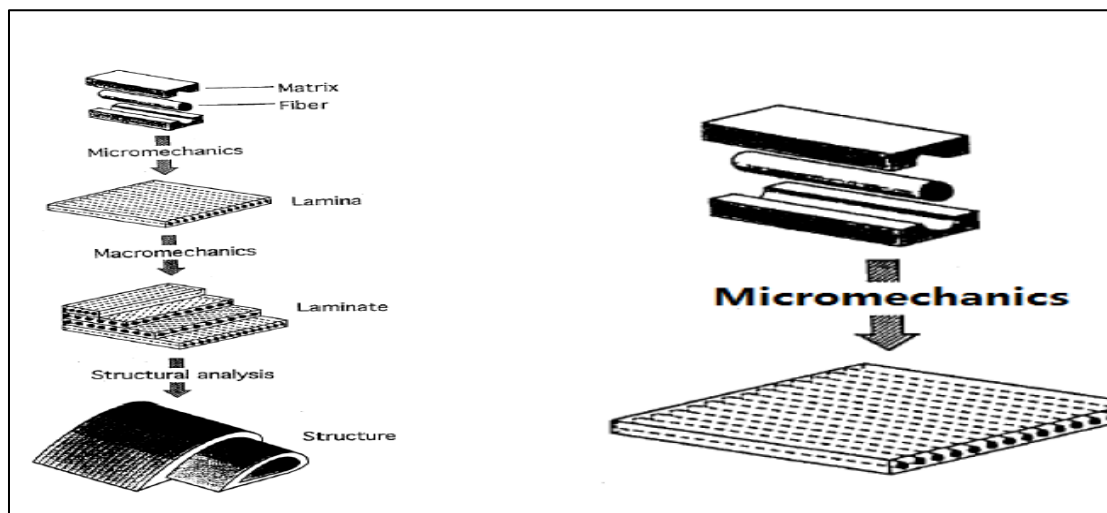


Figure 21: Micromechanics Levels [43].

Eight plies have been chosen in this study with a thickness of 0.25mm for each ply in a stacking sequence as shown in Figure 22 to form a symmetric laminate for all the composite materials in this work. mechanical properties of the three composites have been calculated by the Auto desk Heliux composite version 2017 software like Young's Modulus, Shear Modulus, Poisson's ratio, volume fraction, density, yield stress and strain in the (1,2,3) planes as shown in Figure 23.

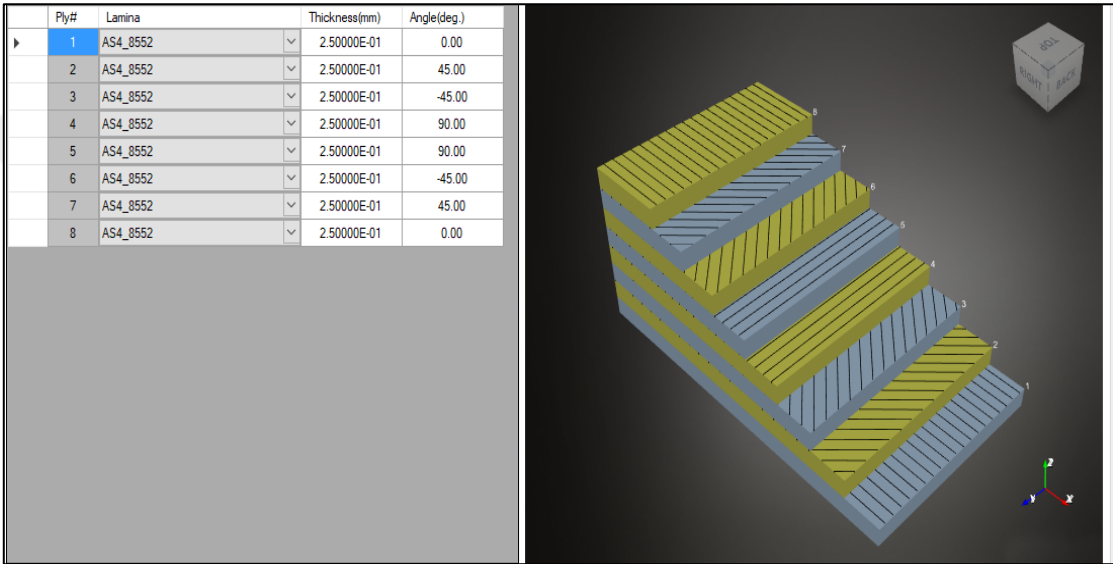


Figure 22: Composite Laminate Plies with Stacking Sequence.

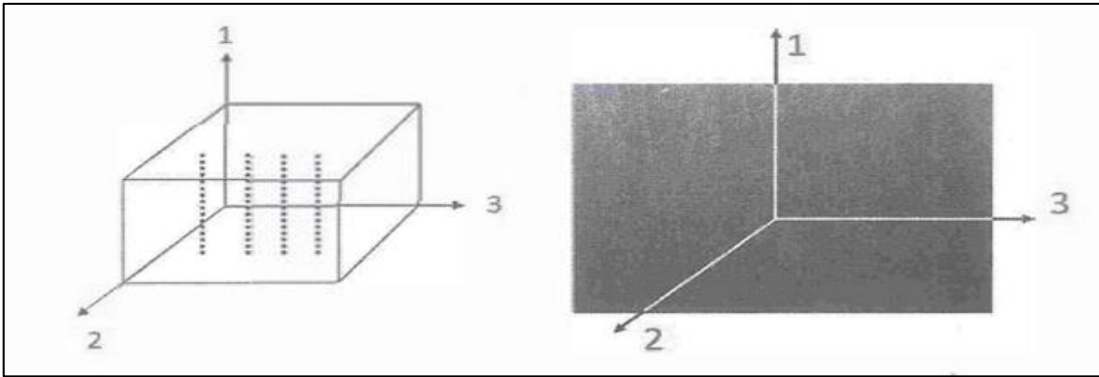


Figure 23: The Three Orthogonal Planes.

The program depends on classical laminate theory (CLT) to predicate the failure behavior of composite materials. Two types of stresses have been applied to the composites axial load on the X-direction and shear load on the XY-direction respectively

as shown in Figure 24. For each type, a failure prediction has been investigated by using three failure criteria to find out the failure behavior for each composite and the effect of each failure criteria on the failure prediction for a certain composite. Comparisons have been made for the results for best comprehensive understanding of the three composites under these conditions.

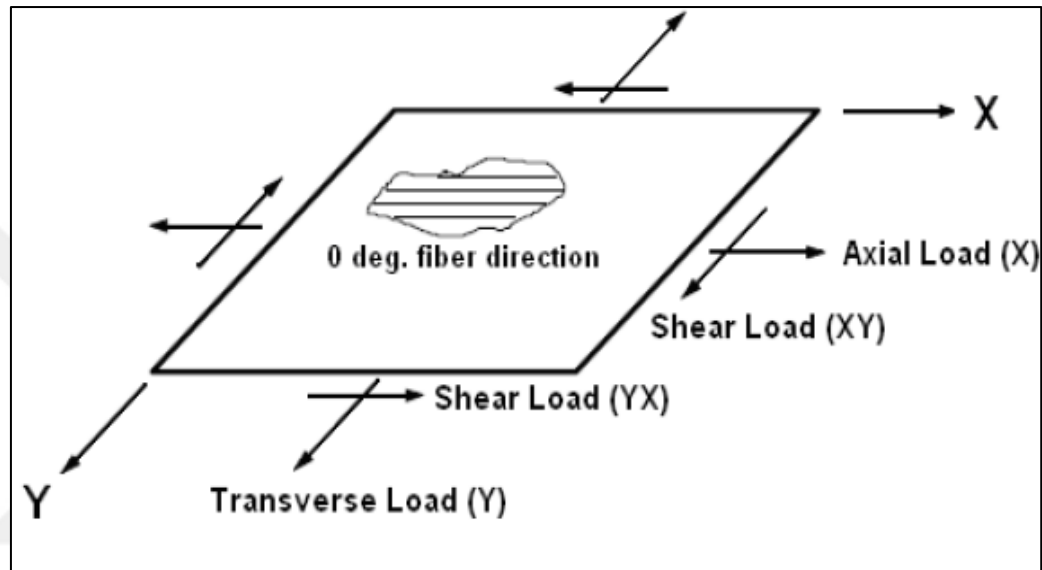


Figure 24: Coordinates System and Loads Directions Definitions.

4.3. Work organization

Three composite materials have been chosen carefully in this study so that they commonly used in wing and wind blade manufacturing to fulfill an investigation to find out their properties, their failure behavior, their failure mood sequence, permissible axial load for each, permissible shear load for each, failure envelope for each. A comparison has been made to show in a simple presentation the limits of each.

Three failure criteria have been chosen to do the investigations which are (maximum stress, Christensen, and Hashin) criteria. Investigations have been done to find out the effect of each criterion on the composites and the differences between the chosen criteria itfelfes. A stacking sequence has been selected to make a laminate of 8 plies (laminas) with symmetric stacking sequence (0, +45, -45, and 90) s for all the three composites in this study with (0.25mm) ply thickness to make laminate of (2mm) thickness.

An axial load stress in the global X-direction (S_{11} -direction), as in Figure 24, has been applied on each composite gradually until the first ply failure has done and keeps loading the laminate until the full composite failure has done.

A pure shear load stress in the XY-plane direction (S_{12} -direction), as in Figure 24, has been applied on each composite gradually until the first ply failure has done and keeps loading the laminate until the full failure has done. Results have presented in this study as three groups: -

1st group is the pure axial load analysis. It consists of two categories:

1st category is to discuss failure mood sequence for all the chosen composites by using a specific failure criterion and make a comparison of the composites behavior for each criterion separately. **2nd category** is to discuss failure mood sequence for a specific composite using the three failure criteria and make a comparison to find out the effect of each failure criterion on each composite separately.

The 2nd group is the failure envelope analysis. It consists of four categories:

1st category is the failure envelope analysis between (S_{11}, S_{22}) that has been done for the three composites with a specific failure criterion for each time. **2nd category** is the failure envelope analysis between (S_{11}, S_{22}) that has done for a specific composite by using the three failure criteria. **3rd category** is the failure envelope analysis between (S_{11}, S_{12}) that has been done for the three composites with a specific failure criterion for each time. **4th category** is the failure envelope analysis between (S_{11}, S_{12}) that has done for a specific composite by using the three failure criteria.

3rd group is the pure shear load analysis. It consists of one category which is:

1st category is about discussing a failure mood sequence for all the chosen composites by using a specific failure criterion separately. It is worthy to notice that by applying a pure shear load, there are no differences in the values of first ply failure values and entirely failure values by changing failure criteria. Therefore, permissible shear stress, first plies failure, and entirely failure have the same values for a specific composite although by using different failure criterion as in Figure (44, 45, and 46). In the present study, Auto Desk Helius Composite Software has been used to do the investigations about the mechanical properties of the chosen composites by using three failure criteria to find

out the comparison and the behavior differences between the failure theories and the composites themselves.

QBlade software version 0.963 has been used to find out the force that has been generated from a wind turbine. For that, a SANDIA_SERI-8 model of wind blade has been adopted in this study to make a simulation for a wind turbine unit where SANDIA_SERI-8 model blade is working under a steady wind speed 15m/s with total simulation time $t = 6.403\text{sec}$. The spar of the blade has been assumed that it carries all the load. QBlade has calculated the normal total aerodynamic load on the blade. Its maximum value has been found when the simulation time step $t = 0.178\text{sec}$, the total normal force = 11000N. This force is acting of the aerodynamic center of the blade. Shifting of this load has been done to the center of the spar to find out the effect of a specific wind speed on each composite and findout the deflection due to this load for each composite.

4.4. Pure Axial Load Analysis

4.4.1. Failure Mood Analysis According Different Failure Criterion

In this section, the effect of each failure criteria has discussed. Mood failure for each composite material has discussed, and comparison has been made to show precisely what the differences between the criteria that have been chosen.

Table 2: Failure Mood Definitions in the Study Tables Below.

Failure Modes	1	2	3
Failure Criteria			
Max Stress	Transverse Failure	Shear Failure	Longitudinal Failure
Hashin	Matrix Failure	Fiber Failure	
Christensen	Matrix Failure	Fiber Failure	

Table 3: Failure Mood Sequence of the Three Composites at Maximum. Stress Criterion.

	SIGMA _x (MPa)	EPSILON _x (mm/mm)	Failed Ply Number(s)	Failure Modes
	681	0.0115	4.5	1.1
im7-977-3	725	0.0134	2.3.6.7	2.2.2.2
	884	0.0163	1.8	3.3
	483.84	0.00961932	4.5	1.1
AS4-8552	824.32	0.0163885	1.8	3.3
	896	0.0196921	2.3.6.7	2.2.2.2
	241.265	0.00491843	4.5	1.1
AS4-3501-	456.09	0.0106188	2.3.6.7	1.1.1.1
	661	0.0153915	1.8	3.3

It is obvious from Table 3, Figure 25 that IM7-977-3 first ply failure has been done at 681MPa for (90^0) which is the weakest plies for the axial load by transverse failure mood. ($\pm 45^0$) plies were starting to fail by shear failure mood at 725MPa. (0^0) plies were carrying the load until they have been failed by longitudinal failure mood with 884MPa axial load with a different slope as shown in Figure 25.

For AS4-8552, first ply failure was (90^0) with 483.84MPa by transverse failure mood, which is very close to that value in Hashin, Christensen criteria. Then it takes extended limit to reach the 2nd step failure which was with (0^0) plies by longitudinal failure mood which is considered a huge difference in failure mood behavior than other failure criteria by the load 824.32MPa. ($\pm 45^0$) was the last ply failed by shear failure mood when the load has reached to 896MPa. For AS4-3501-3 as shown in Figure 25 it is clear where (90^0) plies have been failed first at 241.26MPa, which is the same value with all other criteria with transverse failure mood and have the longest limit to reach the 2nd step failure mood. For ($\pm 45^0$) plies where failed with transverse failure mood and finally to reach last ply failure at 661MPa, which is the same in all failure criteria that have studied in this work for (0^0) plies of longitudinal failure mood. What is notable to say here that, the material has been entirely failed with 661MPa without suffering from shear failure mood during its failure mood sequence.

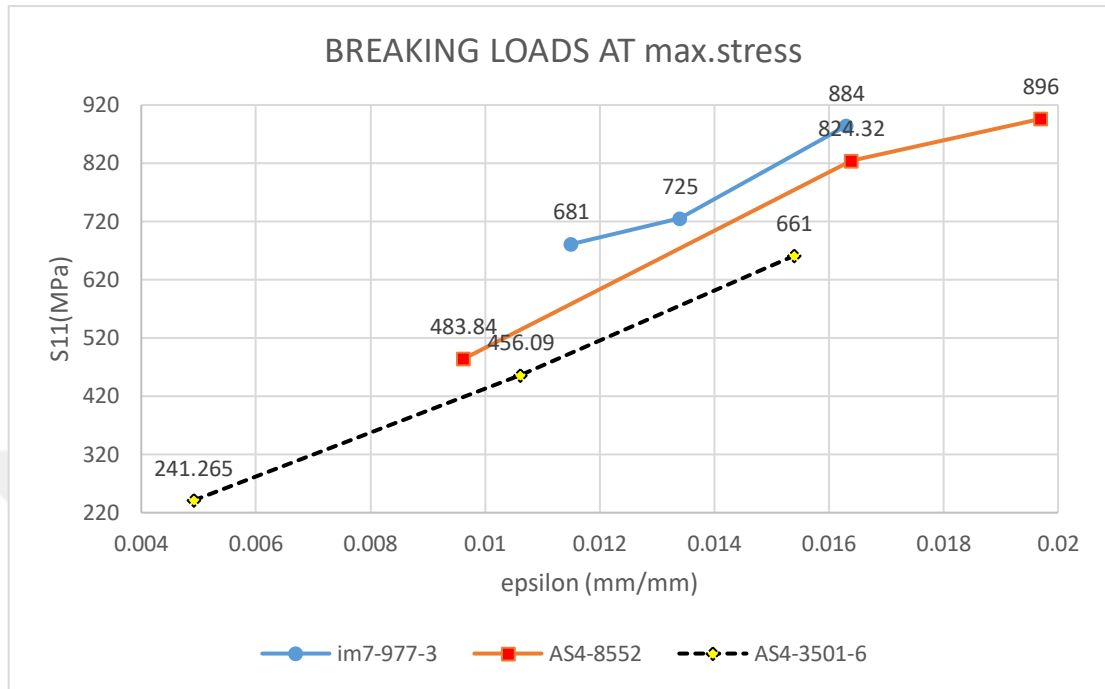


Figure 25: Failure Mood Sequence of The Three Composites at Maximum Stress Criterion.

Table 4: Failure Mood Sequence of the Three Composites at Christensen Criterion.

	SIGMAx (MPa)	EPSILONx (mm/mm)	Failed Ply Number(s)	Failure Modes
im7-977-3	587.86	0.0105156	2.3.6.7	1.1.1.1
	632.06	0.0116509	4.5	1.1
	884	0.016295	1.8	2.2
AS4-8552	479.88	0.00954059	4.5	1.1
	591.48	0.0129989	2.3.6.7	1.1.1.1
	744	0.0163515	1.8	2.2
AS4-3501-6	241.265	0.00491843	4.5	1.1
	297.45	0.00692529	2.3.6.7	1.1.1.1
	661	0.0153915	1.8	2.2

By using Christensen failure criteria, it is cleared from Table 4, Figure 26 that IM7-977-3 has matrix failure mood happened first for plies (2, 3, 6, 7) ($\pm 45^\circ$) at 587.86MPa. It is significant difference in failure mood to fail ($\pm 45^\circ$) before (90°) plies under an axial load stress. These four plies have been failed with matrix mood at the same time leaving the load increases on plies (4, 5) (90°) in the middle of the composite thickness until it

failed at 632.06 MPa with matrix mood failure too. The last ply failure has been done lastly for (1,8) (0⁰) plies by fiber failure mood when the load has reached 884MPa, which was the same full breaking load as with Hashin criteria.

AS4-8552 has been noticed from Table 4, Table 5, that this composite has the same failure mood sequence of Hashin and Christensen criteria so that the behavior of failure are the same except in the ($\pm 45^0$) plies failure load value which was 591.48MPa in Christensen if compared with 643.56MPa in Hashin for the same composite. Also, the limit failure load from 2nd step ($\pm 45^0$) plies matrix failure mood to last ply failure (1,8) (0⁰) fiber failure mood in Christensen, was longer than Hashin criteria for this composite.

It has been clear that AS4-3501-6 also has the same notes that have said about AS4-8552 comparing between Hashin & Christensen where failure criteria are entirely similar to those for AS4-3501-6 except the limit between matrix failure mood for (90⁰) and 2nd step matrix failure mood for ($\pm 45^0$) was shorter than of Hashin criteria.

To summarize all above: it has been evident from Table 4, Figure 26 that IM7-977-3 composite has three failure mood steps not like Hashin, Christensen criteria for the same composite. The ($\pm 45^0$) plies were the first plies to fail before (90⁰) plies, which have been collapsed by matrix failure mood too. If compared with that in Hashin criteria where all ($\pm 45^0$) and (90⁰) plies have been failed at the same time, same load values and same failure mood type.

For AS4-8552 and AS4-3501-6 those tow composites have the same behavior with Hashin and Christensen failure criteria. First ply failure and last ply failure having the same values and failure mood sequence for each, except that AS4-8552 has a more extended limit between matrix failure mood and fiber failure mood than AS4-3501-6. AS4-3501-6 has shorter limit between first ply failure (90⁰) matrix failure mood and 2nd step matrix failure mood of ($\pm 45^0$) plies than what has happened in Hashin failure criteria.

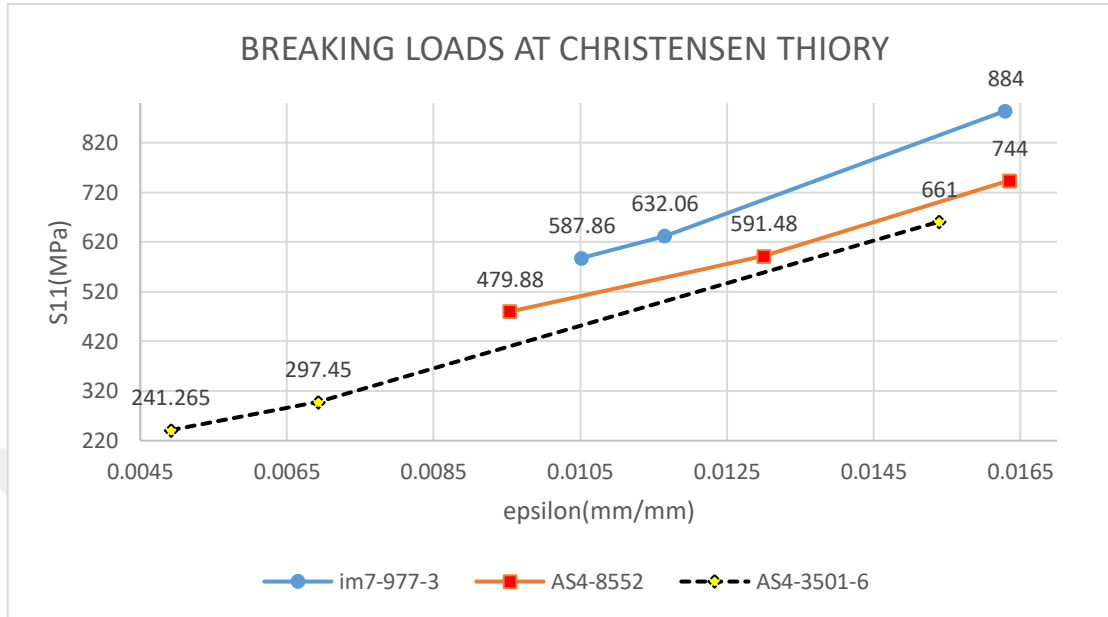


Figure 26: Failure Mood Sequence of The Three Composites at Christensen Criterion.

Table 5: Failure Mood Sequence of The Three Composites at Hashin Criterion.

	SIGMA _x (MPa)	EPSILON _x (mm/mm)	Failed Ply Number(s)	Failure Modes
im7-977-3	645.32	0.0118954	2.3.4.5.6.7	1.1.1.1.1.1
	884	0.016295	1.8	2.2
AS4-8552	479.88	0.00954059	4.5	1.1
	643.56	0.0141434	2.3.6.7	1.1.1.1
	744	0.0163515	1.8	2.2
AS4-3501-6	241.265	0.00491843	4.5	1.1
	327.195	0.00761782	2.3.6.7	1.1.1.1
	661	0.0153915	1.8	2.2

As shown in Table 5 and Figure 27 for AS4-8552 the first plies have been failed are (4,5) because (90°) plies are the weakest against the axial load stresses. The failure happened in matrix failure mood because matrix can only carry the shear load, while fiber can only carry an axial load [28], that's why matrix is very weak against the axial load. Later on, at 643.56MPa, plies (2,3,6,7) which are all (±45°) plies have been failed in the next step in matrix failure mood too. Because (±45°) have been taking the axial loads for this region until they failed at 643.56MPa. The last failure plies have been done when the

load has reached 744MPa.plies (1,8)(0⁰) plies are finally failed with fiber mood failure because they are in the same direction with the load.

AS4-3501-6 has the same failure sequence of AS4-8552 as shown in Table 5. But it is important to notice that with AS4-3501-6, the failure starting in the very early step than AS4-8552 as shown in Figure 27. at 241.26MPa and plies failed at 661MPa, unlike AS4-8552.

From Figure 27, IM7-977-3 has the highest strength than other tow composites in this study. Failure has been entirely happened within two steps only. The limit between first ply failure and last ply failure was shorter than other composites. AS4-8552, AS4-3501-6 have the same failure mood sequence, but AS4-8552 has higher strength than AS4-3501-6 with a shorter limit between first ply failure and last ply failure. In addition, AS4-8552 has a long duration between first ply failure and 2nd step failure than AS4-3501-6. Also, AS4-3501-6 has the most extended limit failure between first ply failure and last ply failure from all other composites. Also, it has a short limit between (90⁰) plies failure with (±45⁰) plies failure than others which have matrix mood failure. At the same time, the limit between matrix mood failure with fiber mood failure was longer than others.

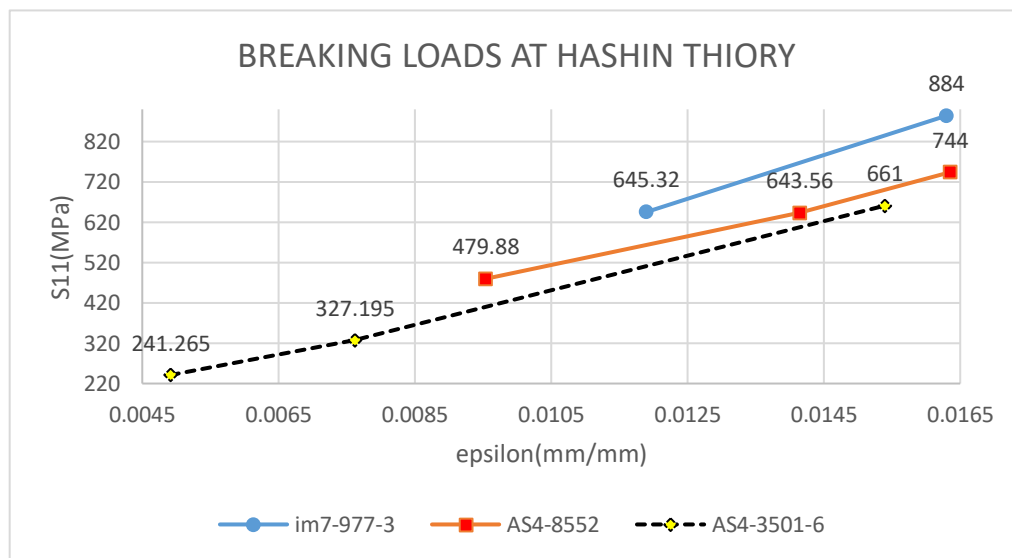


Figure 27: Failure Mood Sequence of The Three Composites at Hashin Criteria.

4.4.2. Failure Behavior of Composites with Different Failure Criteria

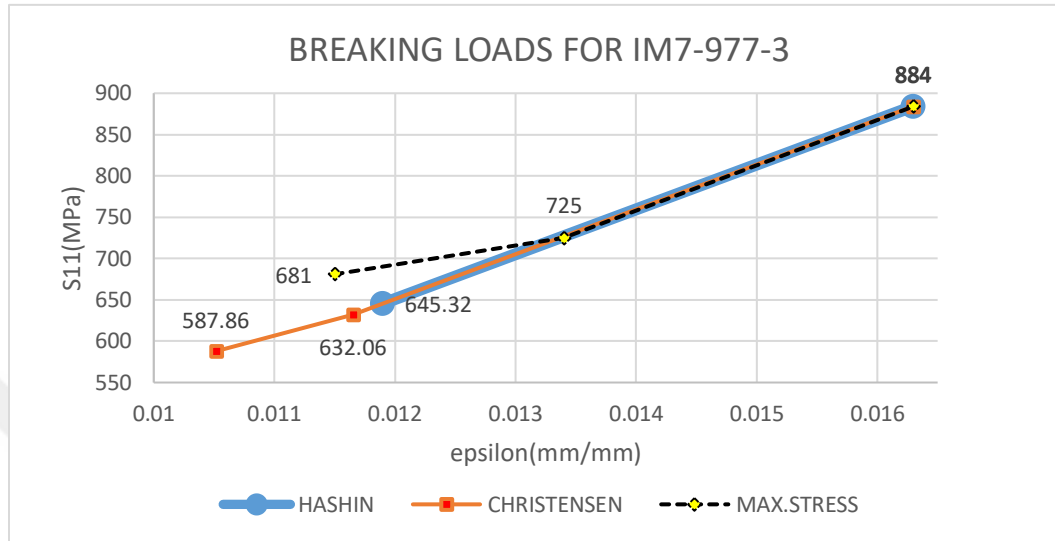


Figure 28: Breaking Axial Load For IM7-977-3 Composite Material.

As shown in Figure 28, the stress-strain diagram for IM7-977-3 composite shows the values of 1st ply failure, 2nd step failure and last ply failure mood by using Hashin, Christensen, and max.stress failure criteria and what is the difference in failure mood sequence when changing applying failure criteria.

By using Hashin , it is clear to notice that the failure starts at 645.32Mpa and ends with 884Mpa at the same slope(linear motion). The full failure is consists of two steps only. 1st step was with matrix failure mood for all plies except (0^0) plies which have been failed with fiber failure mood as mentioned in the discussion of Table 5.

Christensen criterion agree entirely with the slope of Hashin failure criterion except that, in Christensen, the first ply failure starts earlier when the load reaches 587.87Mpa as shown in Table 4. by matrix failure mood at first. Then, 2nd step failure has happened when the load reached 632.06 Mpa which is very close to the first ply failure of Hashin criteria with matrix failure mood for both.

The slope of max. Stress criterion in Figure 28 shows that the failure has two steps. first one is between 1st ply failure with 2nd step failure, which gives an understanding that after 1st ply failure, the material is still try to cope the load by relatively lower rate of elongation until the 2nd step failure took a hardening behavior in the composite which is

expressed by increasing the rate of elongation (ϵ) and increasing the failure slope until last plies that have been failed with fiber failure mood at 884Mpa as discussed in Table 4.

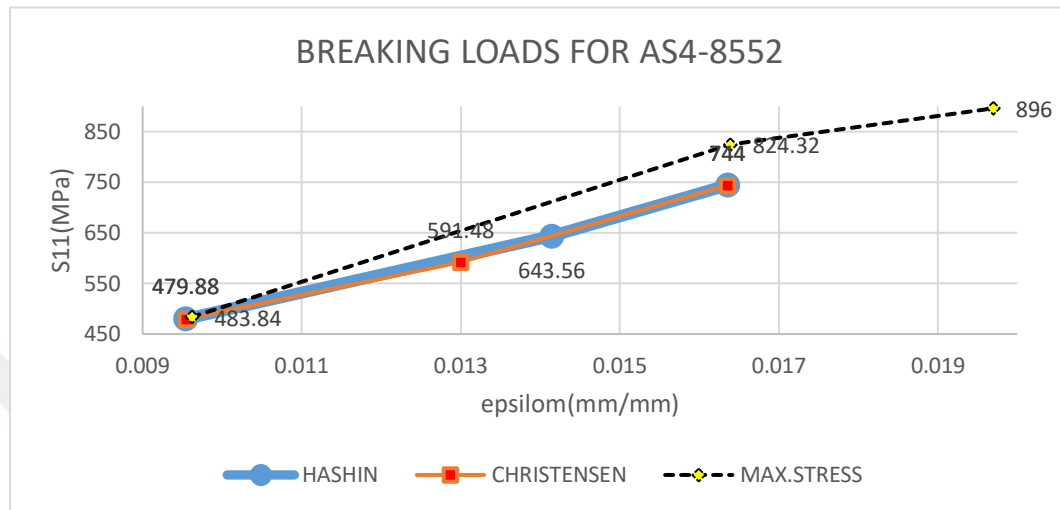


Figure 29: Breaking Axial Load For AS4-8552 Composite Material.

AS4-8552 seems to be sensitive while using different failure criteria as shown in Figure 29 stress-strain curve diagram is different from the other composite. By using Christensen criterion, a very little difference in the rate of elongation against the stress applied with Hashin. And max. Stress criterion which has a higher slope which means that the rate of elongation against stress is lower. Max.stress criterion shows 3 steps of failure sequence which started in specified slope between 1st and 2nd steps and decreasing the slope between 2nd and last ply failure showing a softening in failure behavior. Which means that in the 2nd slope region, the rate of elongation in composite starts to increase until the complete failure has happened.

For AS4-3501-6, all criteria that have used here are precisely identical although there are small differences in slope can be neglected see Figure 30. In addition, AS4-3501-6 has 3-steps of failure sequence with all criteria that have been used. All of them are showing that all composite is completely failed at the same point. It is possible to say that there are no worthy differences with using any of failure criteria for this composite.

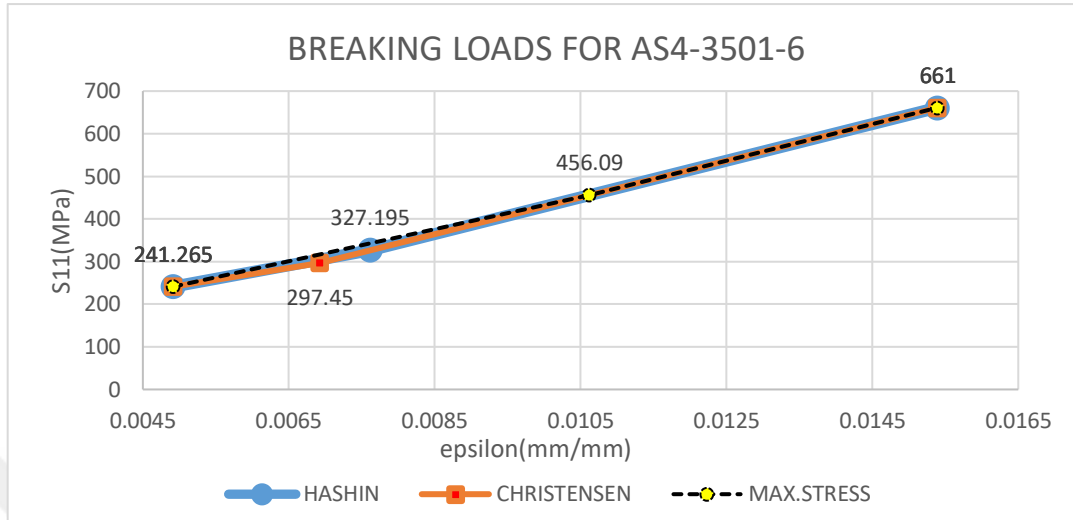


Figure 30: Breaking Axial Load For AS4-3501-6 Composite Material.

4.5. Progressive Failure Analysis (failure envelope)

Failure envelope is a way to predict the failure in laminate under the specific situation and draw a safety boundary for any composite material, giving the designers a comprehensive image about usage limits for any application. Certainly, this failure envelope includes both linear and quadratic areas with important jumps in expected failure loads as the biaxial loading sweeps throughout the two quadrants. As the biaxial S_{11}, S_{22} load changes, the stresses, and strains of each lamina change. This fact compounded by important changes in tensile and compressive strengths for the material used and creates different ply failure mixtures at every area of the failure envelope.

4.5.1. Failure Envelope Analysis With Specific Criteria -Different Composites (Axial with Transverse Loaded)

Figure 31 shows that failure envelope of the three composites by using max. Stress criterion. Which shows that IM7-977-3 failure envelope in the 1st quarter is the largest among the others. The 2nd quarter IM7-977-3 has a larger limit at the range when $(-S_{11}, +S_{22})$ are from step (186 to 67). Meanwhile, AS4-8552 shows high compressive strength than IM7-977-3 within the triangle of steps (67,74,89) as shown in Table 6. AS4-3501-6 has the smallest area in the diagram as in Figure 31, that means its strength in tension-

compression is the lowest if compared with the others. What have been said about 2nd quarter, is also true for the 4th quarter. For the values within the triangle of steps (160,177,186) where AS4-8552 has a higher strength capability than IM7-977-3. AS4-3501-6 has the lowest area for the 1st, 2nd and 4th quarter if compared with other composites. But it agrees mostly for the 3rd quarter with other composites except for slight differences in the boundaries for each composite as shown in Figure 31. In addition, all the composites have linear lines in the failure envelope that is mean there is no interactions between the stresses.

Table 6: Failure Envelope Turning Values Of (S_{11}, S_{22}) of the Composites Using Max. Stress Criterion.

IM7-977-3			AS4-8552			AS4-3501-6		
Step	S11(MPs)	S22(MPs)	Step	S11(MPs)	S22(MPs)	Step	S11(MPs)	S22(MPs)
26	659.944	665.174	26	481.337	485.152	26	241.091	243.001
54	-68.7677	667.799	67	-268.269	476.16	76	-241.257	235.61
67	-265.435	471.129	74	-427.922	474.25	109	-647.371	-178.035
89	-533.764	202.801	89	-533.771	202.804	126	-778.155	-809.489
94	-597.47	124.37	109	-644.025	-177.115	140	-221.042	-658.991
126	-849.35	-883.551	126	-790.092	-821.906	142	-172.126	-645.779
140	-235.912	-703.325	140	-220.218	-656.535	175	235.671	-237.539
157	129.004	-596.109	142	-171.2	-642.305			
160	177.695	-558.873	160	172.509	-542.564			
186	499.958	-236.613	177	474.326	-421.245			
197	672.659	-63.9064	186	476.676	-225.595			

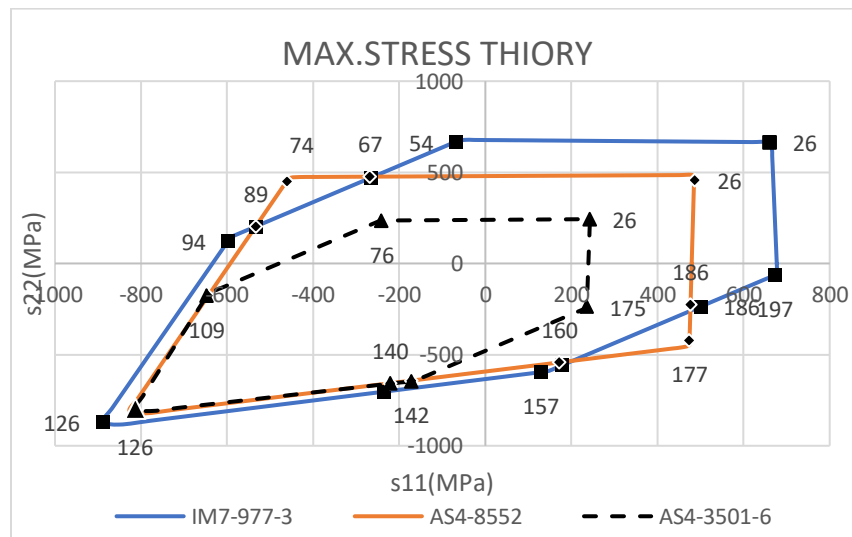


Figure 31: Failure Envelope Diagram for Composites Using Max. Stress Criteria.

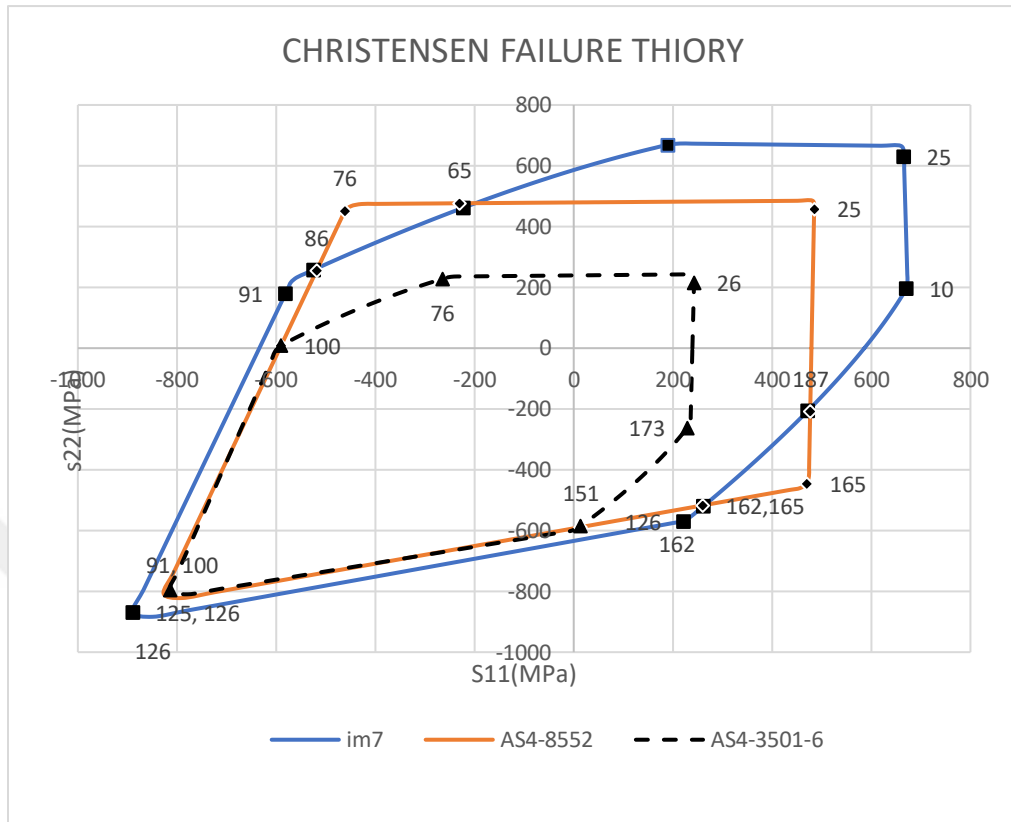


Figure 32: Failure Envelope Diagram for Composites Using Christensen Criterion.

Applying Christensen criterion for the three composites that have been studied as in Figure 32 gives the same overall understanding about IM7-977-3 that having the widest range in failure envelope. Then, AS4-8552 comes next and AS4-3501-6 has the lowest strength capability. It is worthy to note that, IM7-977-3 has quadrant curves if compared with Figure 31 that is mean, there is an interaction between the stresses. Also, there is quadrant curve for AS4-3501-6 in the 4th quarter while other composites have almost the same form with slight differences in their values.

Table 7: Failure Envelope Turning Values Of (S_{11} , S_{22}) of the Composites Using Christensen Criterion.

im7-977-3			AS4-8552			AS4-3501-6		
Step	S11(MPs)	S22(MPs)	Step	S11(MPs)	S22(MPs)	Step	S11(MPs)	S22(MPs)
10	671.076	196	25	484.877	458.8	26	241.091	243.001
25	665.714	629.911	65	-230.192	476.623	76	-241.257	235.61
65	-223.042	461.82	76	-461.764	450.957	100	-590.168	9.31769
86	-524.099	258.243	86	-518.483	255.476	125	-814.037	-794.985
91	-581.203	179.756	100	-589.922	9.31381	151	13.8531	-584.895
126	-849.35	-883.551	126	-790.092	-821.906	173	229.04	-262.038
162	221.336	-568.981	151	13.9404	-588.582			
165	261.31	-519.933	162	207.152	-532.517			
187	472.427	-205.59	165	259.936	-517.197			
			187	476.893	-207.533			

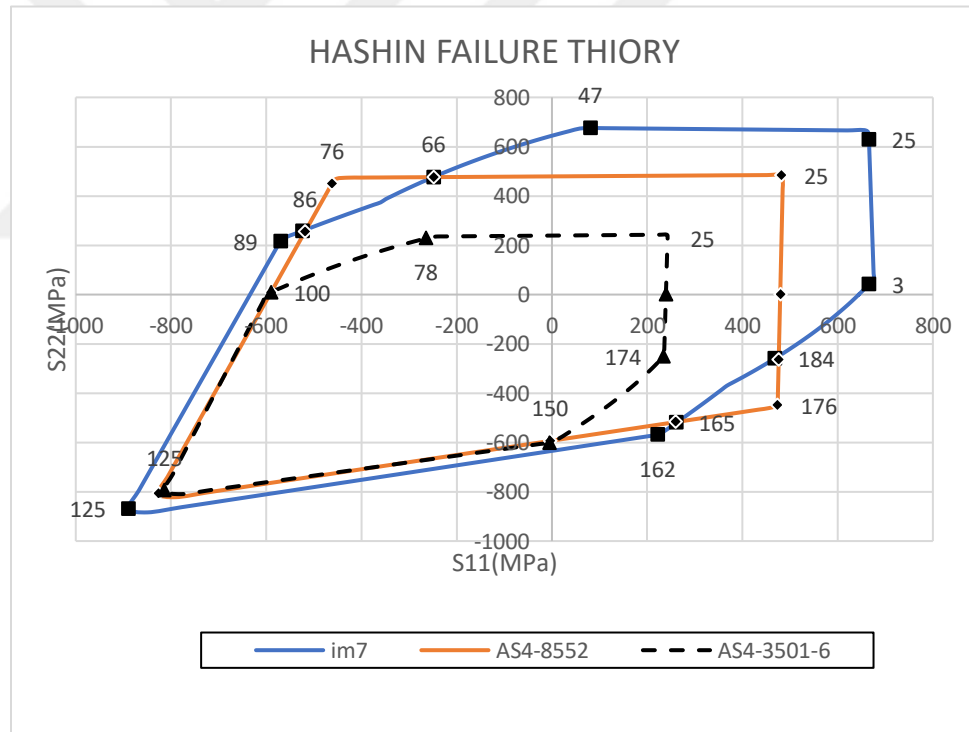


Figure 33: Failure Envelope Diagram for Composites Using Hashin Criterion.

Table 8: Failure Envelope Turning Values of (S_{11}, S_{22}) of the Composites Using Hashin Criterion.

IM7-977-3			AS4-8552			AS4-3501-6		
Step	S11(MPs)	S22(MPs)	Step	S11(MPs)	S22(MPs)	Step	S11(MPs)	S22(MPs)
3	665.718	42.0945	25	484.877	458.8	25	242.829	229.769
25	665.714	629.911	66	-248.925	476.395	78	-264.736	227.737
47	80.3682	675.601	76	-461.764	450.957	100	-590.168	9.31769
66	-249.058	476.648	86	-518.483	255.476	125	-814.037	-794.985
86	-524.099	258.243	100	-589.922	9.31381	150	-4.74056	-600.556
89	-570.342	216.698	125	-826.998	-807.642	174	234.112	-251.364
125	-889.123	-868.313	150	-4.68868	-593.985	200	239.307	4.62E-12
162	221.336	-568.981	165	259.936	-517.197			
165	261.31	-519.933	176	473.766	-448.286			
184	468.363	-259.027	184	476.219	-263.372			
200	644.369	1.25E-11	200	479.377	9.22E-12			

It is obvious from Figure 33 that there are also a quadrant curve for AS4-3501-6 in the 4rd quarter as in Christensen. For IM7-977-3 in the 2nd and 4th quarter has quadrant curves reflect an interaction between stresses in these areas. In the regions between the steps (66 to 88) and (165 to 184) there are a critical point that turn the shape of the curves as seen in Table 8.

4.5.2. Analysis with Certain Composite -Different Criteria (axial with transverse loaded)

Figures (34, 35, and 36) are showing the differences for each failure criterion on the composites.

It is clear from Figure 34 that in the 1st quarter the three failure criteria are identical for most the area except near the X-axis, and Y-axis, where there are few differences, when Christensen criterion is more conservative than others. Hashin criterion come after, and the last is max. Stress criterion.

2nd and 4th quarter have clear differences between the three criteria that have used in this study. Where there are some differences in the shape of failure envelope diagram for each failure criterion. According to the values in Table 6 for IM7-977-3, the slope between the values within steps (157,197) has large strength than Christensen between steps (10,162) as shown in Table 7. Hashin is in between max. Stress and Christensen where the slope lies within steps (3,162) as shown in Table 8 and Figure 34. Hashin has almost the same slope of the failure envelope with Max. Stress criterion in the 1st and 3rd

quarters except slight differences in values in the 2nd and 4th quarters. In general, all the three failure criteria are roughly identical for IM7-977-3. The 3rd quarter has a larger area from other quarters, and failure criteria in it are completely identical.

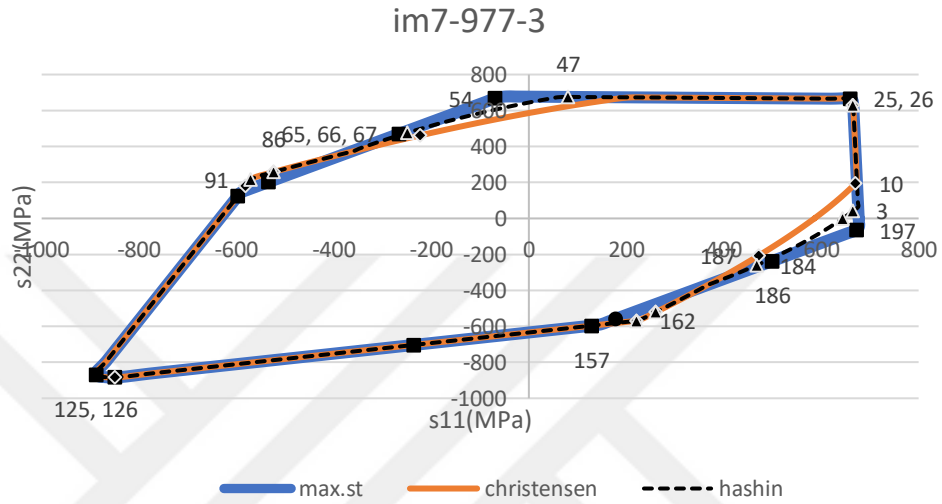


Figure 34: Failure Envelope for IM7-977-3 by Applying Different Failure Criterion.

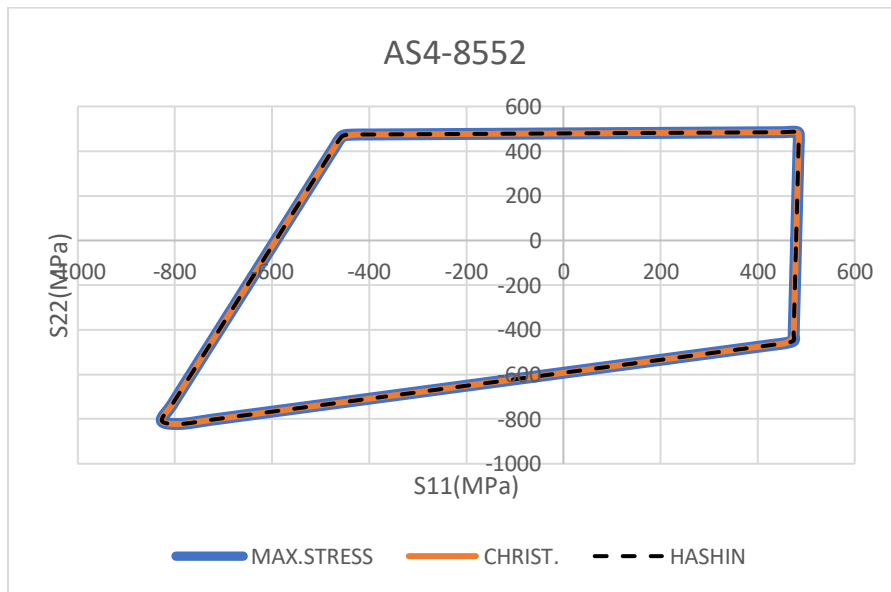


Figure 35: Failure Envelope For AS4-8552 by Applying Different Failure Criteria.

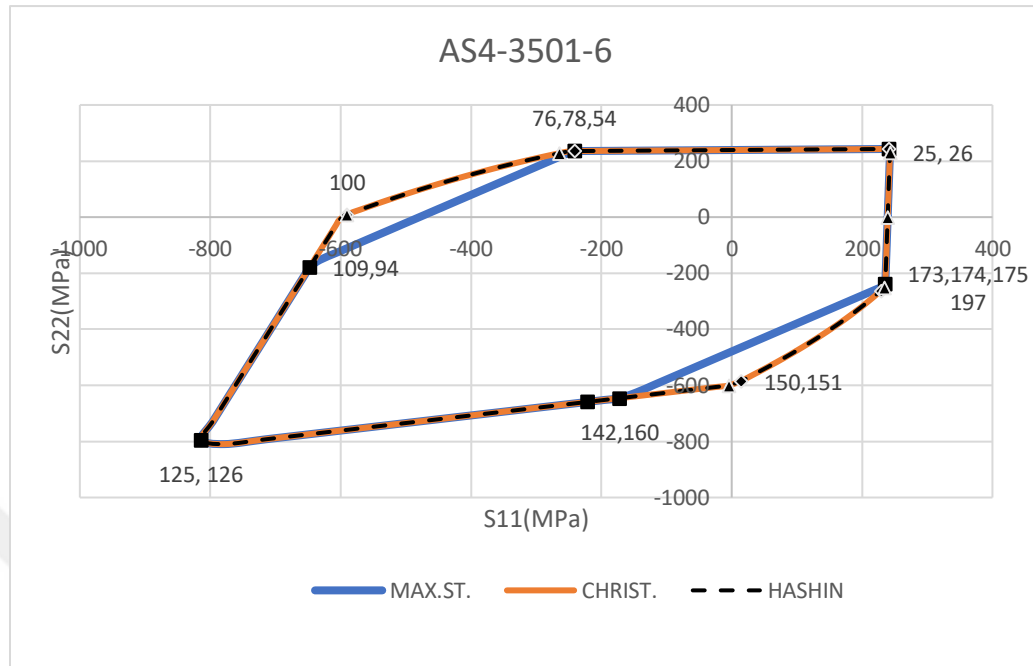


Figure 36: Failure Envelope for AS4-3501-6 by Applying Different Failure Criteria.

AS4-8552 has the same shape of failure envelope although when different failure criteria have been used. It shows a full match of boundaries to the four quarters. The 1st quarter is entirely symmetrical about (45°) plies due to the nature of quasi-isotropic laminate.

Different failure criteria have been applied on AS4-3501-6 as shown in Figure 36, that shows a complete match between Christensen and Hashin failure criteria for all the diagram (4 quarters). But at the same time, there is a clear difference with max.stress criterion in 2nd and 4th quarters. Where the diagram tells that max.stress is more conservative in these quarters than other criteria. For instance, in 2nd and 4th quarters as shown in Table (6, 7 and 8) the values between steps (160 to 197) as shown in Table 6 have different failure envelopes for IM7-977-3 in one hand with both AS4-8552 and AS4-3501-6. On the other hand, IM7-977-3 is more conservative than Christensen and Hashin for the same range quarter's parts. The Same explanation can be said in the similar area in the 2nd quarter between points steps of (54 to 94) as shown in Table 6.

4.5.3. Analysis with Certain Criterion -Different Composites (axial with shear loaded)

Figures (37, 38 and 39) respectively show how failure envelope will be for all the composites that have been examined in this work according to specific failure criteria for each diagram of (max.stress, Christensen,Hashin).

Figure 37 shows the effect of max. Stress criteria on the three composites and how the failure envelope will could be. IM7-977-3 has a more comprehensive range of stresses where this material can take a vertical line appointed between the points of step (1 to 30) as shown in Table 9 then it takes another path to reach step 35 after this point failure prediction line takes a horizontal path until step 156 after that the path will take a declined path to reach step 171 finally down vertically until reached step 200 so that the area is more comprehensive than other composites.all the diagram include linear lines because there is no interaction between stresses as mentioned befor.

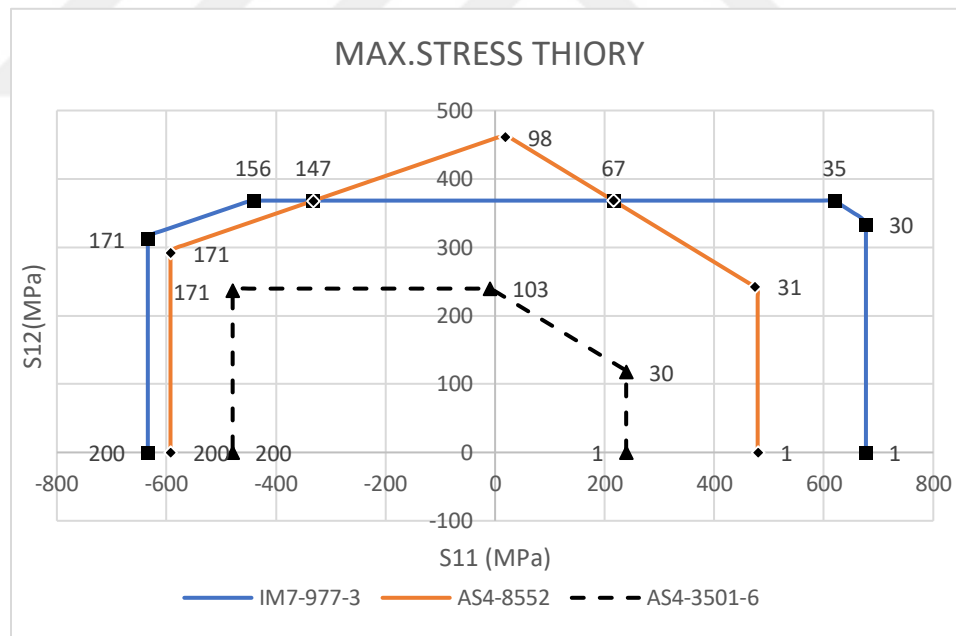


Figure 37: Failure Envelope Using Max. Stress Criteria on The Three Composites.

Table 9: Failure Envelope Turning Values Of (S_{11} , S_{12}) of the Composites Using Max. Stress Criterion.

IM7-977-3			AS4-8552			AS4-3501-6		
Step	S11(MPs)	S12(MPs)	Step	S11(MPs)	S12(MPs)	Step	S11(MPs)	S12(MPs)
1	677.05	2.16E-14	1	479.377	-6.90E-15	1	239.307	-1.70E-15
30	677.047	333.606	31	473.382	242.614	30	239.309	117.917
35	618.934	368.282	67	215.382	368.56	103	-9.46011	239.571
67	215.221	368.284	98	18.2109	461.179	171	-479.129	236.085
147	-332.309	368.286	147	-332.048	367.997	200	-479.136	-4.60E-12
156	-442.044	368.284	171	-592.629	292.01			
171	-634.013	312.401	200	-592.629	-5.70E-12			
200	-634.014	-6.10E-12						

AS4-8552 is more conservative than IM7-977-3 and has a lower stiffness than IM7-977-3 except in a specific range closed around Y-axis. A triangle shaped of three point steps (67,98,147) respectively. This triangle has higher failure predication strength than IM7-977-3 as shown in Figure 37. Otherwise, all the boundary conditions are lower than IM7-977-3. Also there are no interactions between the stresses as in Christensen and Hashin. As shown in Figure 38, Figure 39).

AS4-3501-6 has the smallest failure envelope if compared with the other composites and significant differences in values with other composites.

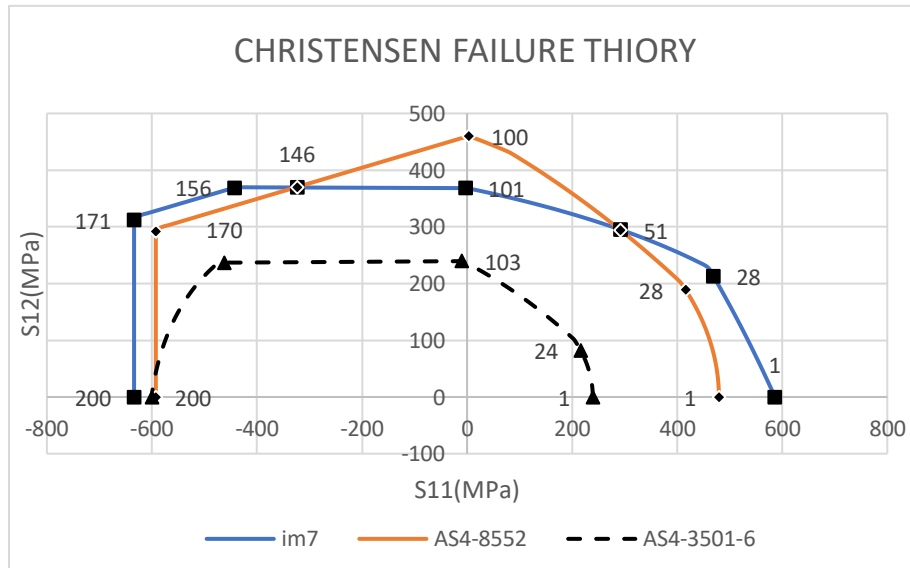


Figure 38: Shape of Failure Envelope Using Christensen Criteria on The Three Composites.

Figure 38 shows that failure envelope of the three composites using Christensen failure criterion. In general, Max. Stress criterion, IM7-977-3 has also the widest range of failure envelope. Then AS4-8552 comes next so where it is more conservative than IM7-977-3 except for a triangle shaped area between the points of steps (51,100,146). So if any application has designed stresses within this area, only AS4-8552 can satisfy this condition among other composites. Otherwise, it is considered more conservative than IM7-977-3 for all other regions. AS4-3501-6 has the most conservative failure envelope than others. In the 2nd quarter, it takes a horizontal path from step (103 to 170) with no interactions between the stresses. Then the safe boundaries take a curve path between steps (170 to 200) reflecting an interaction between the stresses in this area like between the steps (1 to 103). Also, an interaction is existing for AS4-8552 between the steps (1 to 100).

Table 10: Failure Envelope Turning Values Of (S_{11}, S_{12}) of the Composites Using Christensen Criterion.

im7-977-3			AS4-8552			AS4-3501-6		
Step	S11(MPs)	S12(MPs)	Step	S11(MPs)	S12(MPs)	Step	S11(MPs)	S12(MPs)
1	586.073	-6.90E-15	1	479.377	-6.90E-15	1	239.307	-1.70E-15
28	469.018	212.974	28	416.019	188.908	24	216.187	82.1389
51	292.589	294.907	51	291.962	294.276	103	-9.45793	239.515
101	-2.90716	368.293	100	3.63089	459.978	170	-462.104	236.834
146	-322.868	369.384	146	-323.666	370.296	200	-599.279	-5.80E-12
156	-443.052	369.124	171	-592.629	292.01			
171	-634.013	312.401	200	-592.629	-5.70E-12			
200	-634.014	-6.10E-12						

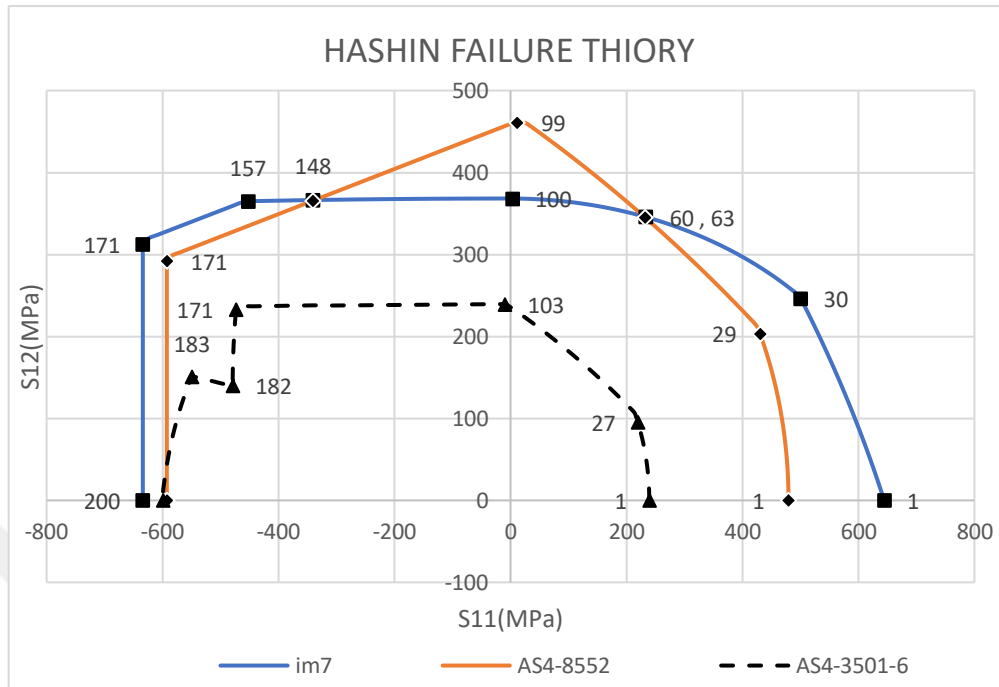


Figure 39: Shape of Failure Envelope Using Hashin Criteria on The Three Composites.

Figure 39 shows the failure envelopes for the three composites by using Hashin failure criterion. A quick look at the figure is quite enough to understand that the path of each composite for its prediction failure behavior is very similar to that in Christensen failure criterion. Except for AS4-3501-6, where as obvious in the 2nd quarter. There is a significant clear jump in strength between steps (182,183). Hashin is very sensitive here because it is Fully interactive criterion to the sequence of matrix failure. The jump was from the linear behavior to the quadrant curve. AS4-3501-3 can be significantly affected by the sudden reduction of matrix stiffness, resulting jump in strength as shown in the Table 11.

Table 11: Failure Envelope Turning Values Of (S_{11}, S_{12}) of the Composites Using Hashin Criterion.

IM7-977-3			AS4-8552			AS4-3501-6		
Step	S11(MPs)	S12(MPs)	Step	S11(MPs)	S12(MPs)	Step	S11(MPs)	S12(MPs)
1	644.369	-7.10E-15	1	479.377	-6.90E-15	1	239.307	-1.70E-15
30	500.392	246.562	29	430.145	203.573	27	219.473	95.5098
63	232.589	345.873	63	232.103	345.15	103	-9.45793	239.515
100	2.9027	367.727	99	10.9202	461.065	171	-473.24	233.183
148	-341.246	366.392	148	-340.555	365.651	182	-479.129	139.938
157	-452.375	364.949	171	-592.629	292.01	183	-549.3	151.064
171	-634.013	312.401	200	-592.629	-5.70E-12	200	-599.279	-5.80E-12
200	-634.014	-6.10E-12						

4.5.4. Analysis with Certain Composite -Different Criteria (axial with shear loaded)

Figures (40, 41 and 42) show differences in failure criteria on a specific composite to find out which one is more suitable for certain design conditions and where are the critical values for each.

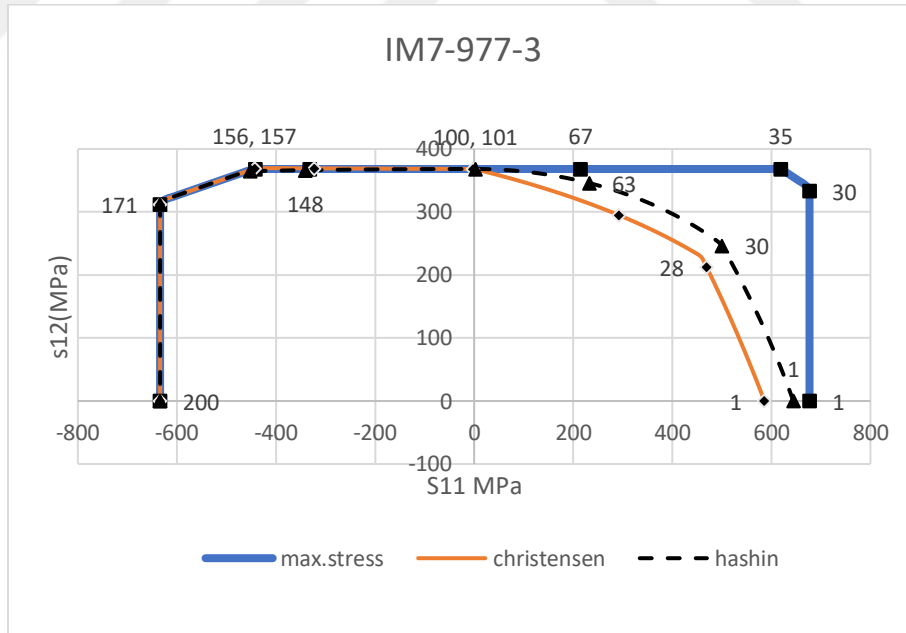


Figure 40: Failure Envelope of Axial With Shear Load For IM7-977-3 Using Different Failure Criteria.

Figure 40 shows that IM7-977-3 in the 1st quarter has different starting points for failure envelope diagram for each criterion and shows no interaction between the stresses. Christensen is the most conservative in this concept which starts at step1C. While Hashin

comes next with step1H. The highest value was for max. Stress criterion starting in step1M as shown in Table 12. After which, the failure envelope of max. Stress criterion goes vertically not like other criteria which gives the max. Stress criteria the wider range of failure envelope shape. In the 2nd quarter, it is obvious that all failure criteria yield roughly the same laminate strengths. For Christensen and Hashin there are interactions between the stresses in the 1st quarter for each of them expressed by the quadrant curves for their failure envelopes.

Table 12: Failure Envelope Turning Values Of (S_{11}, S_{12}) of the IM7-977-3 With Different Failure Criteria.

Step	Max. stress		Step	Hashin		Step	Christensen	
	S11(MPs)	S12(MPs)		S11(MPs)	S12(MPs)		S11(MPs)	S12(MPs)
1M	677.05	2.16E-14	1H	644.369	-7.10E-15	1C	586.073	-6.90E-15
30	677.047	333.606	30	500.392	246.562	28	469.018	212.974
35	618.934	368.282	63	232.589	345.873	51	292.589	294.907
67	215.221	368.284	100	2.9027	367.727	101	-2.90716	368.293
147	-332.309	368.286	148	-341.246	366.392	146	-322.868	369.384
156	-442.044	368.284	157	-452.375	364.949	156	-443.052	369.124
171	-634.013	312.401	171	-634.013	312.401	171	-634.013	312.401
200	-634.014	-6.10E-12	200	-634.014	-6.10E-12	200	-634.014	-6.10E-12

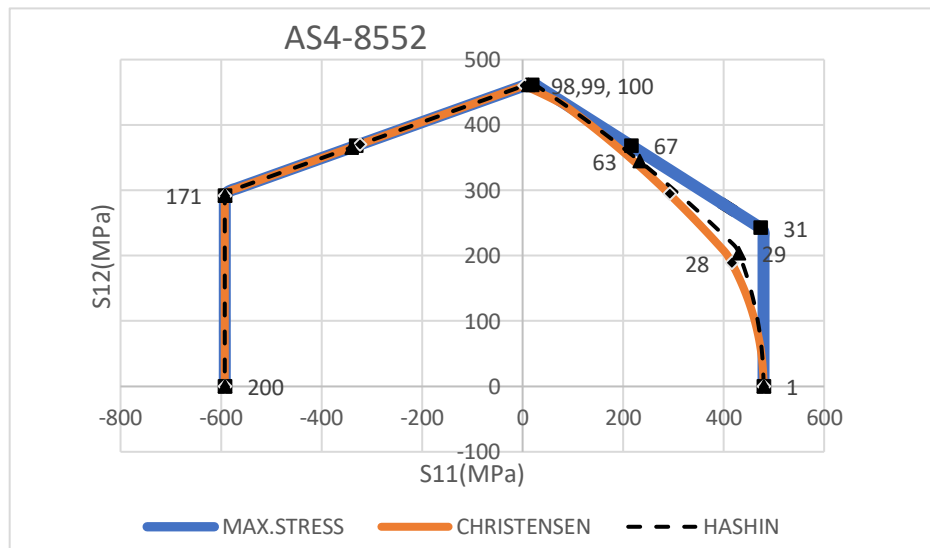


Figure 41: Failure Envelope of Axial With Shear Load For AS4-8552 Using Different Failure Criteria.

Table 13: Failure Envelope Turning Values of (S_{11}, S_{12}) of the AS4-8552 with Different Failure Criteria.

Step	Max. stress		Step	Hashin		Step	Christensen	
	S11(MPs)	S12(MPs)		S11(MPs)	S12(MPs)		S11(MPs)	S12(MPs)
1	479.377	-6.90E-15	1	479.377	-6.90E-15	1	479.377	-6.90E-15
31	473.382	242.614	29	430.145	203.573	28	416.019	188.908
67	215.382	368.56	63	232.103	345.15	51	291.962	294.276
98	18.2109	461.179	99	10.9202	461.065	100	3.63089	459.978
147	-332.048	367.997	148	-340.555	365.651	146	-323.666	370.296
171	-592.629	292.01	171	-592.629	292.01	171	-592.629	292.01
200	-592.629	-5.70E-12	200	-592.629	-5.70E-12	200	-592.629	-5.70E-12

Figure 41 shows that Failure envelopes of AS4-8552 with different failure criteria. In the 1st quarter all of them start roughly at the same starting point. Max. Stress criteria then go vertically with no interactions between the stresses until the step (31). Hashin and Christensen take quadrant curves with interactions between the stresses until the steps (29, 28) respectively. Then they take another slope until the steps (89, 99) which gives an ability to order them as:

- 1- Max. Stress criteria have a wider range of failure envelope.
- 2- Hashin criterion come next.
- 3- Christensen is the most conservative criterion.

After all the mentioned points, in the 2nd quarter, all the failure criteria yield roughly the same laminate strengths with no interactions between the stresses.

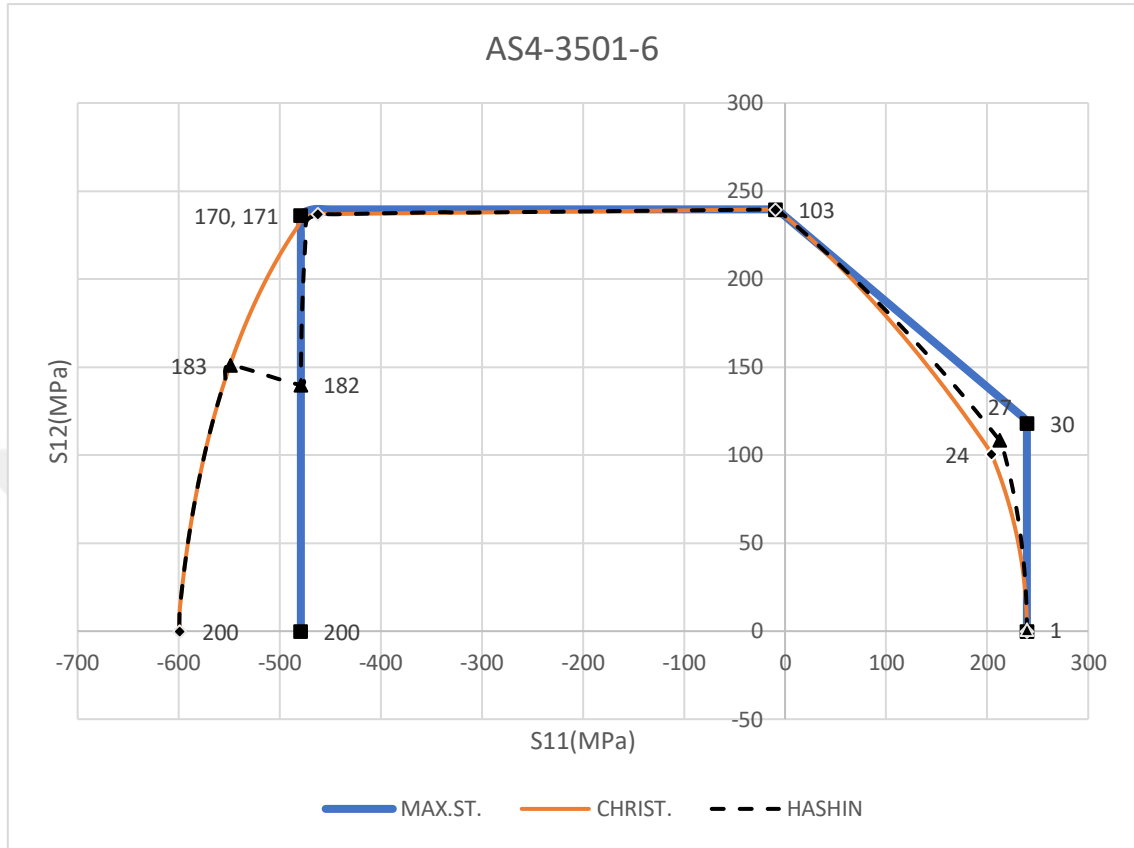


Figure 42: Failure Envelope of Axial with a Shear Load For AS4-3501-6 Using Different Failure Criteria.

Failure envelopes of AS4-3501-6 as in Figure 42 shows that 1st quarter quietly takes the same behavior of AS4-8552 with slight differences in values. So they make the same orders as in Figure 41. In the 2nd quarter, it is worthy to notice that Hashin criterion are matching with max. Stress criterion partially with a linear line and suddenly jump to match with Christensen in another part with a quadrant curve through the points between steps (182,183) as shown in Table 14 this critical Region existed because of Hashin's sensitivity to the matrix failure, and this can induced a sudden jump in strength. This kind of critical points need more practical investigations for more understanding of the nature of this composite behavior in failure.

Table 14: Failure Envelope Turning Values of (S_{11}, S_{12}) of the AS4-3501-6 With Different Failure Criteria.

Max. stress			Hashin			Christensen		
Step	S11(MPs)	S12(MPs)	Step	S11(MPs)	S12(MPs)	Step	S11(MPs)	S12(MPs)
1	239.307	-1.70E-15	1	239.31	-1.70E-15	1	239.307	-1.70E-15
30	239.309	117.917	27	219.47	95.5098	24	216.187	82.1389
103	-9.46011	239.571	103	-9.458	239.515	103	-9.45793	239.515
171	-479.129	236.085	171	-473.2	233.183	170	-462.104	236.834
200	-479.136	-4.60E-12	182	-479.1	139.938	200	-599.279	-5.80E-12
			183	-549.3	151.064			
			200	-599.3	-5.80E-12			

4.6. Pure Shear Load Analysis.

Table 15: Shear Load Failure Mood Sequence of the Three Composites at Maximum Stress Criteria.

	SIGMAxy (MPa)	EPSILONxy (mm/mm)	Failed Ply Number(s)	Failure Mode
	370	0.0177	1.4.5.8	2.2.2.2
im7-977-3	444	0.0215	3.6	3.3
	673	0.0329	2.7	3.3
AS4-8552	460.89	0.0264458	1.3.4.5.6.8	2.3.2.2.3.2
	569	0.0331948	2.7	3.3
AS4-3501-	236.22	0.0142652	1.3.4.5.6.8	2.1.2.2.1.2
	508	0.0313385	2.7	3.3

By applying pure shear load using Max. Stress failure criterion as shown in Table 15. It is clear to see that IM7-977-3 first ply failure was ($0^0, 90^0$) as shown in Figure 43 where 4 plies at the same time are failed when the load is 370MPa with shear failure mood. It is like a tear effect for them. Next, (-45^0) plies have been failed at 444MPa with longitudinal failure mood according to the direction of positive shear load that has applied. Then, they are attached to (90^0) plies that have been failed already. Finally, the laminate has been failed completely when the load reaches 673MPa causing failure of ($+45^0$) plies with longitudinal failure mood. They stand for to be last failed plies because of their direction with positive shear load direction. It is worth to note that with the shear load by using max. Stress criterion, there is no transverse failure mood, because there is no pure load perpendicularly applied on fiber direction. Also, there is the relatively reasonable

limit between first ply failure, and last ply failure as shown in Figure 44, failure mood sequence consists of three steps, not like other composites as shown in Table 15.

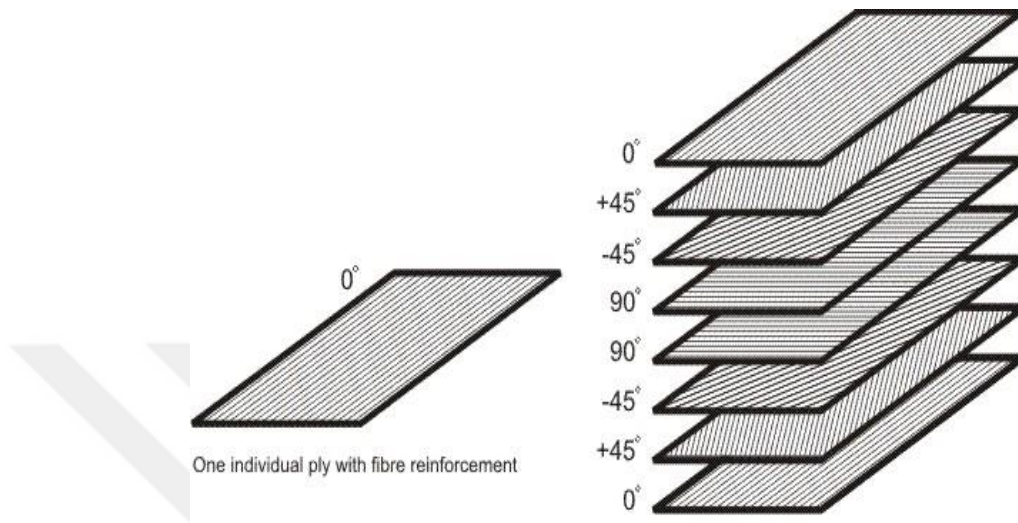


Figure 43: Laminate Stacking Sequence.

AS4-8552 as shown in Table 15 has a failure mood sequence consists of two steps, not as in IM7-977-3. Starting at shear load 460.89 MPa causing failure to $(0^0, 90^0)$ as shown in Figure 43 by shear failure mood and (-45^0) by longitudinal one. All of them at the same load. There is a high degradation for this composite against shear load causing failure of 6 plies at the same time. When the load has reached 569MPa, last plies $(+45^0)$ have been failed with longitudinal failure mood as illustrated in IM7-977-3, but it seems to have a higher strength to carry the load until first ply failure has happened at 460MPa.

AS4-3501-6 as shown in Table 15 first ply failure has happened at shear load 236.22 MPa. It is early failed if compared with the other composites. Plies that have failed are $(0^0, 90^0)$ plies with shear failure mood at the same time. Plies of (-45^0) as shown in Figure 43 that have failed with transverse failure mood. This composite is the only one that (-45^0) plies have failed with transverse failure mood. It depends on the mechanical properties of the composite itself. After the failure of 6 plies have happened, the laminate stay carrying the load until the last ply failure has happened for $(+45^0)$ with longitudinal failure mood when the load reached 508 MPa. From Figure 44 the completed failure has

happened within two steps and the limit between the first ply failure and the last ply failure is the largest compared with the other composites.

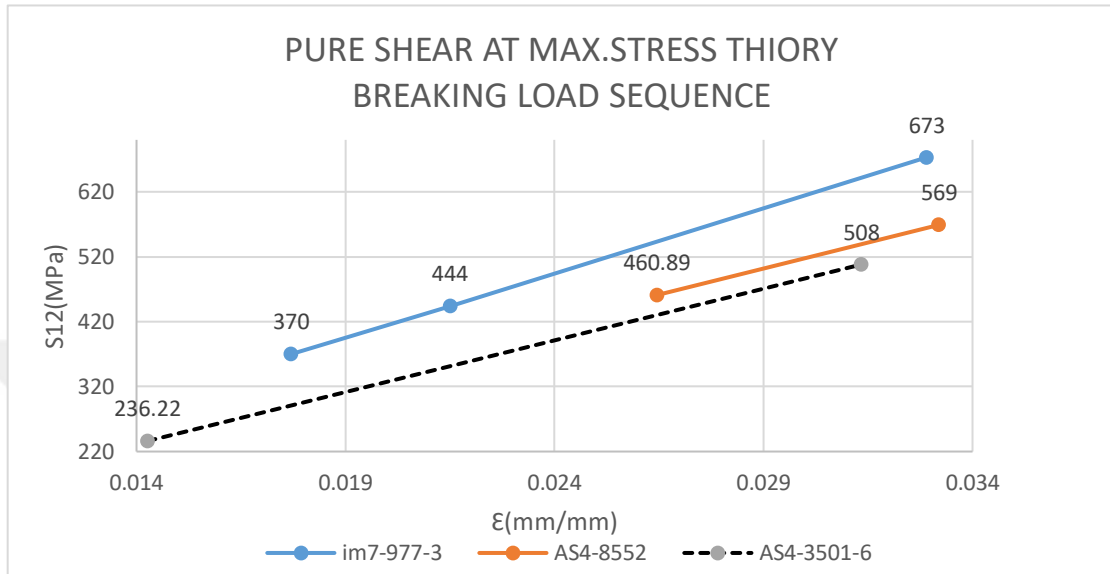


Figure 44: Shear Load Failure Mood Sequence of The Three Composites at Maximum. Stress Criterion.

Table 16: Shear Load Failure Mood Sequence of The Three Composites at Hashin Criterion.

	SIGMAxy (MPa)	EPSILONxy (mm/mm)	Failed Ply Number(s)	Failure Modes
im7-977-3	370.15	0.0177111	1.4.5.8	1.1.1.1
	444.18	0.0215022	3.6	2.2
	673	0.0329482	2.7	2.2
AS4-8552	460.89	0.0264458	1.3.4.5.6.8	2.2.2.2.2.2
	569	0.0331948	2.7	2.2
AS4-3501-6	236.22	0.0142652	1.3.4.5.6.8	2.1.2.2.1.2
	508	0.0313385	2.7	2.2

Using Hashin failure criterion to analyze the progressive failure for applying shear load on the composites as shown in Table 16 and Figure 45, where IM7-977-3 has the same failure values with that in Table 15 except the failure mood sequence where the first ply failure ($0^0, 90^0$) have been failed by matrix failure mood. (-45^0) and ($+45^0$) plies have failed with fiber failure mood. AS4-8552 also has a similar of failure behavior in Hashin with max. Stress criterion except in the failure mood sequence. Where

(0° , -45° , 90°) those 6plies, as shown in Figure 43, are failed by fiber failure mood at the same time and then ($+45^{\circ}$) plies also failed for the same reason. That means fiber failure mood completely happens with the fiber before any failure in the matrix. This behavior is unique to happen in the failure mood sequence if compared with the other composites. AS4-3501-6 as shown in Table 16 and Figure 45 there where a big similarity between failure behavior for this composite between Hashin and max. Stress failure criterion, except in the failure mood of ply failure for ($+45^{\circ}$) with fiber failure mood. Practically it is not a big difference. It is related to the definition of failure mood for each criterion.

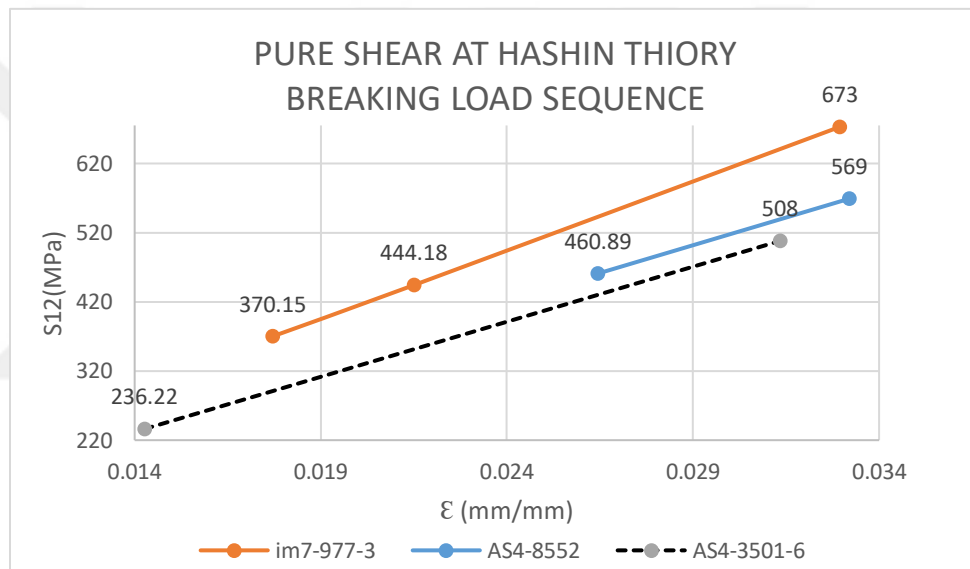


Figure 45: Shear Load Failure Mood Sequence of The Three Composites at Hashin Criterion.

Table 17: Shear Load Failure Mood Sequence of the Three Composites at Christensen Criterion.

	SIGMAxy (MPa)	EPSILONxy (mm/mm)	Failed Ply Number(s)	Failure Modes
im7-977-3	370.15	0.0177111	1.4.5.8	1.1.1.1
	444.18	0.0215022	3.6	2.2
	673	0.0329482	2.7	2.2
AS4-8552	460.89	0.0264458	1.3.4.5.6.8	1.2.1.1.2.1
	569	0.0331948	2.7	2.2
AS4-3501-	236.22	0.0142652	1.3.4.5.6.8	1.1.1.1.1.1
	508	0.0313385	2.7	2.2

Table 17 and Figure 46 show that IM7-977-3 has no difference in failure mood between hashin and Christensen. It has the same notes that have mentioned before. In Figure 45 and Figure 44, AS4-8552 has failure loads values like Hashin criterion as shown in Table 16 and Table 17 except, $(0^\circ, 90^\circ)$ plies that have failed with matrix failure mood instead of fiber failure mood that have happened in Hashin criterion.

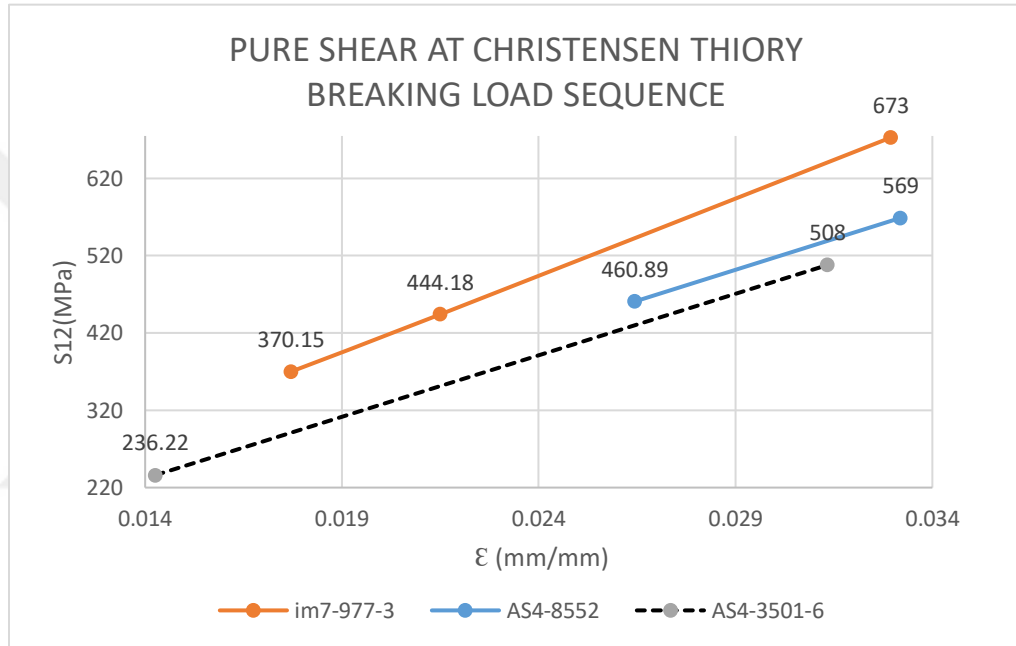


Figure 46: Shear Load Failure Mood Sequence of The Three Composites at Christensen Criterion.

AS4-3501-6 as shown in Table 17 shows that the Plies $(0^\circ, -45^\circ, 90^\circ)$ have been failed with matrix failure mood at 236.22MPa and $(+45^\circ)$ plies have failed with fiber failure mood at the same load. Not like in Hashin criterion which have just (-45°) plies have failed with matrix failure mood, and other plies have failed with fiber failure mood.

4.7. Aerodynamic Force Analysis Using QBlade Software Version 0.963

To findout the effect of wind speed on a specific composite using in a wind blade, SANDIA_SERI-8 model has been taken to make a simulation.

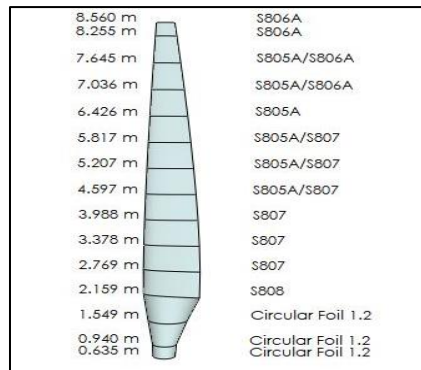


Figure 47: SANDIA_SERI-8.

Figure 47 shows that blade model has been divided into 15 line to facilitate the analysis showing different airfoils with specific data for each airfoil as shown in Table 18.

Table 18: SANDIA_SERI-8 Model Database.

BLADE DATA and 0.64m hub radius					
segments	pos(m)	chord(m)	twist	foil	polar
1	0	0.4191	0	Circular Foil 1.2	CD=1.2 360 Polar
2	0.3048	0.452882	0	Circular Foil 1.2	CD=1.2 360 Polar
3	0.9144	0.747522	0	Circular Foil 1.2	CD=1.2 360 Polar
4	1.524	1.1176	20	S808	TO_Re1.000_M0.00_N9.0 360 M
5	2.1336	1.09449	14.81	S807	TO_Re1.000_M0.00_N9.0 360 M
6	2.7432	1.05207	10.61	S807	TO_Re1.000_M0.00_N9.0 360 M
7	3.3528	0.997458	7.29	S807	TO_Re1.000_M0.00_N9.0 360 M
8	3.9624	0.932434	4.74	S805A/S807	TO_Re1.000_M0.00_N9.0 360 M
9	4.572	0.858774	2.87	S805A/S807	TO_Re1.000_M0.00_N9.0 360 M
10	5.1816	0.777494	1.57	S805A/S807	TO_Re1.000_M0.00_N9.0 360 M
11	5.7912	0.689102	0.74	S805A	TO_Re1.000_M0.00_N9.0 360 M
12	6.4008	0.593852	0.27	S805A/S806A	TO_Re1.000_M0.00_N9.0 360 M
13	7.0104	0.49276	0.06	S805A/S806A	TO_Re1.000_M0.00_N9.0 360 M
14	7.62	0.38526	0	S806A	TO_Re1.000_M0.00_N9.0 360 M
15	7.9248	0.3302	0	S806A	TO_Re1.000_M0.00_N9.0 360 M

Steady wind speed of 15m/s has been assumed to make simulation on this model to findout the load that has been generated on the blade as shown in Figure 48.

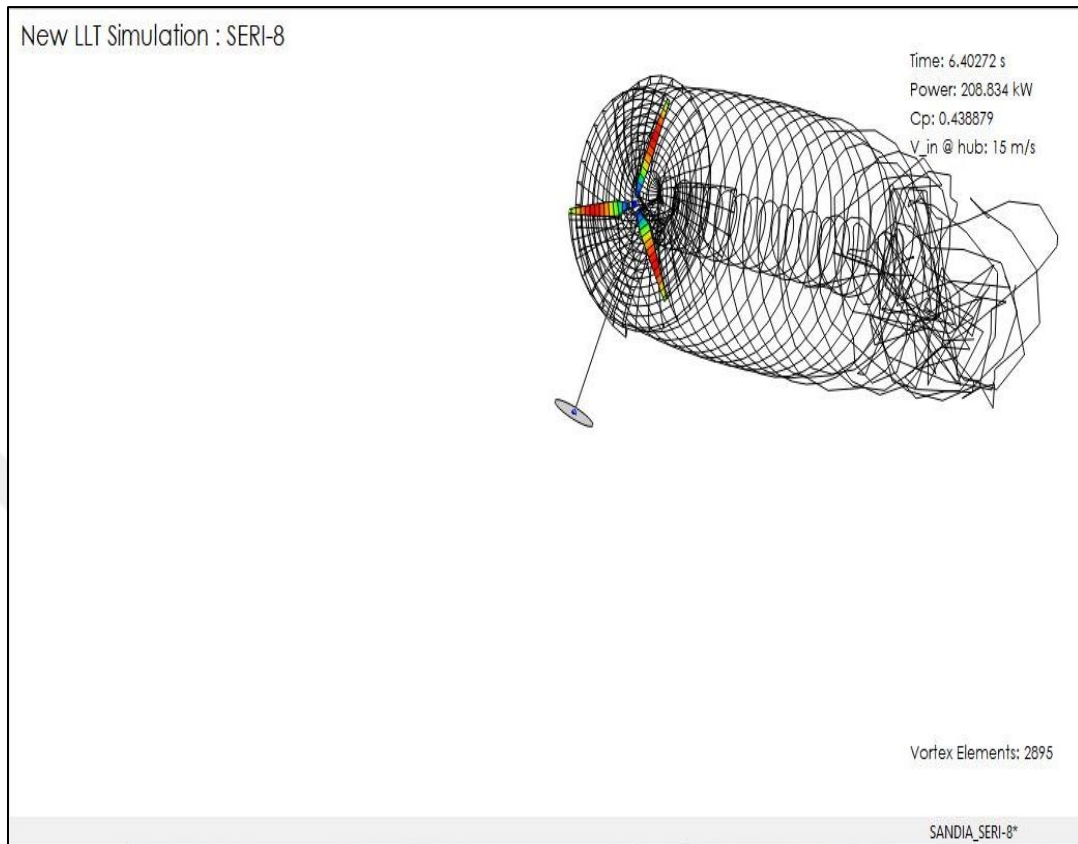


Figure 48: SANDI_SERI-8 Simulation At $V=15\text{m/S}$.

Simulation time was 6.403sec, where Qblade has shown the changing in load values from zero sec to 6.403sec. Peak load has been investigated to find out that at time step $t=0.178$ sec the load has the maximum value which is total normal force = 11000N.

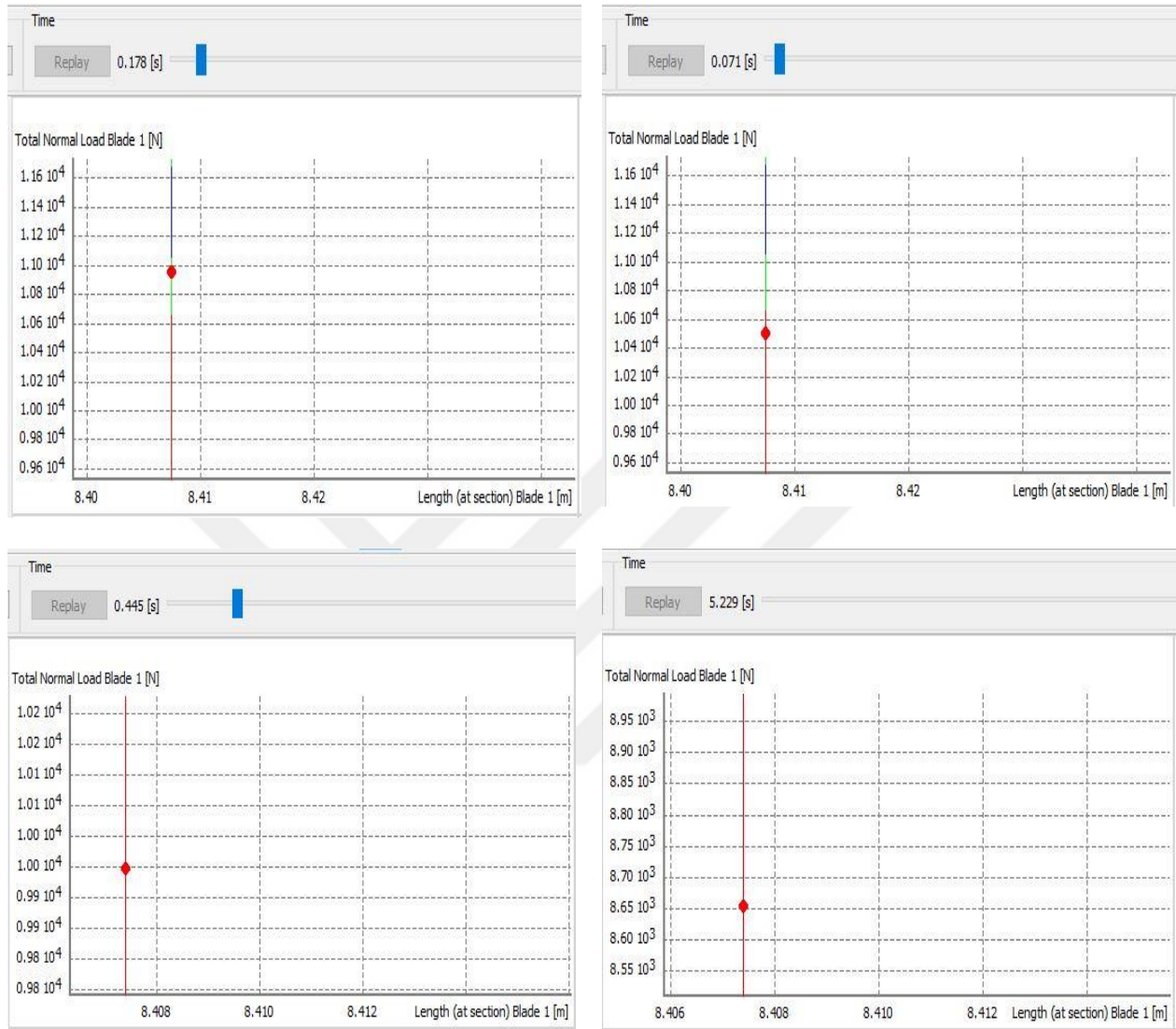


Figure 49: Normal Force at Different Time Steps on The Blade.

Figure 49 shows different time step simulation for SANDIA_SERI-8 which are (0.178, 0.071, 0.445, 5.229) sec to prove that at $t=0.178$, maximum total normal load has been applied on the blade model. This load has been taken to be used as an input in bending analysis for Helius Composite software to investigate what the deferences in composite behavior among the three composites that have been choosen in this study.

4.8. Composite Material Behavior Due to Aerodynamic Force Analysis

An important assumptions have been adopted before using the maximum total normal force in Helius Composite software.

4.8.1. Assumptions

Spar of SANDIA_SERI-8 wind blade model has been assumed to carry the total load of the wind speed. The blade has been divided into three sections to facilitate taking average dimension values for the spar as an input of the analysis. Section 1 for circular airfoils, section 2 for the thick airfoils, section 3 for thin airfoils as shown in Figure 50 (b). All the dimensions of Ibeam sections (1.2.3) are taken from the height of the part segments of SANDIA_SERI-8 database as shown in Figure 50 (c). The cross section of the spar has been assumed to be as an I Beam with H =height of the Ibeam and W =width of the I beam from the database of the SANDIA_SERI-8. Average values of H_1, H_2, H_3 are (540,201.2,71)mm respectively as shown in Figure 50 (c). W has been assumed as $(0.6H)$. Average dimensions of all blade spar length as shown in Figure 50 (d) has been taken as another case study to investigate the beam deflection. Center of spar has been assumed to be at $0.325(C_m)$ [44], where C_m is the mean chord value of the sections as in Figure 50(f).

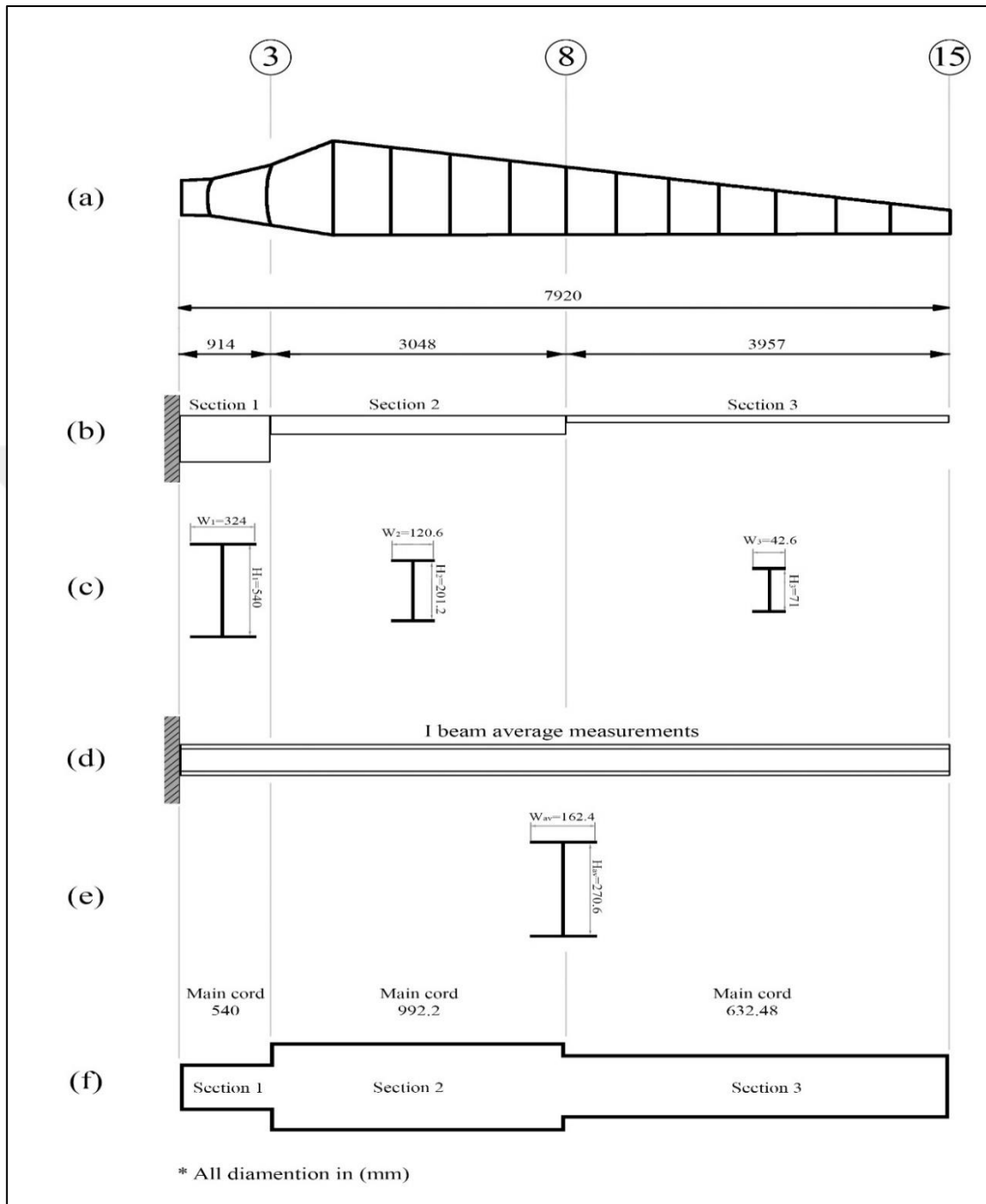


Figure 50: (A) The Blade Segment Number, (B) Main I-Beam Sections for Spar, (C) I-Beam Spar Cross Section Dimensions, (D) I-Beam Spar Average Dimensions, (E) I-Beam Spar Average Cross Section, (F) Main Cord Values for Spar Sections (Blade Top View).

4.8.2. Calculations

In addition to calculation the three sections dimensions that have been mentioned before, another case study has been taken. Considering one section spar having average

dimensions with H_{av} and W_{av} which are calculated from eqns.(24,25) are carrying the load on the blade model as shown in Figure 50(e).

$$\text{Where} \quad H_{av} = \frac{H_1+H_2+H_3}{3} \quad (24)$$

$$W_{av} = 0.6H_{av} \quad (25)$$

Maximum deflection has been calculated for all the I-beam sections for each composite material due to aerodynamic force. A comparison has been fulfilled to show the behavior of each composite material as shown in Table 19.

Table 19: Max. Deflection Table for All Sections of the Three Composites.

	UNDER WIND SPEED V=15m/s		TOTAL NORMAL LOAD=11000N	UNIFORM LOAD =11000N/7920mm =1.39 N/mm	
IM7-977-3X2					
	SECTION 1	SECTION2	SECTION3	SUM of 1,2,3	OVER ALL AVERAGE SECTION
LOAD (Mpa)	0.6513	52.4668	717.598		195.277
DEFLECTION (mm)	-0.00816	-19.63	-1169.32	-1188.96	-361.467
AS4-8552X2					
LOAD(Mpa)	0.6513	52.4668	717.598		195.277
DEFLECTION(mm)	-0.0095	-22.287	-1360.19	-1382.49	-420.47
AS4-3501-6x2					
LOAD(Mpa)	0.6513	52.4668	717.598		195.277
DEFLECTION(mm)	-0.00966	-22.662	-1383.37	-1406.04	-427.635

Table 19 shows that the maximum summation value of three section deflections along all the blade length was for AS4-3501-6 with the value of total deflection= (-1406.04) mm. AS4-8552 comes next with maximum total deflection= (-1382.49) mm. The minimum total deflection went to IM7-977-3 with (-1188.96) mm. While the deflection of the overall average section was (-.427.635, -420.47, -361.467) mm respectively. It is obvious that the deflection of the spar section of the wind blade is depending on tow factors: the length of the section and the mechanical properties of the composite itself.

CHAPTER FIVE

CONCLUSION AND SUGGESTIONS

5.1. Conclusion

By applying a pure shear load, there is no effect of changing the failure criteria. Therefore, permissible shear stress, first plies failure and last ply failure have the same values for a specific composite. AS4-8552 has a more extended limit between matrix failure mood and fiber failure mood than AS4-3501-6. Applying an axial load with Hashin criterion shows that with AS4-3501-6, the failure starting in the very early step than AS4-8552, as shown in Figure 27. From Figure 27, IM7-977-3 has the highest strength than other tow composites in this study. AS4-8552 is more conservative with failure sequence analysis than other criteria. For AS4-3501-6, all criteria that have used here are precisely identical although there are tiny differences in slope can be neglected as shown in Figure 30. Applying shear load on AS4-8552 with Hashin gives a result where the fiber failure mood is completely happening with the fiber before any failure in the matrix. This behavior is interesting to happen among the failure mood sequence if compared with the other composites. Testing the materials with applying an aerodynamic force comes from steady state wind speed simulation of 15m/s on the wind blade SANDIA_SERI-8 model is showing that the blade deflection of the composite materials has the maximum value for AS4-3501-6 then AS4-8552 comes next and the minimum deflection was for IM7-977-3 composite.

5.2. Suggestions

A more practical investigation is needed to be done on the AS4-3501-6 composite under shear load, focusing on the sudden jump in strength using Hashin failure criterion for more understanding to such a sudden jump in strength for this composite. More diversity of stacking sequences is needed to be investigated in a similar work to find out what is the effect of changing stacking sequence on the composite structure to carry the load.



REFERENCES

- [1] B. A. A. & V. A. Eker, "Using of composite material in wind turbine blades.," *Journal of Applied Sciences*, 6, 2917-2921, (2006).
- [2] J. F. S. D. D. & A. P. Mandell, "Composite materials fatigue issues in wind turbine blade construction," *SAMPE 2008.*, (2008).
- [3] D. D. A. P. & M. J. F. Samborsky, *Effects of Glass Fabric and Laminate Construction on the Fatigue of Resin Infused Blade Materials.*, (2008, January).
- [4] S. Żółkiewski, "Selection and impact of parameters in composite materials designing.," In *Proceedings of the 13th IFToMM Congress*, Guanajuato, Mexico, (2011).
- [5] D. T. & A. T. D. Griffith, *The Sandia 100-meter all-glass baseline wind turbine blade: SNL100-00.*, Sandia National Laboratories, Albuquerque, Report No. SAND2011-3779, (2011).
- [6] K. J. Z. M. D. V. D. C. P. S. K. J. & B. D. Jackson, *Innovative design approaches for large wind turbine blades.*, *Wind Energy*, 8(2), 141-171, (2005).
- [7] D. A. & A. T. D. Griffin, *Alternative composite materials for megawatt-scale wind turbine blades: design considerations and recommended testing.*, In *ASME 2003 Wind Energy Symposium* (pp. 191-201). American Society of Mechanical Engin, (2003, January).
- [8] B. B. T. S. P. A. & D. L. Hillmer, *Aerodynamic and structural design of MultiMW wind turbine blades beyond 5MW.*, In *Journal of Physics: Conference Series* (Vol. 75, No. 1, p. 012002). IOP Publishing, (2007).

- [9] P. S. A. T. D. S. H. J. L. D. L. L. D. W. G. D. A. & M. A. Veers, *Trends in the design, manufacture and evaluation of wind turbine blades.*, Wind Energy, 6(3), 245-259, (2003).
- [10] P. L. H. & L. A. Brøndsted, *Composite materials for wind power turbine blades.*, Annu. Rev. Mater. Res, 35, 505-538, 2005.
- [11] J. F. M. J. G. & R. A. L. Manwell, "Wind energy explained: theory, design and application," John Wiley & Sons, (2010).
- [12] A. J. Salaman, *Tensile and impact properties of polystyrene matrix composites reinforced by palm natural fibers and carbon fibers*, Academic Research International, 3(2), 114, (2012).
- [13] B. Attaf, *Advanced Technologies for Design and Manufacturing of Composite Wind Turbine Blades*, Conference Paper · , December 2015.
- [14] L. B. & S. M. M. Lessard, *Two-dimensional modeling of composite pinned-joint failure*, Journal of composite materials, 29(5), 671-697, (1995).
- [15] F. P. S. L. J. H. S. R. & W. M. R. Van der Meer, *Computational modeling of complex failure mechanisms in laminates*, Journal of Composite Materials, 46(5), 603-623, (2012).
- [16] A. & S. H. Puck, *Failure analysis of FRP laminates by means of physically based phenomenological models*, Composites Science and Technology, 58(7), 1045-1067, (1998).
- [17] C. T. & T. J. Sun, *Prediction of failure envelopes and stress/strain behaviour of composite laminates*, Composites Science and technology, 58(7), 1125-1136, (1998).
- [18] N. G. & G. S. N. Vasjaliya, "Aero-structural design optimization of composite wind turbine blade," In Proceedings of the 10th World Congress on Structural and Multidisciplinary Optimization Accessed July (Vol. 21, p. 2014), (2013).
- [19] Y. A.-A. A. P. I. D. z. E. Ö. & D. A. Kim, "Experimental and Computational Investigation of Turbulence Effect on Performance and Wake of Wind Turbines," (2016).

- [20] F. O. E. Diss, *TURBINE, WIND*, ISTANBUL AYDIN UNIVERSITY, 2015.
- [21] C. V. B. W.-H. J. H. K. M. S. O. K. J. J. & B. E. Skamris, *Type approval scheme for wind turbines. Recommendation for design documentation and test of wind turbine blades*, 2002.
- [22] R. P. L. Nijssen, *Fatigue life prediction and strength degradation of wind turbine rotor blade composites*, 2006.
- [23] B. F. J. E. D. C. P. J. F. M. J. H. M. J. T. K. & H. K. Sørensen, *Improved design of large wind turbine blade of fibre composites based on studies of scale effects (Phase 1). Summary report*, 2004.
- [24] F. Aymerich, "Composite materials for wind turbine blades, issues and challenges," Italy, 2012.
- [25] O. T. Thomsen, *Sandwich materials for wind turbine blades—present and future*, *Journal of Sandwich Structures & Materials*, 11(1), 7-26, 2009.
- [26] B. W.-H. J. & B. P. Hayman, *Materials challenges in present and future wind energy*, *Mrs Bulletin*, 33(4), 343-353, 2008.
- [27] L. & F. O. Mishnaevsky Jr, *Composite materials in wind energy technology*, *Thermal to Mechanical Energy Conversion: Engines and Requirements*, EOLSS Publishers: Oxford, UK, (2011).
- [28] K. Y. Lin, *Composite materials: materials, manufacturing, analysis, design and repair*, 2015.
- [29] "<http://int.search.myway.com/search/AJimage.jhtml?&n=782b4616&p2=%5EBSB%5Exdm011%5ES18314%5Etr&pg=AJimage&pn=1&ptb=E125D79D-77D8-43F1-AE5A-CB954164C9C1&q=&searchfor=carbon+fiber+material&si=CJis-Or5s8CFRa3Gwodav8MMA&ss=sub&st=tab&tp=hst&trs=wtt&ots=1508>".
- [30] J. A. GRAND, *Wind power blades energize composites manufacturing*, *Plastics technology*, 54(10), 2008.
- [31] S. Joncas, *Thermoplastic Composite Wind Turbine Blades: An Integrated Design Approach*, (2010).

- [32] L. A. A. T. K. H. V. T. L. L. V. J, *Hybrid yarn for thermoplastic fibre composites. Summary of technical results*, Final report for MUP2 Framework Program No 1994-503/0926-50. Risi,-R-1034(EN), (1998) .
- [33] J. G. J. D. C. S. E. J. & W. B. K. Smith Jr, "Hypervelocity Impact Testing of IM7/977-3 with Micron-Sized Particles," in *Structural Dynamics, and Materials Conference In 51st AIAA/ASME/ASCE/AHS/ASC Structures, 18th AIAA/ASME*, (2010, January).
- [34] S. G. L. I. R. D. Z. T. J. S. J. K. P. L. I. M. L. S. & S. D. A. Miller, *Face-Sheet Quality Analysis and Thermo-Physical Property Characterization of OOA and Autoclave Panels*, (2012).
- [35] K. Gripple, *A Comparison of the Compression Response of Thick (6.35 mm) and Thin (1.60 mm) Dry and Moisture Saturated AS4/3501-6 Laminates (No. DTRC-SME-90/74)*, DAVID TAYLOR RESEARCH CENTER BETHESDA MD SHIP MATERIALS ENGINEERING DEPT, 1990.
- [36] P. D. H. M. J. & K. A. S. Soden, *Lamina properties, lay-up configurations and loading conditions for a range of fibre-reinforced composite laminates*, *Composites Science and Technology*, 58(7), 1011-1022, 1998.
- [37] P. C. P. W. P. & B. Portela, *Analysis of morphing, multi stable structures actuated by piezoelectric patches*, *Computers & Structures*, 86(3), 347-356, 2008.
- [38] "<https://damassets.autodesk.net/content/dam/autodesk/www/products/simulation-composite-design/docs/pdfs/nasa-goddard-space-flight-center-customer-story.pdf>".
- [39] R. M. Jones, *Mechanics of composite materials*, CRC press, 1998.
- [40] R. M. Christensen, *The comparison and evaluation of three fiber composite failure criteria*, (No. UCRL-CONF-209972). Lawrence Livermore National Laboratory (LLNL), Livermore, CA, (2005).

- [41] "<https://knowledge.autodesk.com/support/helius-composite/learn-explore/caas/CloudHelp/cloudhelp/2017/ENU/ACMPDS/files/GUID-A6A702F1-6416-421A-BA81-E9D3DDA4257E-htm.html>".
- [42] "http://www.ecourses.ou.edu/cgi-bin/ebook.cgi?topic=me&chap_sec=07.4&page=theory".
- [43] Y. MAO, 2011. [Online]. Available: http://www2.mech.unsw.edu.au/BET_files/live/A151612A91E9387287E65FB85D348305.pdf.
- [44] D. A. Griffin, *Blade system design studies volume I: Composite technologies for large wind turbine blades*, Sandia National Laboratories, Paper No. SAND-1879, (2002).
- [45] U. Ustunel, *Modern multiaxials improve performance. Reinforced Plastics*, 50(4), 34-38, (2006).
- [46] C. T. Sun, *COMPARATIVE EVALUATION OF FAILURE ANALYSIS METHODS FOR COMPOSITE LAMINATES*, (No. DOT/FAA/AR-95/109), (1996).
- [47] F. & J. K. E. Paris, *A study of failure criteria of fibrous composite materials*, (2001).
- [48] A. Y. R. I. A. P. J. & L. H. Chehouri, *Optimal design for a composite wind turbine blade with fatigue and failure constraints*, Transactions of the Canadian Society for Mechanical Engineering, 39(2), 171-186, (2015).
- [49] I. M. I. O. D. I. M. & D. I. Daniel, *Engineering mechanics of composite materials (Vol. 3, pp. 256-256)*, New York: Oxford university press, (1994).
- [50] A. K. Kaw, *Mechanics of composite materials*, CRC press, (2005).

CURRICULUM VITAE

PERSONAL INFORMATION

Surname, Name: Al-Faris, Ali
Nationality: Iraqi (IQ)
Date and Place of Birth: 2 January 1975
Marital Status: Married
Phone: +90 5378738137 WhatsApp: 009647701631282
Email: ali75f@gmail.com

EDUACTION

Degree	Institution	Year of Graduation
BS	University of Mosul\ Mosul	1997
High School	Al-Resalah High School	1993

WORK EXPERIENCE

- Head of mechanical courses department** 2012-Present
Ministry of electricity (MOE)
Training & development directorate (T&D) - NEINAVA branch.
Responsibilities: Managing all the mechanic's courses in the branch.
- Head of quality management department** 2011-2012
(MOE) general directory for power production- north region. Power Industry
Responsibilities: Responsible for preparation to implement quality management system.
- An employee in internal audit section.** 2010-2011
(MOE) general directory for power production- north region. Power Industry
Responsibilities: responsible for preparation to implement internal audits in the directory.
- An employee in Quality Management Section** 2009-2010
Mosul dam hydro power station / main dam. Power Industry
Responsibilities: Responsible for preparation to implement quality management system
- Senior Mechanical Engineer** 2008-2009
Mosul dam hydro power station / main dam. Power Industry

Responsibilities: Implementing maintenance on mechanical parts in regulating dam

Operating engineer / senior 2006-2008

Mosul dam hydro power station / regulating dam. Power Industry

Responsibilities: Operating and Supervising the operation of power units in regulating dam & 132kv substation.

Operating Engineer 2004-2006

Mosul dam hydro power station / main dam. Power Industry

Responsibilities: Operating the power units in main dam &400 KV substation.

Inspection Engineer 2000-2004

The general company of rehabilitation power plants. Power Industry

Responsibilities: Implementing the inspection procedures on all the boiler components, condenser, air ducts all welded joints. for more than 4 power stations spread across the country.

FOREIGN LANGUAGES

Arabic : Fluent

English : Very good